Institute of Paper Science and Technology

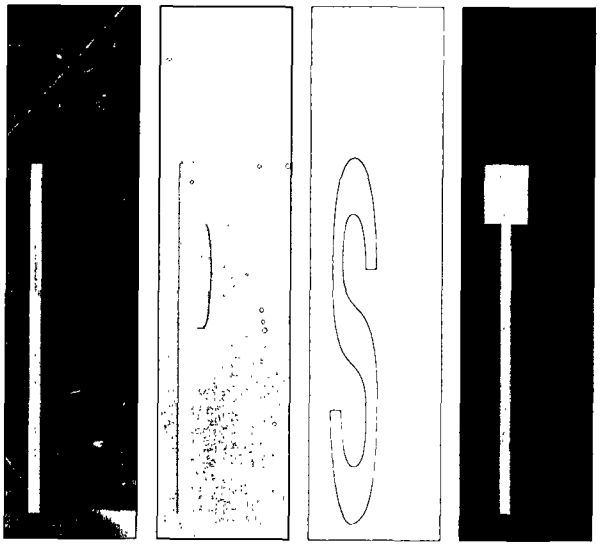

Atlanta, Georgia

A STUDY OF TRANSVERSE MOISTURE DISTRIBUTION AND MOVEMENT DURING HOT-SURFACE DRYING OF PAPER

A thesis submitted by

Arthur Charles Dreshfield, Jr.

B.S. 1951, University of Illinois
M.S. 1953, Lawrence College

in partial fulfillment of the requirements
of The Institute of Paper Chemistry
for the degree of Doctor of Philosophy
from Lawrence College,
Appleton, Wisconsin

June, 1956

TABLE OF CONTENTS

INTRODUCTION

Hot-surface drying is the process of placing a wet material in contact with a surface hotter than the material. Heat is transferred to the material; this vaporizes water, and the water vapor subsequently leaves the material. Hot-surface drying is therefore a complex operation involving simultaneous transfer of heat and mass in a multiphase system.

The operation of hot-surface drying is in widespread use in the paper industry. Nearly all of the paper and paperboard produced is subjected to this operation during manufacture. The conduct of drying has very significant bearing on the cost, quality, and properties of the product. Thus, it is an operation of great importance to the paper industry.

The following literature survey of the field will show that there are considerable gaps in the present knowledge of the process. Specifically lacking is a clear picture of the mechanism of hot-surface drying. That is, knowledge is lacking concerning the location and movement of liquid water within a sheet, concerning the location of the zone in which vaporization occurs, and concerning the movement of water vapor out of the sheet. A better understanding of these phenomena should contribute to knowledge of the factors causing and limiting drying; better understanding of the mechanism of hot-surface drying should contribute to more intelligent operation of existing equipment and better design of new equipment.

AIR DRYING OF PULP AND PAPER

In air drying, transfer of heat to the wet sheet is from air moving past the sheet. The process is much slower than hot-surface drying, and it is used much less widely in the pulp and paper industry. However, it has received considerably more study than hot-surface drying, probably because it is amenable to simpler experimental and theoretical analysis.

Higgins (1) has recently made a thorough literature survey and laboratory investigation of air drying. The interested reader is referred to Higgins for prior references; only those aspects of air drying which contribute to an understanding of hot-surface drying are emphasized here.

A typical air-drying process is found to consist of two general periods of drying. In the first, the rate of drying of every point on the surface is constant; this is consequently called the constant-rate period. During this period, however, the drying rate is not constant across the surface of the sheet. It has been shown that drying during this period corresponds closely to evaporation from a surface of water. This indicates that the surface of the sheet must be saturated with water, and that liquid water is moving from the interior to the surface of the sheet. Higgins has measured the temperature of a sheet during drying and has found that the sheet is nearly isothermal and is close to the wet-bulb temperature during constant-rate drying. During this period, drying can be predicted closely by calculations based on adiabatic humidification theory. Higgins calculated heat- and mass-transfer coefficients from his data, and he found that both could be correlated with the mass velocity of the air passing over the sheet. Figure 1 is Higgins' correlation of

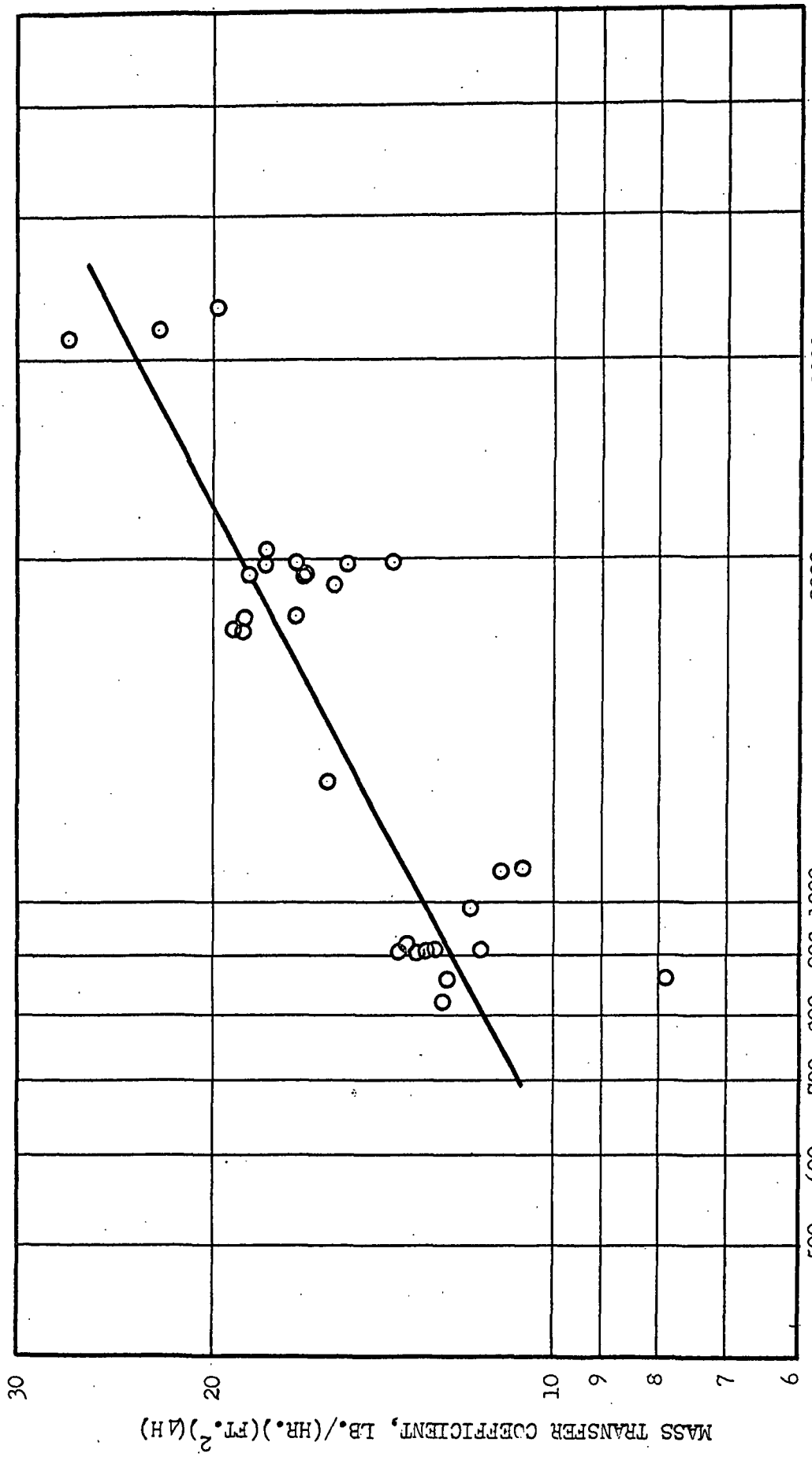

Figure 1. Effect of Mass Velocity on the Mass Transfer Coefficient

mass-transfer coefficient, K; it can be seen that K varies linearly with the square root of G, the mass velocity of the air.

Constant-rate drying continues until the "critical moisture content" of the sheet is reached. This is defined as the over-all moisture content of the sheet at which the rate of drying is observed to decrease. For air drying, it occurs when the surface of the sheet at the upstream side of the sheet is such that the air-surface interface is no longer saturated. Sheet properties, sheet size, and drying conditions determine the value of the critical moisture content.

Below the critical moisture content, drying occurs at a continuously decreasing rate; this is the "falling-rate period." Experimental evidence (2 - 5) indicates that unsaturated-surface drying is the predominate mechanism in thin sheets, sub-surface vaporization in thick sheets. There is probably no sharp distinction between these two processes.

HOT-SURFACE DRYING OF PULP AND PAPER

Studies of drying have been of two general types; studies of the effect of variables, both internal and external on the over-all drying rate of a sheet, and studies of moisture and temperature distribution within a sheet during drying. Most of the published data refer to paper-machine operation. Reports on the effect of sheet properties and drying conditions on drying rate are often contradictory, probably because of the difficulty of obtaining accurate measurement and control of significant variables. Burstein (6) presents an adequate review of such literature up to 1944; little can be deduced concerning the mechanism of hot-surface drying. TAPPI Data Sheets 155 (7) summarize drying and production-

rate data for various grades of paper and pulp. Montgomery (8) presents additional information of this nature. Montgomery (9) gives a discussion of paper machine drying principles and factors affecting drier operation. Schmidt (10), Nuki (11), and Goumeniouk (12) discuss principles of paper machine drying. Nissan (13) presents a mathematical analysis of paper machine drying.

Studies of particular machines have been reported by Lewis, McAdams and Adams (14) and by Sherwood, Gardner, and Whitney (15). Both groups found an initial preheating period in which the drying rate was increasing, a constant-rate period, and a falling-rate period. Sherwood et al., estimated the over-all heat-transfer coefficient, U, from their data. They found it to be approximately 50 B.t.u./(hr.)(ft.^{2})(°F.) during the constant-rate period. It became steadily less during the falling-rate period.

Laboratory simulation of paper machine drying (alternate heating of each side of the sheet) has been conducted by two workers. Burstein (6) studied the effects of sheet properties, hot-surface temperature, and air conditions on the over-all drying rate of sheets. He interpreted his results to show that drying took place in two constant-rate periods, the second with a lower rate than the first. From his work, Burstein deduced that a zone in the center of the sheet was saturated with water; on either side, a zone of unsaturation existed in which vaporization occurred. He also concluded that the air and vapor between the sheet and the hot surface represented an appreciable portion of the resistance to heat transfer. Burstein dried some sheets with one side in continuous

contact with a heated surface. He found that the drying rate under this condition was slightly less than when the sides were heated alternately.

Smith and Attwood (16, 17) have developed a device which appears to be more versatile and amenable to control than Burstein's. Their results have shown the effect of felt properties, felt tension, air temperature, cylinder size, cylinder spacing, and drier surface temperature on the rate of drying of sheets. They found that drying rate increased linearly with the temperature of the hot surface, which is in accord with the findings of Burstein. However, their data indicated a constant-rate period and a falling-rate period.

Flyate (18) has investigated some of the factors affecting hot-surface drying of thin sheets. He found that the type of pulp had only a small effect on the drying rate. Beating had little effect on the constant-rate period, but it caused considerable reduction in drying rate during the falling-rate period. He also found that the drying rate during the constant-rate period decreased as the basis weight of the sheet increased. For thin sheets, the critical moisture content was independent of the temperature of the hot surface and was approximately 30% of the dry sheet weight.

McCready (19) has published the most complete study to date pertaining to the mechanism of hot-surface drying. He used sheets 1/4-inch thick for most of his work. He measured the effect of several variables on the over-all drying rate of sheets. He obtained transverse temperature distribution during drying and also the transverse moisture distribution at one time during drying.

Figure 2A

Temperature Distribution in Sheet
[From McCready (49)]

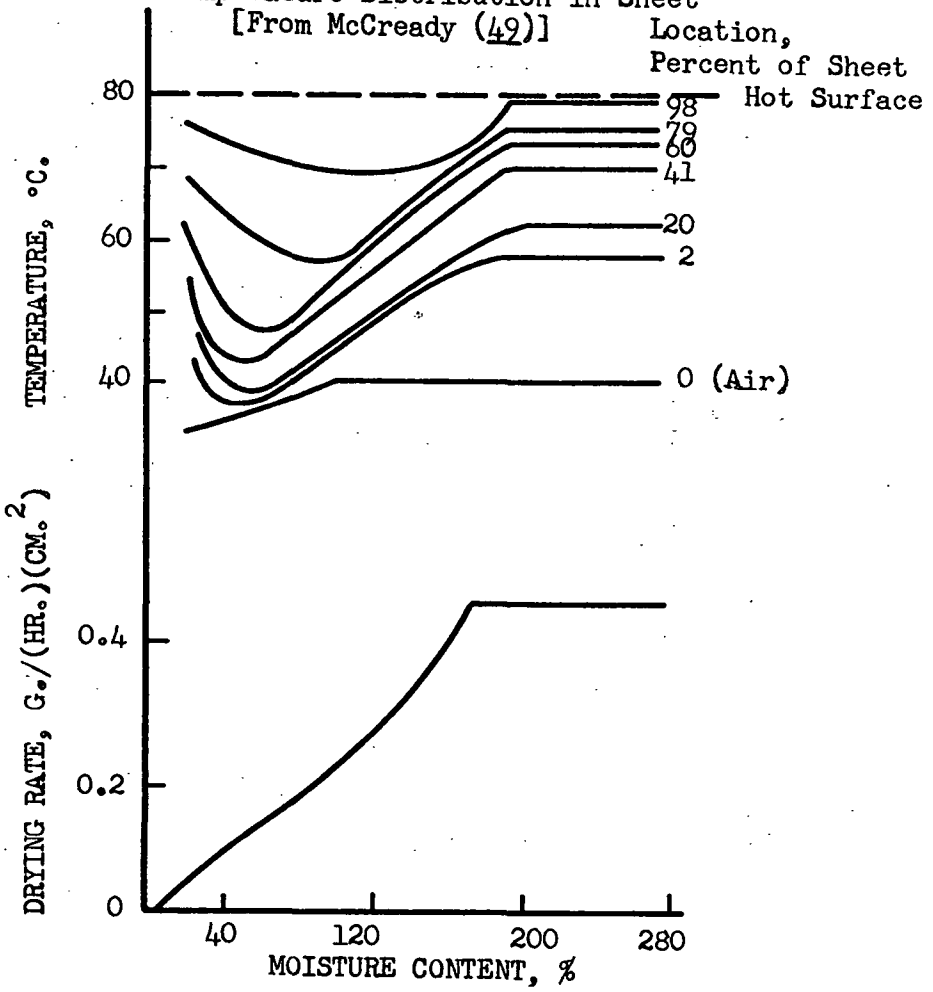

Figure 2B

Temperature Distribution Sheet

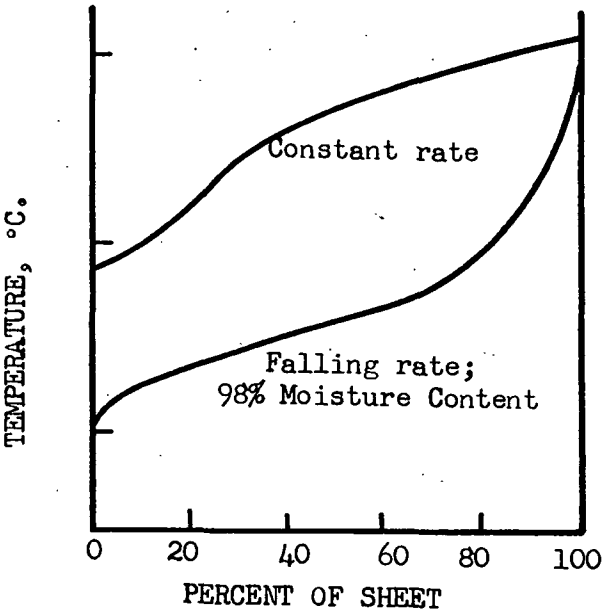

McCready differentiated two types of drying; one characterized by a minimum temperature within the sheet; the other by continuously decreasing temperature from the hot to the cold surface of the sheet. The drying rate and temperature distribution in a sheet of the second type are shown in Figure 2. The temperature distribution during the constant-rate period and at one moisture content during the falling-rate period is shown in Figure 2A, replotted from Figure 2. At this moisture content, the third of the sheet nearest the hot surface had a moisture content of 37%, the middle third of the sheet and the third nearest the air surface each contained 128% moisture. Referring to Figure 2, the temperature distribution within the sheet remained constant during the period of constant-rate drying. At the critical moisture content, the temperature in all portions of the sheet began to decrease, and the temperature distribution changed continuously throughout the falling-rate period. At any depth within the sheet, the temperature reached a minimum value for that region at some time during the falling-rate period, then it began to increase. The region of the sheet nearest to the hot surface reached its minimum value first; then regions progressively farther from the hot surface reached their minimum value successively.

McCready interpreted these results to show that vaporization occurred at the hot-surface interface during the constant-rate period; during the falling-rate period, the zone of vaporization was receding from the hot surface of the sheet.

McCready also calculated the apparent mass-transfer coefficient at the air-interface from the constant-rate data. He showed that this

coefficient satisfactorily predicted the drying rate during the falling-rate period until a sheet of moisture content of about 50% was reached. From this he concluded that the constant-rate period was saturated-surface drying at constant surface temperature and that the vapor leaving the air interface of the sheet was in equilibrium with the water at that interface. Most of the falling-rate period, therefore, was also saturated surface drying, the water vapor leaving the sheet being in equilibrium with the water at the air-interface of the sheet. This interface was at a lower temperature than during constant-rate drying due to the increased thermal resistance of the sheet at the hot-surface interface.

INVESTIGATIONS RELATED TO DRYING MECHANISM

Although not directly concerned with hot-surface drying of pulp and paper, several workers have conducted investigations which shed light on phenomena which could be of importance in this operation. Marshall and Friedman (20) have recognized five possible mechanisms which could cause moisture movement within solids. These are

1. Flow caused by capillary forces.
2. Flow caused by diffusion of either liquid or vapor due to a gradient in concentration or partial pressure.
3. Flow caused by gravity or by an over-all pressure gradient.
4. Flow caused by vaporization-recondensation cycles within the material.
5. Flow caused by shrinkage forces.

CAPILLARY FORCES

Flow of liquid by capillary forces arises from the well-known fact that the pressure beneath a concave interface is less than that beneath

a flat surface. The pressure difference is expressed by the equation

$$\Delta P = \gamma[(1/r_1 + (1/r_2)] \cos\theta_c \qquad (1)$$

where ΔP = pressure difference across the liquid interface

γ = interfacial tension

r_1 and r_2 = radii of curvature of the two principle planes of the meniscus.

θ_c = contact angle between the liquid and the solid.

Consistent units are implied.

For a porous system, this pressure difference is generally called the "capillary suction."

A related concept worthy of consideration is that of "entry suction," originally presented by Haines (21) for a bed of spheres. As water is removed from such a bed, the radius of curvature of water held between the spheres at the surface of the bed decreases as the centers of the menisci recede from the surface. When the center of a meniscus reaches a point on the plane defined by center lines of three spheres, the pressure difference is at a maximum because the radius of curvature of the meniscus is at a minimum. Any further water removal will cause an increased radius of curvature, and air will be drawn into the bed. This critical suction value is called the entry suction of the bed.

For a series of capillaries of varying length and diameter, a similar concept can be developed. As water is removed, the level in the larger capillaries recedes. When a meniscus reaches a point of minimum radius of curvature, the entry suction for that capillary is reached. Because of the distribution of sizes and shapes, a sharp value for a real

bed is not found, but air can undoubtedly be drawn into a bed by such a mechanism. The mechanism also predicts a continuous redistribution of liquid water during drying, the water being moved from larger to smaller pores.

For a complex capillary system such as exists in pulp, it is impossible to measure the pore size and shape distribution. Rather, the capillary suction is measured as a function of moisture content. Barkas and Hallan (22) have done this for several pulps. Ceaglske and Hougen (23), and Pearse, Oliver, and Newitt (24) have measured capillary suction as a function of moisture content for sand and glass beads, respectively. Both groups also conducted air drying experiments and found fair agreement between the moisture distribution found in the bed and that predicted for capillary suction equilibrium.

Krischer (25) presented a somewhat different treatment of capillary movement. He considered flow to be caused by a capillary "conductivity" times a moisture gradient, mathematically analogous to diffusion. His values for conductivity varied over wide ranges, being a strong function of moisture content. Such a treatment seems inferior to the capillary suction concept.

DIFFUSION

Hougen, McCauley, and Marshall (26) have shown that capillary migration explains moisture distribution during air drying much better than does diffusion theory. Capillary flow is to be expected as long as a continuous water network exists. At low moisture content, however,

discrepancies exist, and diffusion becomes the more important mechanism. Liquid diffusion may be responsible for the movement of water below the "fiber saturation point"*; vapor diffusion plausibly accounts for the movement of water when the moisture content of the material is very low. Hougen et al. (26) and Marshall and Friedman (19) give references to earlier work in which diffusion of liquid or vapor was assumed to be the mechanism of water movement.

GRAVITATIONAL AND OVER-ALL PRESSURE GRADIENTS

Gravitational forces and external pressure are used to remove the major portion of water from the fiber slurry used for papermaking. Water removed by evaporation is normally that which cannot be removed by mechanical means. Higgins (1) has shown that no gravitational gradients existed in sheets 6 inches long, hung vertically, containing 120% moisture. The slope of the capillary suction curves presented by Barkas and Hallan (22) indicate that transverse moisture gradients due to gravity would be negligible in sheets containing up to 1000% moisture or more. Nissan (27) has proposed that pressure caused by heating air entrapped at the sheet-drum interface on a paper machine could move water mechanically into a felt. In the discussion following this paper, however, Whitney notes that Preston and Chen (28) have shown liquid migration in textiles to be in the opposite direction from that proposed by Nissan. Dreshfield notes that calculations based on the data of Barkas and Hallan (22) show that the pressure generated is insufficient to overcome the capillary suction holding the water in the sheet; therefore it could not cause migration of liquid water.

*"Fiber saturation point" is a value, not sharply defined, at which the vapor pressure of the water in the system is measurably less than the equilibrium vapor pressure of liquid water at the same temperature.

VAPORIZATION-RECONDENSATION

Preston and co-workers (28-30) have studied nonlevelness of dyeing. They found that a nonsubstantive dye migrates to a hot surface during drying. The higher the initial moisture content, the more rapid and pronounced was the migration. The rate of migration decreased greatly when the critical moisture content was reached. These experiments were qualitative in nature, some being performed with a textile web which was initially level-dyed, others using a stack of filter paper in which the center sheet was dyed.

These results are interpreted by Preston as verification of a vaporization-recondensation cycle occurring within the material during drying. Since a temperature gradient existed, vapor formed at the hot side had a higher partial pressure than the saturation pressure of the remainder of the sheet. Therefore, some vapor condensed in the cooler portions of the sheet. Thus, a cycle was set up with liquid water moving toward the hot surface, vaporizing there, and part of the vapor condensing within the sheet.

Evidence for the existence of vaporization-recondensation phenomena has been shown for other materials. Sheppard, Hadlock, and Brewer (31), drying sand in uninsulated trays, found that apparent thermal conductivity of the wet matrix was higher than that of water by about 2 B.t.u./hr. $ft.^2$ °F. Since convection within the bed was unlikely, they attributed the added heat transfer to vapor movement. McCready (19) also observed higher thermal conductivity than water in his pulp sheets during drying on a hot surface.

Hutcheon and Paxton (32) measured thermal conductivity and moisture distribution in sawdust which was totally enclosed and maintained under a temperature gradient. Vassilou and White (33) presented similar data for clays, and their results were convincing evidence that vaporization-recondensation was primarily responsible for the transfer of water vapor and of heat. Eisenstadt (34) also found vaporization-recondensation to be occurring in wet glass beads which were maintained under a temperature gradient.

SHRINKAGE FORCES

Higgins (1) has shown that shrinkage during air drying of paper was not sufficient to account for water removal. It is likely that shrinkage in paper is caused primarily by capillary suction forces generated during drying. Shrinkage is therefore probably a result of drying, rather than a cause of it.

PRESENTATION OF THE PROBLEM

The preceding literature review indicates that a general knowledge of the various phenomena which could be involved in drying is extant. However, for the drying of pulp and paper on a hot surface, the mechanism of drying is not clearly understood. The distribution of water in a 1/4-inch lap has been shown (19). Moisture distribution data alone are insufficient to elucidate the mechanism of drying; data showing the movement of moisture are also required. Furthermore, there has been no evidence which proves that the mechanism of drying in thin sheets is the same as in laps 1/4-inch thick.

The only technique which has been employed to study moisture distribution within a material during drying has been to interrupt a drying cycle, separate the material being dried into several layers, and determine the moisture content of each layer. This technique requires rapid and careful handling of a sheet, and evaporation during handling makes the technique unfeasible when the time of a drying run is short or when the amount of moisture involved is small. Consequently, a new technique without these limitations is needed to determine moisture distribution during drying of sheets which approach the basis weight of paper or paperboard.

The availability of a wide variety of radioactive isotopes has made such a technique possible. It has long been known that the absorption of beta rays (high-energy electrons) by matter is a function of the atomic number of the matter and the mass per unit area of the matter (35). In recent years, this principle has been applied industrially to measure

the basis weight of sheets and webs of material by measuring the beta-ray transmission. If a means could be found to measure and record the beta-ray transmission of a sheet of paper during drying, the transmission could be related to the mass per unit area of the sheet and hence the moisture content of the sheet. Drying of a sheet of paper could thus be followed. Furthermore, if the beta-ray source could be placed at a known depth within the sheet, and if the change in backscatter of beta rays from the material beneath the source was small compared with the change in transmission of the material above the source of radiation, then the drying of the fraction of the sheet above the source could be followed by placing the radiation detector above the sheet. By drying a set of sheets differing only in the depth at which the source of radioactivity was located, the drying curves for different fractional thicknesses of a sheet could be determined. Cross-plotting of such data would enable calculation of the moisture distribution within a sheet at various times during drying. This technique would completely eliminate the necessity of interrupting a drying run or delaminating a wet sheet.

A second technique of value is the use of a nonvolatile, nonsubstantive solute. Such a substance should migrate with liquid water and be deposited where evaporation occurs. This is the technique used by Preston and co-workers (28-30) and by Eisenstadt (34). The results of such a study should contribute evidence concerning the movement of liquid water within a sheet during drying.

It is the purpose of this thesis to determine the transverse distribution and the transverse movement of water during hot-surface drying of

paper. From the data obtained, it should be possible to deduce the internal mechanism of drying. This should represent a contribution to existing knowledge concerning hot-surface drying of pulp and paper.

NOMENCLATURE

SYMBOLS

A Area, cm.^{2} (ft.^{2} where noted); atomic weight of an element

C Capacitance, farads

E Energy of an electron, million electron volts

G Mass velocity, lb./hr. ft.^{2}

H Absolute humidity of air, lb. water/lb. air

h Heat-transfer coefficient, B.t.u./hr. ft.^{2} °F.

K Mass-transfer coefficient, lb./(hr.)(ft.^{2})(unit ΔH)

k Thermal conductivity, B.t.u./hr. ft.^{2} (F./ft.)

N Number of beta particles detected per unit time, sec.$^{-1}$

n Number of beta particles detected, dimensionless

P Pressure, dynes/cm.^{2}

q Rate of heat transfer, B.t.u./hr.; electrical charge, coulombs

R Maximum range of electrons in aluminum, (mg./cm.^{2})$^{-1}$; electrical resistance, ohms.

R_f Relative migration of solute, compared to solvent, on a chromatogram, dimensionless

r Radius of curvature of a meniscus, cm.

T Transmission by matter of beta radiation, ratio of N when material is present to N when material is absent, dimensionless

t Temperature, °F.

U Over-all heat-transfer coefficient, B.t.u./(hr.)(ft.^{2})(°F.)

W Weight of water in a sheet, lbs.

X Thickness, ft.

x Mass per unit area of material, mg./cm.^{2}

Z Atomic number of an element

$\bar{Z}$ Average atomic number of a compound

γ Interfacial tension between a solid and a liquid, dynes/cm.

Δ Difference between values

θ Time, sec., (hr. where noted)

θ_c Contact angle between a liquid and a solid, dimensionless

μ_a Absorption coefficient of the beta radiation by matter, $(mg./cm^2)^{-1}$

Defined by equation

$$\underline{dN/N} = -\mu_a \underline{dx}$$

$\underline{\sigma}$ Standard deviation of a value, dimensionless

Subscripts

o Beginning of a drying run

a Air

ai Air interface

d Dry sheet

f Fluid

s Source of beta-radiation

w Water

1/2 Condition when T = 0.5

min. Minimum

max. Maximum

Abbreviations

c Counts

e Exp. = base of natural logarithms

f.p.m. Feet per minute

g.p.m. Gallons per minute

M.e.v. Million electron volts

mmu mμ = Millimicrons

VAC Volts, alternating current

μc. Microcurie

DESCRIPTION OF APPARATUS

A 20-gage galvanized iron duct is used for the purpose of supplying, measuring, and controlling the temperature, relative humidity, and flow rate of air which is passed over the hot surface on which drying is conducted. Air flow is parallel to the cylindrical axis of the hot surface. A schematic diagram is shown in Figure 3; a photograph in Figure 4.

Air enters the inlet duct at A. This duct is 8.5 inches in diameter and 18 inches long. It is insulated with magnesite. The main duct into which fan D discharges is 9 inches square and 90 inches long. It is covered with asbestos paper. The hot surface is located on the floor of the tunnel at H, one foot from the duct discharge.

Air temperature is measured by a thermometer located at G. Temperature regulation is obtained by controlling the current to two 1000-watt cone heaters at C. One is connected through a switch to the 115 VAC line, the other through a Variac, so that continuous regulation from zero to maximum input can be obtained.

Relative humidity is measured by a wet-bulb thermometer located at G with the dry-bulb thermometer. Regulation is achieved by injecting steam into the inlet duct through perforated pipe B. High pressure steam is throttled by a pressure-reducing valve; final adjustment of steam flow is made with a needle valve.

Air flow is measured by a 3-inch diameter flow nozzle at E. This is connected to an inclined water manometer. The nozzle has been calibrated by the dilution method, using a rotameter as a standard, and it was found

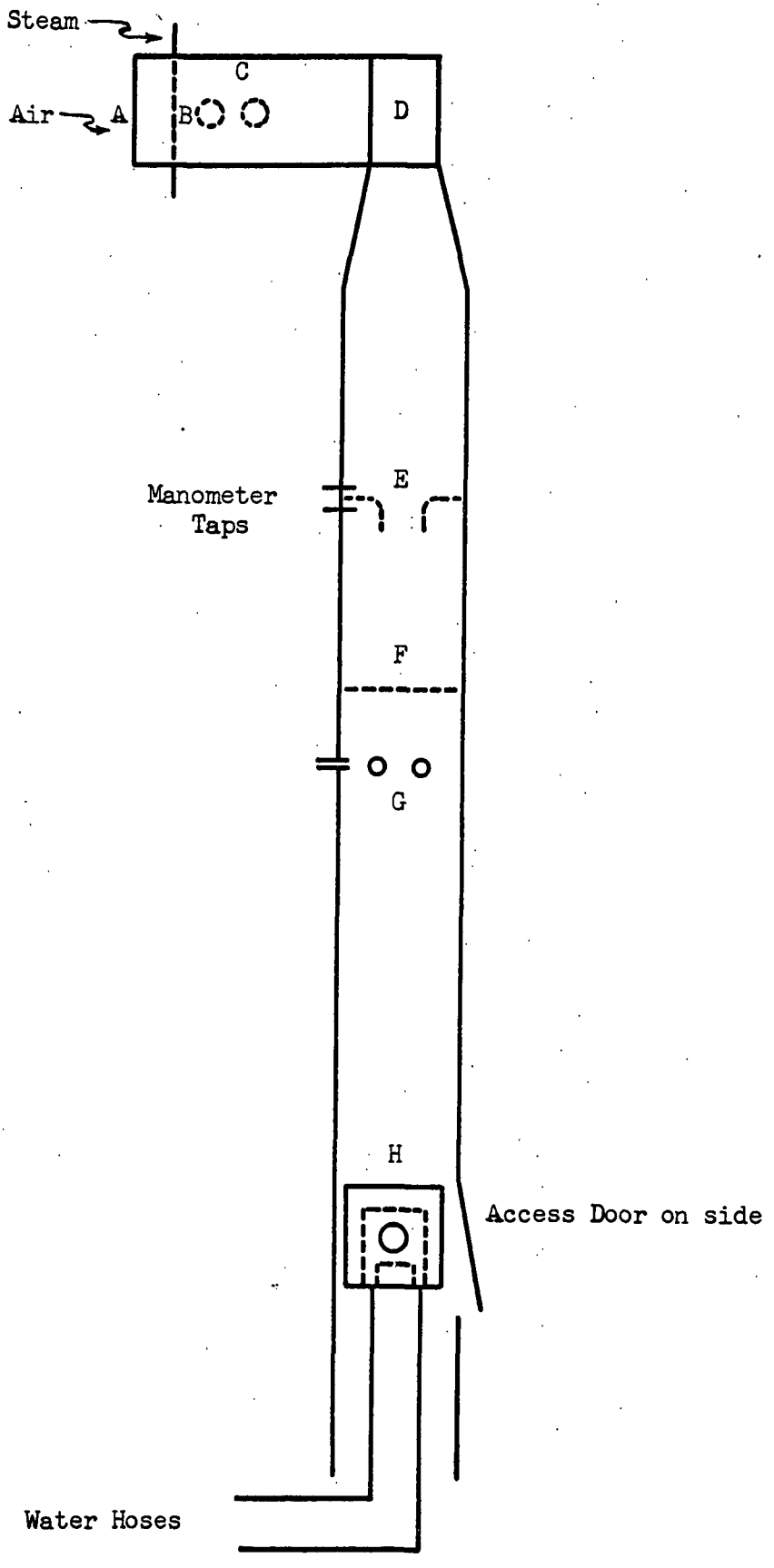

Figure 3. Schematic Diagram of Ductwork

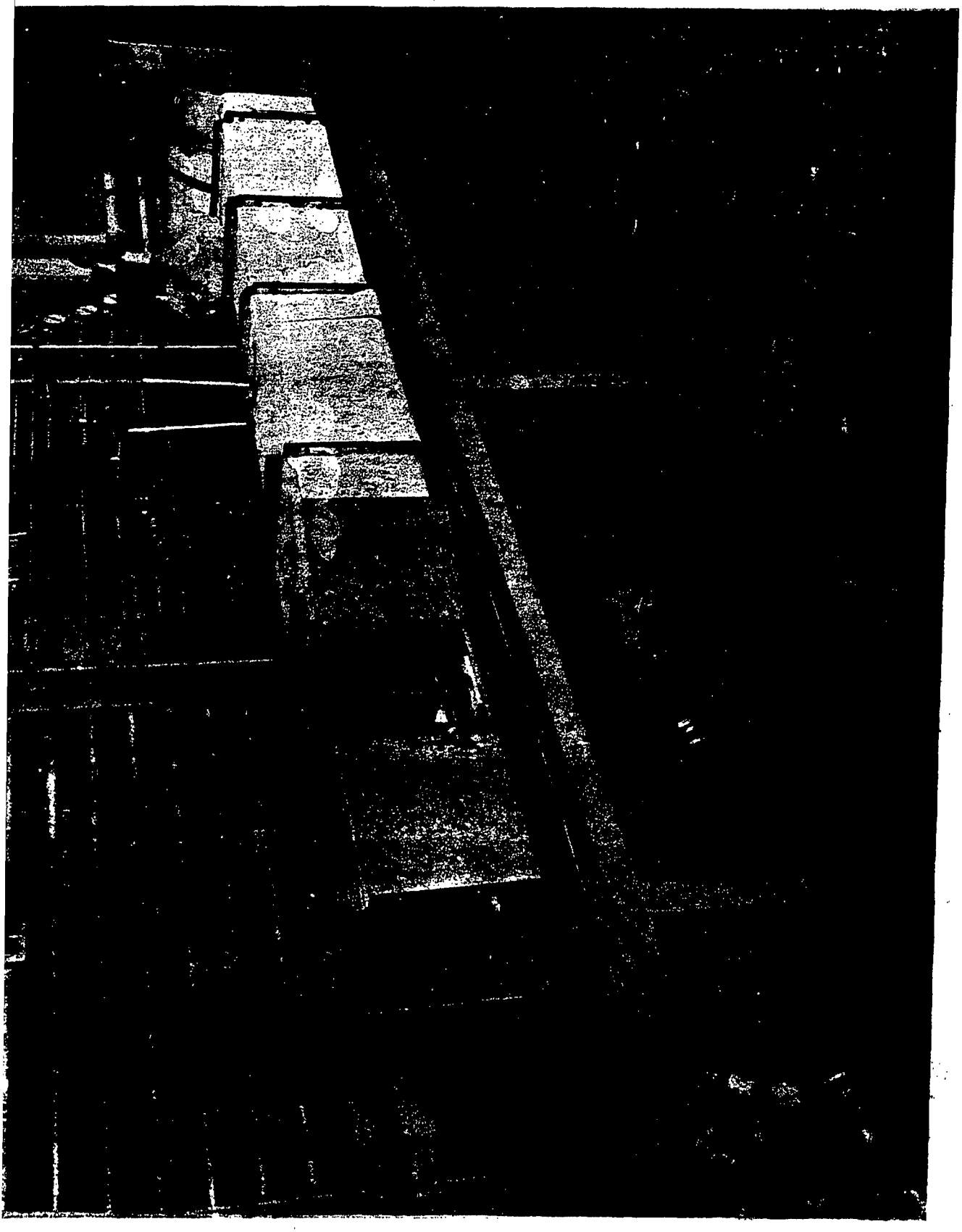

Figure 4. Photograph of Apparatus

to have a discharge coefficient of 0.98. Coarse regulation of air flow is achieved by setting of the variable pulleys connecting the blower motor to the blower, thus controlling the speed of rotation of the blower. Final regulation is obtained with a damper located at A.

A screen at F serves to aid uniform air distribution from the flow nozzle.

Drying is conducted on the surface shown in Figures 5 and 6. It consists of a hollow brass base with a 3/32-inch thick aluminum plate gasketed and screwed over it. The usable portion of the plate is approximately 4 inches square and is approximately cylindrical with a radius of curvature of 2.5 feet. Liquid enters and leaves the unit through 1/2-inch brass pipes which have a 1/8-inch slit in the side beneath the aluminum plate.

The unit is mounted on a block of wood by two 1/16-inch brass rods which extend the length of the hot surface on each side of it. Each end of each rod is threaded and is inserted through the wood; a nut and washer draw each end firmly against the wooden base. The base is held on the tunnel floor by wood screws inserted from the bottom of the tunnel.

Figure 7 is a schematic diagram of the units for supplying hot liquid for heating the surface. The liquid is forced through the surface from a 15-gallon tank by a centrifugal pump. The flow rate is approximately 15 g.p.m. Water is circulated at temperatures up to 200°F.; ethylene glycol at higher temperature. The temperature of the circulating liquid is measured by a thermometer in the tank and is controlled by a Fenwal thermoswitch and relay controlling a 500-watt heater immersed in the tank.

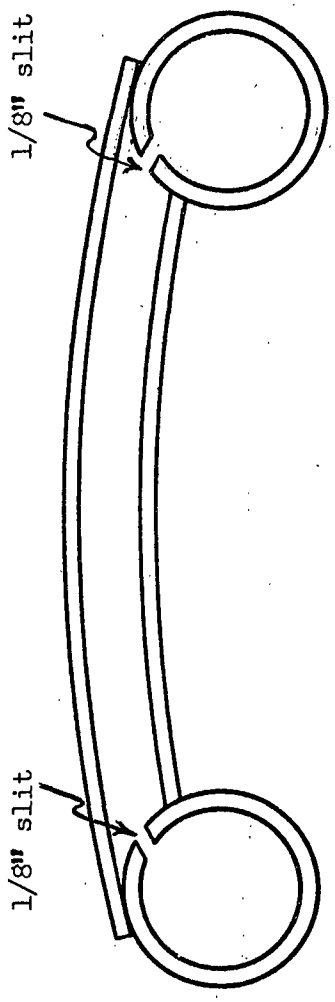

Figure 5. End View of Hot Plate

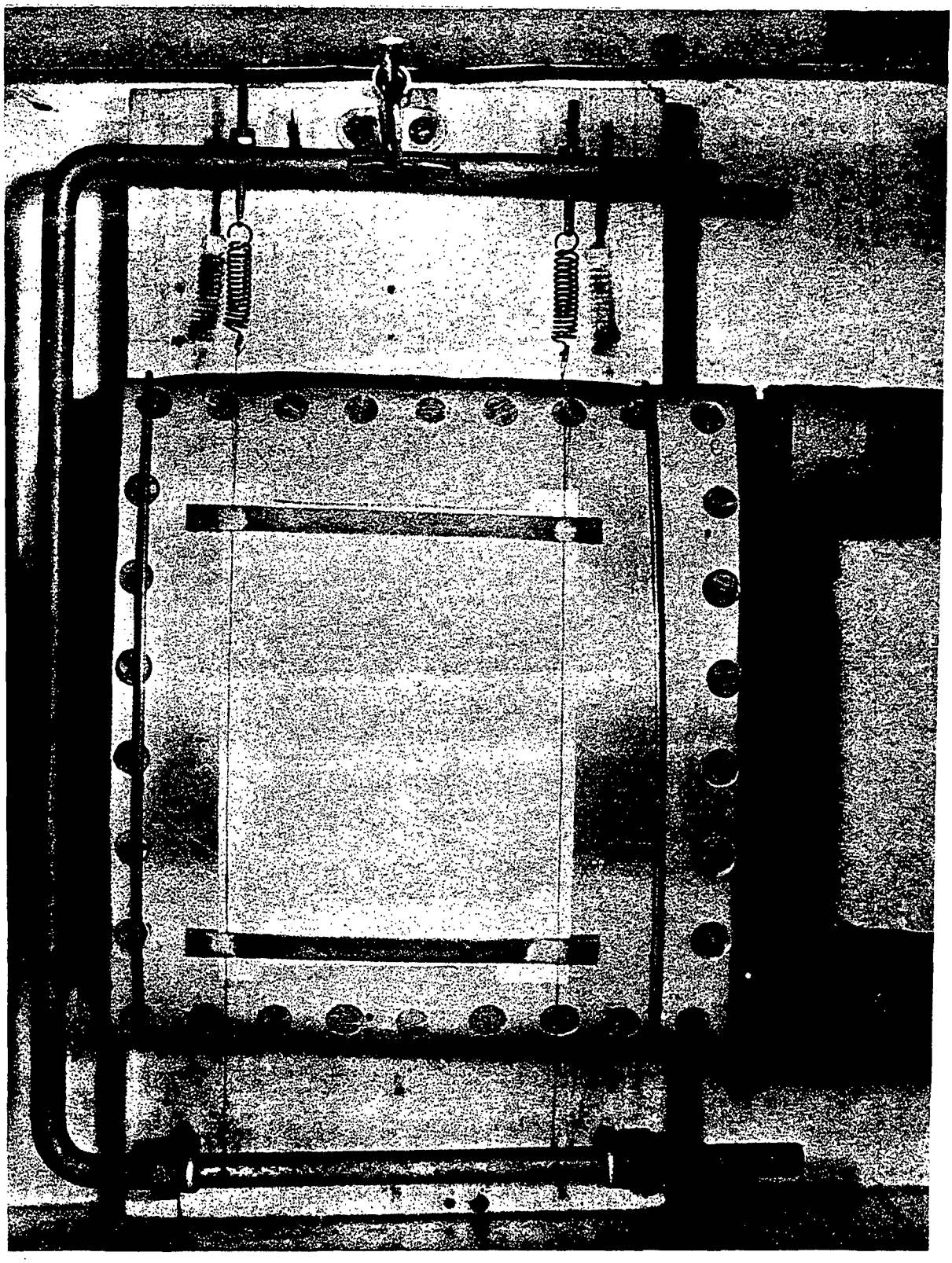

Figure 6. Top View of Hot-Surface Unit

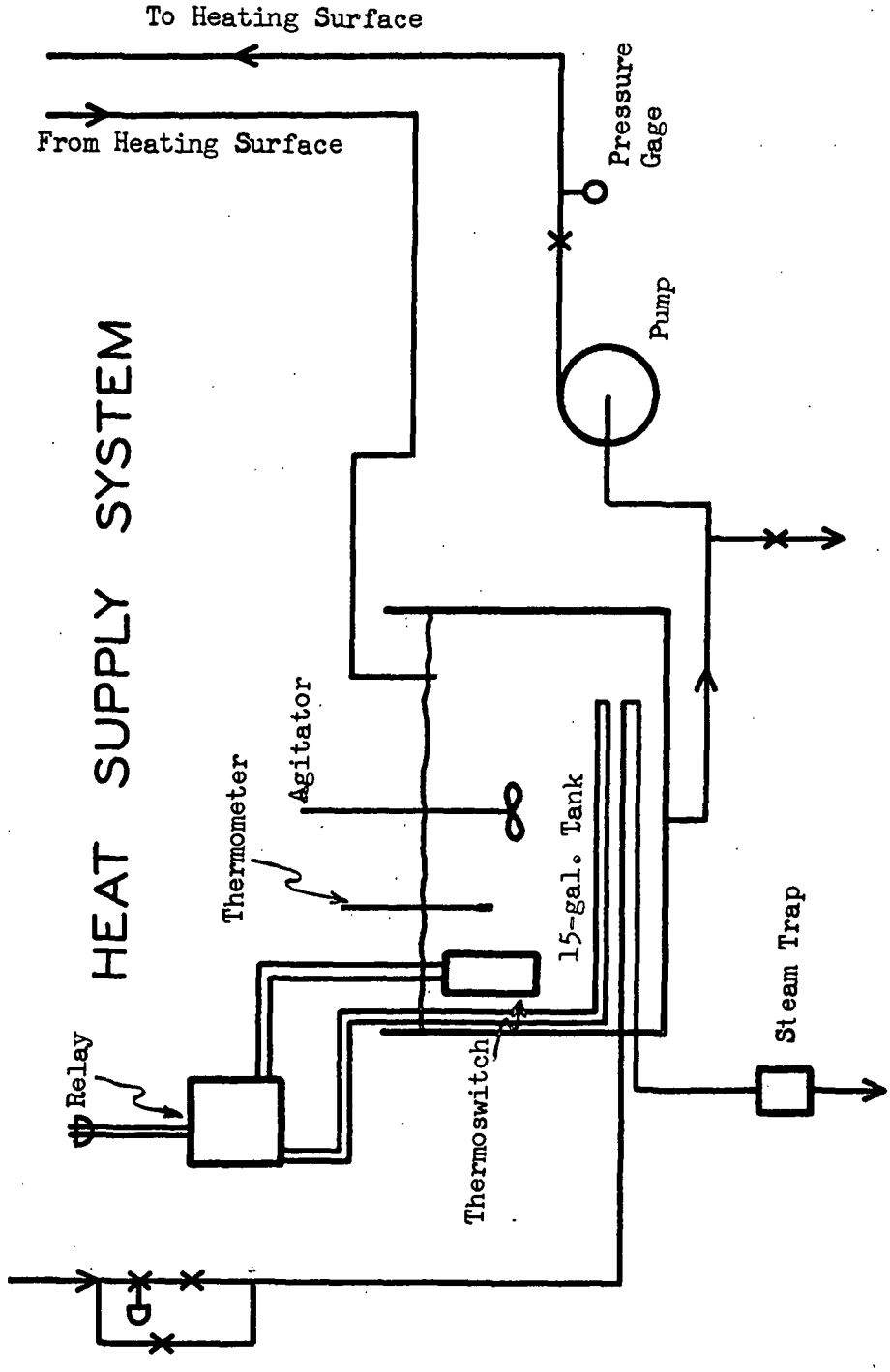

Figure 7. Schematic Diagram of Heating System

The tank contains 3 feet of 1/4-inch iron pipe with a steam trap on one end. High pressure steam can be admitted to this pipe for rapid warmup of the fluid; throttled steam can be admitted so that the electric heater supplies only part of the total load during operation. The liquid in the tank is kept in vigorous agitation by a 1/20-horsepower stirrer.

Clamping of the sheet is accomplished by the removable C-frame which is shown in Figures 5 and 6. This has two 0.01-inch wires attached to it 2.38 inches apart. Two pieces of 1/16-inch thick by 3/16-inch wide by 3 inches long brass stock are soldered to them with the inside edges 3 inches apart. These pieces of stock are slightly bent with the ends up. The pressure exerted by this unit is adjusted by adjusting the tension on the springs which connect the front end of the wires to the front of the C-frame.

The frame is held in the tunnel by two hookeyes mounted on the wooden base behind the hot plate and by a snap latch mounted on the wooden base in front of the hot plate. The hookeyes have been partly cut away so that the C-frame can be inserted and removed from them.

Figure 8 is a schematic diagram of the apparatus for measuring and recording the rate at which beta radiation is coming from the sheet. This will subsequently be referred to as a "beta gage." Considerations leading to the selection of this apparatus are discussed in Appendix 1. A is the source of radiation, thallium 204. It is either mounted on the hot surface or within sheets being dried by the techniques described in the Experimental Procedures. B is a scintillation head, Tracerlab Model P20-A, a device for detecting beta radiation and converting each beta ray

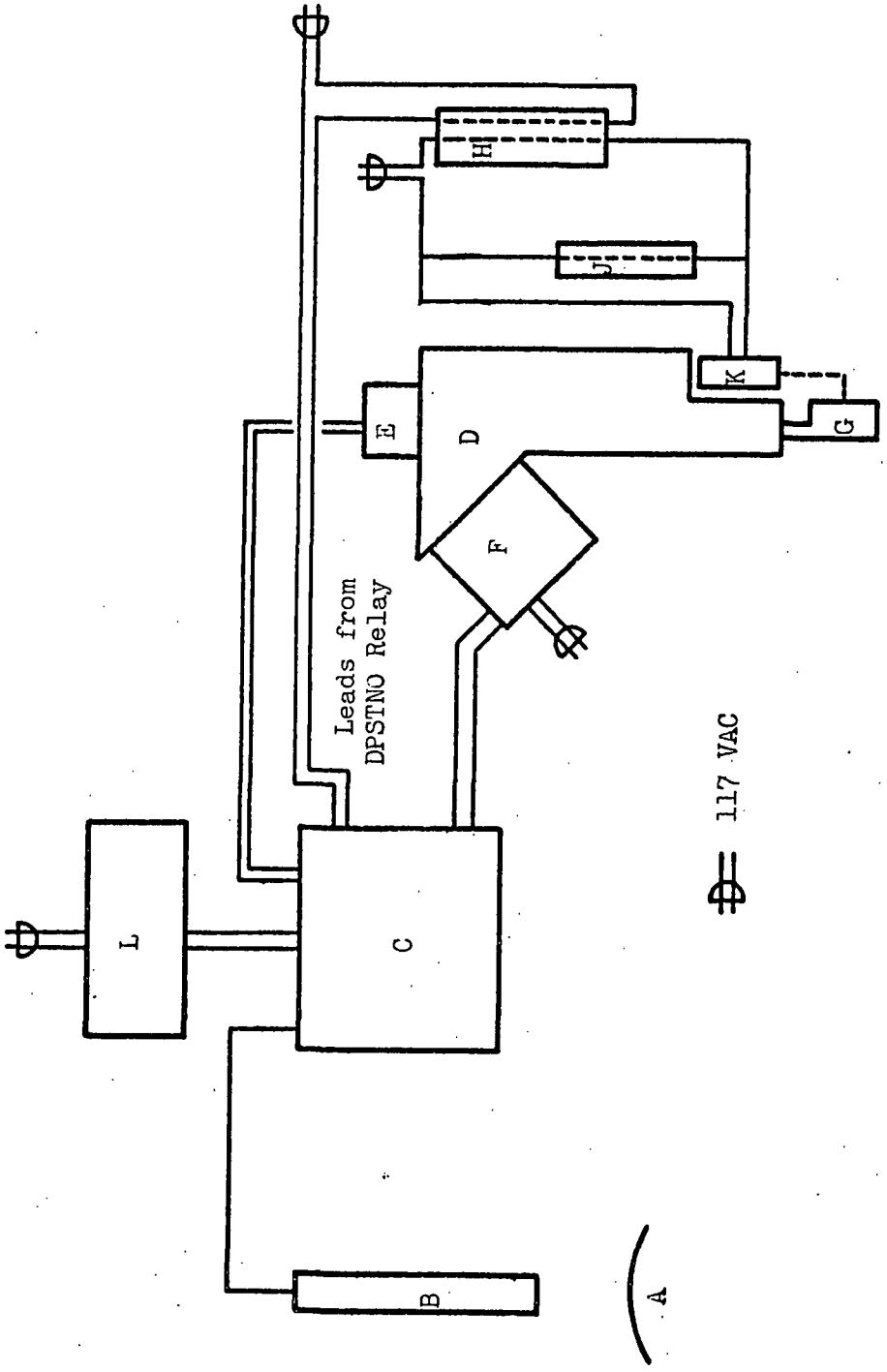

Figure 8. Schematic Diagram of Beta-Gage

above a minimum energy level to an amplified electric pulse. C is an electronic scaler, Tracerlab Model SC-51 containing Model SC-41A decade scaling units. This device supplies necessary power to the scintillation head, and it amplifies the pulses from the scintillation head, counts them, and exhibits the total number. For this work, the scaler has been equipped with a double-pole, (DPSTNO) relay which is momentarily closed every time a preselected number of counts is scaled. D is a light-tight box. Timer E, which has a 1-second full-sweep hand and a 1-minute full-sweep hand, is mounted facing into the box. Strobotac F is mounted so as to illuminate the clock face. G is a 16-mm. camera facing clock E. This camera has had its shutter removed and has been so modified that activating the firing button advances the film one frame. It contains a +2 closeup attachment over the lens. Eastman Super-XX film is used at f-4.5. H is a power relay, and J is a spark-quenching circuit consisting of a 20-ohm power resistor and a 450-microfarad paper capacitor connected in series. K is a solenoid connected by a spring to the firing button of the camera. L is a Sorenson voltage regulator which supplies power to the scaler.

Operation of the unit is as follows: With the scaler on Manual and the Count Selector on 10,000, the timer starts when the scaler is started. When 10,000 counts have been collected on the scales, the scaler resets to zero and momentarily closes the relay which has been built into it. One set of contacts fires the Strobotac, illuminating the clock face. Since the camera contains no shutter, this yields a picture of the clock showing the timer reading when 10,000 counts were reached. The other set of contacts closes power relay H. This energizes solenoid K, advancing the camera one frame and making it ready for the next picture. The

mechanical delay of the solenoid assures that the picture will be taken before the film in the camera begins to move.

After the film has been developed, fixed, washed and dried, it is conveniently read on a microfilm reader. The actual clock reading is the elapsed time since the start of scaling; the difference between successive readings is the time required for 10,000 counts to have been received at the detector. This is the reciprocal of the rate of beta-ray reception at the detector.

For steady-state work, the power relay operating the camera is removed and an electromechanical register is connected in its place to totalize counts.

OVER-ALL DRYING-RATE STUDIES

EXPERIMENTAL PROCEDURES

PREPARATION OF A BETA-RAY SOURCE

To study the over-all drying rate of sheets, it was necessary to have the source of radiation below the sheet and the radiation detector above. To obtain reproducible contact at the hot-surface interface of the sheet, it was desirable to have the radioactive source fixed to the hot surface rather than to deposit the radioactive source on the bottom of every sheet to be dried.

To do this, the source of radiation (thallium 204) was affixed to a thin sheet of aluminum foil, and the foil was pulled and held taut on the hot surface with the radioactive material beneath it. Appendix III describes the experiments conducted to establish a suitable procedure for depositing the radioactive source and the details of the procedure used.

CALIBRATION OF THE BETA-RAY SOURCE

As used in this thesis, the "calibration curve" for the beta gage with any source refers to the relation between mass per unit area of the material between the source and the detector and the transmission of beta rays of that material. Transmission is the ratio of the number of counts per unit time received when the material is between the source and the detector to the number of counts per unit time received when the material is absent.

There are several factors which affect the calibration curve observed. These, and any factors which affect the counting rate observed, must be kept constant throughout the work. A discussion of these can be found in Appendix IV. Appendix I contains a brief discussion of the characteristics of beta radiation and its interaction with matter and of instruments used for radiation detection and measurement. Details of the calibration procedure, calibration data, and a sample calculation of a calibration point are found in Appendix IV.

The calibration curve for pulp was obtained by determining the beta-ray transmission of a series of dry sheets. The mass per unit area of the sheets was obtained by weighing and measuring each sheet.

The calibration curve for water was obtained by first preparing a series of wet sheets containing various amounts of water. These sheets were wrapped in aluminum foil to prevent evaporation during use. The beta-ray transmission of the wrapped wet sheets and of the dry sheets was determined. The weight of the wrapped wet sheets, the wrapper, and the dry sheets was determined. The mass per unit area of the dry sheets was determined. From these data, the beta-ray transmission of the water in each sheet and the mass per unit area of water in each sheet was calculated.

PREPARATION OF SHEETS

All sheets were made in a British sheet mold from lightly beaten bleached sulfite pulp. The sheets were couched from the wire directly onto a clean sheet of 0.0015-inch aluminum foil. This foil was subsequently placed in intimate contact with the hot surface; in this manner the contact between the hot surface and the sheet was reproducible.

The sheets were pressed; then samples for drying studies were cut from them. These samples were air dried to the desired wet weight and were sprayed with a little starch. The starch served to keep the sheet in contact with the aluminum foil throughout the entire run; without the addition of starch, sheets tended to cockle and pull away from the foil at the end of the constant-rate period. Appendix V contains details of the sheet preparation procedures.

PROCEDURE FOR DRYING RUNS

The C-frame shown in Figure 6 was used to insert and clamp the sheet onto the hot surface. A tab 2 inches long by 0.2-inch deep was cut in each end of the sheet. The sheet was centered beneath the wire and shims with the aluminum foil down, and the tabs were folded over the shims. This served to hold the sheet on the frame.

Before each run, a piece of Masonite with the date and run number chalked onto it was put into the light-tight box over the clock face and photographed. It was then removed, and the timer and the scaler were reset to zero. The sheet, mounted on the C-frame, was inserted into the tunnel, care being exercised to touch neither the hot surface nor the scintillation head. The back end of the C-frame was engaged into the hookeyes and the front end pulled down to engage the snap-latch. The scaler was started and the tunnel door closed. Operation for the remainder of the run was automatic as given in the description of the apparatus.

After a little practice, the insertion procedure could be conducted with about 5 seconds of air drying and 1-2 seconds of hot-surface drying before the scaler was started.

EXPERIMENTAL RESULTS

ACCURACY AND REPRODUCIBILITY

The circular points of Figure 9 show the relationship which was found between mass per unit area of pulp and water and beta-ray transmission of pulp and water by the calibration procedure. The relationship was nearly linear on semilogarithmic axes, indicating that the assumption of exponential absorption of radiation, i.e., $\ln T = - \mu_a x$, made for purposes of preliminary design calculations, was a reasonable approximation. Appendix I contains an outline of these calculations.

From the slopes of the curve for water of Figure 9, it is calculated that the apparent absorption coefficient, μ_a, varied from 0.021 $(mg./cm.^2)^{-1}$ at 0 $mg./cm.^2$ of water to 0.031 at 60 $mg./cm.^2$ of water. Each raw datum point on a drying curve is obtained from 10,000 beta emissions received at the radiation detector. As discussed in Appendix I, each datum point, therefore, has a standard deviation of 1% transmission. Thus, the standard deviation of a point ranged from 0.32 $mg./cm.^2$ when the maximum amount of water was present to 0.48 $mg./cm.^2$ as a sheet approached dryness. The accuracy of the line faired through the data points for each run is somewhat better than that indicated by the standard deviation of a single point on it, depending upon the rate of drying and the number of points obtained. The standard deviation values can therefore be considered as a conservative estimate of the expected reliability of the data.

An experimental check of the accuracy of the sheet preparation work was obtained by calculating the initial beta-ray transmission of the wet sheets and the beta-ray transmission of the dry sheets. The intended

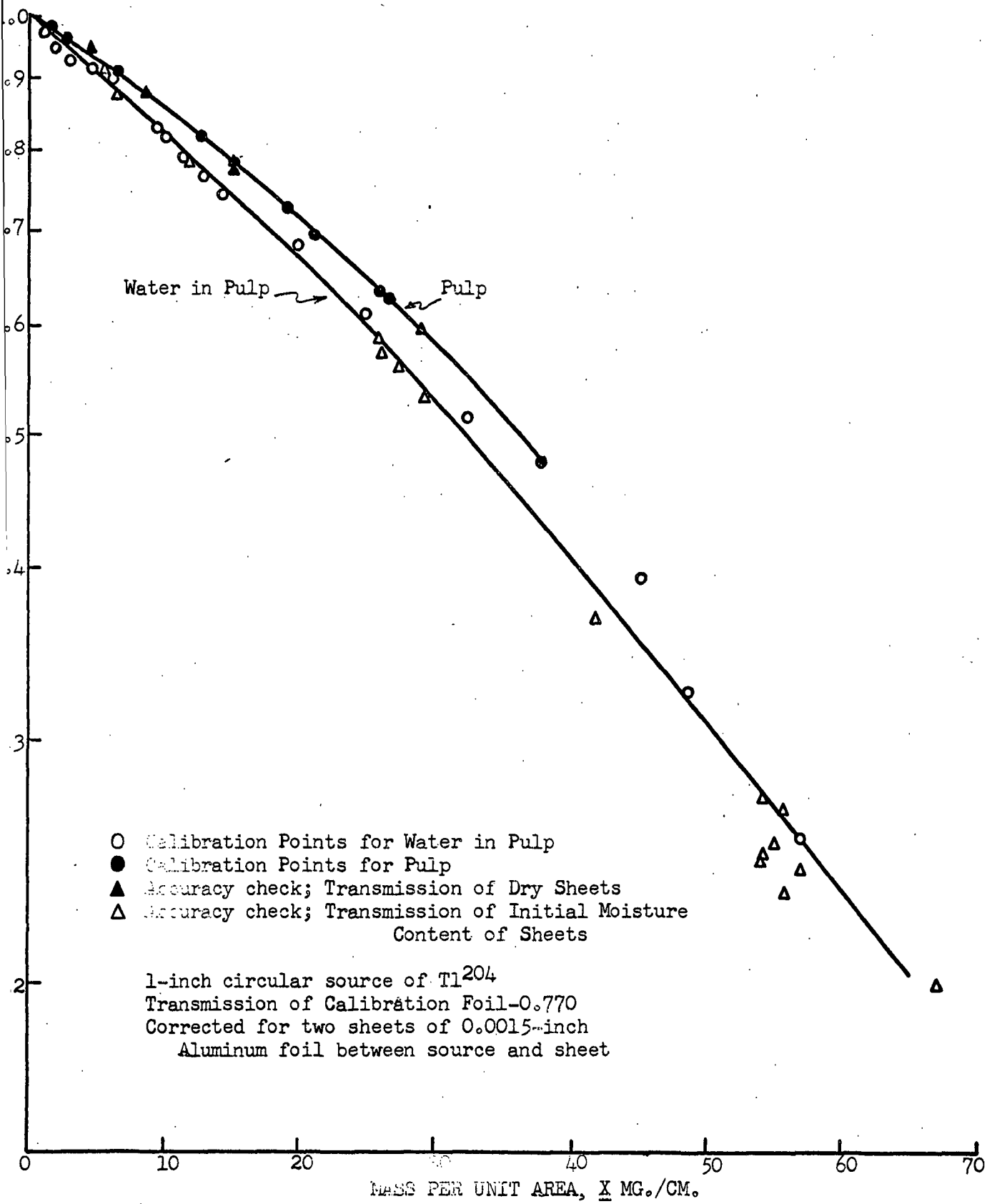

Figure 9. Calibration Curve and Accuracy Check of Beta Gage

initial mass per unit area of water and dry basis weight of the sheets were known. If all the work were correct, each transmission value, when plotted against the appropriate mass per unit area, should fall on the calibration curve, Figure 9. The actual points calculated in this fashion are shown in Figure 9.

The agreement for the dry sheets was very good, the maximum observed deviation being less than ± 1 mg./cm.^{2} and less than this for lighter sheets. Such deviations can be expected as variations in the sheets.

The accuracy of the initial moisture content determination of the sheets was not as good. The maximum deviation observed was 4.5 mg./cm.^{2} and the average deviation was about 1/3 of this. This is explained from the fact that sheets were brought to known initial total weight. Any variations in the dry basis weight of the sheets or the area of the sheets would be reflected as variations in the initial mass per unit area of water in the sheets. Any variations in moisture loss between the time the sheets were weighed and the time the scaler was started would also be reflected as scatter in the initial moisture content of the sheets.

The reproducibility of drying data is shown in Figure 10. The data points shown are those calculated by subtraction of successive frame readings of the film for each run. The data for Run 169A are tabulated in the sample calculations; for the other runs, the faired values of these curves are tabulated in Table XIX. The data points plotted are recorded in Research Notebooks 1387 and 1414 of The Institute of Paper Chemistry. These data were actually obtained for a check of artifacts introduced by the lamination procedure, and as such will be referred to again. They

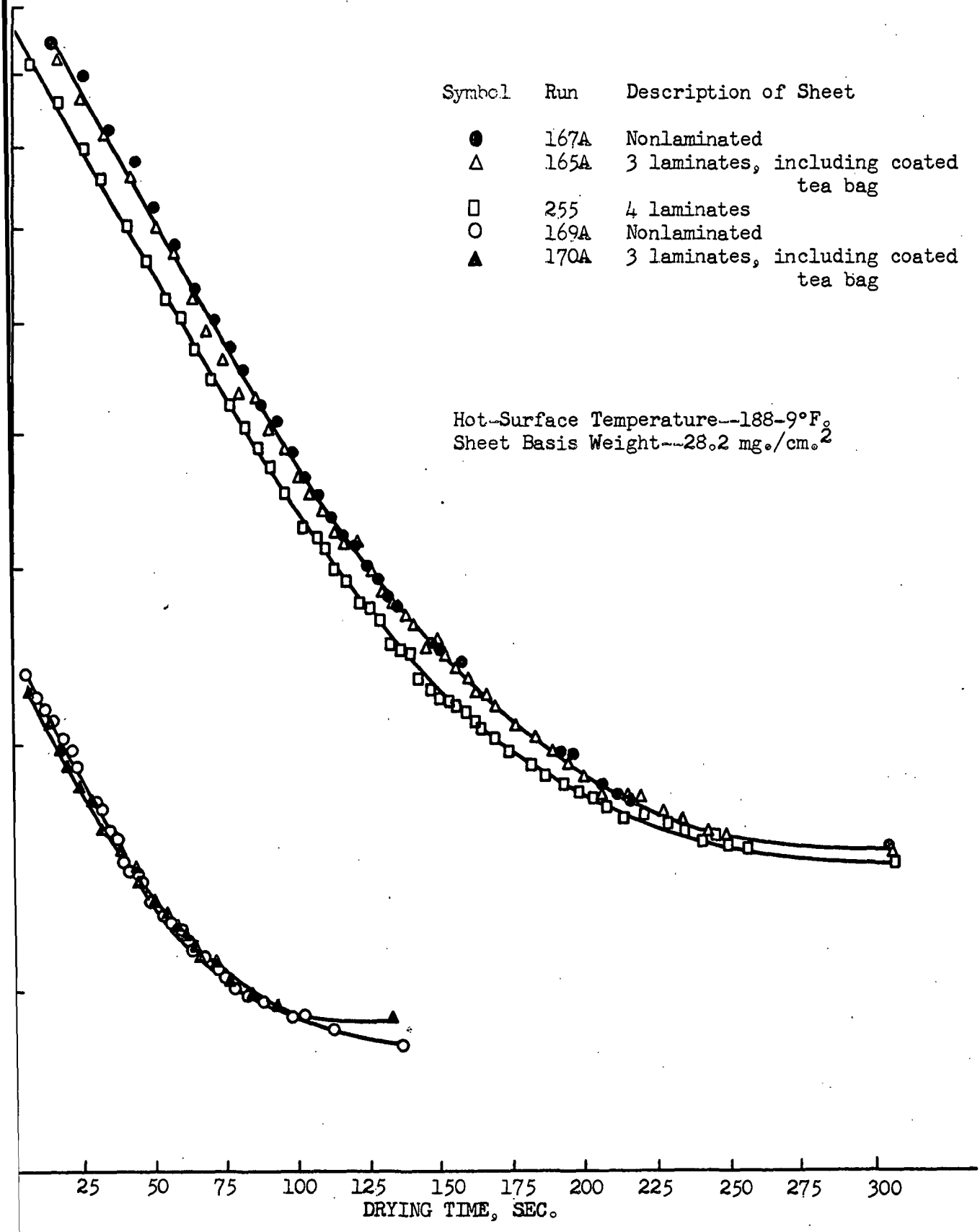

Figure 10. Transmission Curves for Over-all Drying

also serve to show that drying rates can be closely reproduced. The replicate constant-rate drying rate for all sheets of given dry basis weight containing a laminate with up to 30% resin on it agreed to within 2%. The fact that the curves do not cross one another during the constant-rate drying period is evidence that the scatter observed in the zero-time transmission data shown on Figure 9 was actually caused by the differences in initial moisture content. The reproducibility of constant-rate drying rate is evidence that reproducible contact between the sheet and the hot surface was being attained.

There are then two major factors limiting the range of sheet basis weight and drying rate which can be studied with the present apparatus and technique. The first is the limitation imposed by emission statistics and beta-ray absorption. As discussed previously, the precision with which the moisture content at any time during a drying run is known is about ± 0.5 mg./cm.^{2} for a light sheet. For example, for a sheet of 5 mg./cm.^{2} basis weight, this corresponds to $\pm 10\%$ moisture content. In Figure 11, which shows the drying curves for a series of sheets dried at 190°F., the size of the calculated points shown gives visual evidence of the precision imposed by emission statistics. It was impossible to obtain sufficient precision, for example, to state whether or not the constant-rate drying rate of the 3.5 mg./cm.^{2} sheet was greater than that of the 7.1 mg./cm.^{2} sheet. As discussed in Appendix 1, a less energetic beta emitter such as calcium 45 could be used to obtain increased precision for light sheets.

The second factor limiting the useful range of study is the reproducibility of start-up and handling procedures. Referring to Figure 11 or

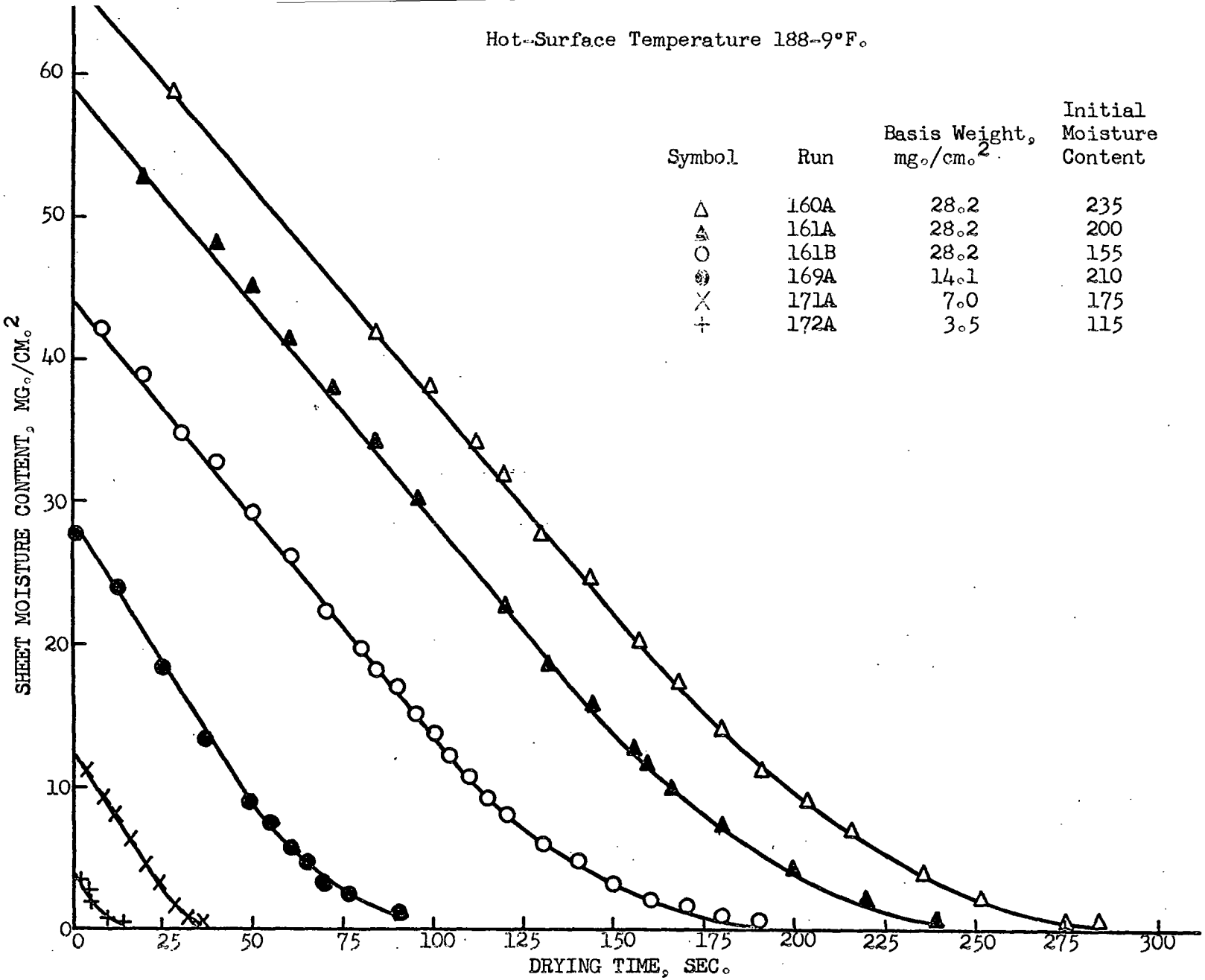

Figure 11. Over-all Drying Curves for Sheets

Table I, the constant-rate drying rate for a 3.5 mg./cm.^{2} sheet dried at 190°F. was 0.45 mg./cm.^{2} sec. The time that the sample was on the hot surface before the scaler was started was 1-2 seconds, corresponding to a moisture loss of 0.45 to 0.90 mg./cm.^{2}, or from 15 to 30% moisture content. Thus, a more rapid and reproducible means of starting a drying run would be required for a study of lighter sheets.

Calculations using the mass-transfer coefficient obtained by Higgins (1) indicate that the rate of air drying in the tunnel was less than 0.01 mg./cm.^{2} sec., so that less than 0.05 mg./cm.^{2} of water was lost from the time that the sheet was inserted into the tunnel until the time that it was placed in contact with the hot surface. This is negligible for all sheets studied in this work, but it could become a factor of importance in the study of very light sheets.

CHARACTERISTICS OF OVER-ALL DRYING CURVES

As shown in Figure 11, the drying of each sheet studied consisted of two periods. During the first, the rate of drying was constant. At some value of the moisture content, the rate of drying began to decrease. Thus, the typical behavior consisting of a constant-rate period, a critical moisture content, and a falling-rate period has been found. It should be noted that the rate of change of drying rate at the critical moisture content was small; the critical moisture content was, therefore, difficult to determine with accuracy.

Some investigators (14, 15) have detected an initial heating period at the beginning of a drying run, during which the rate of drying was increasing. Such a period existed in the sheets studied in this work, but it was of too short a duration to be detected.

TABLE I

SUMMARIZED OVER-ALL DRYING DATA

1-in. Circular Thallium Source
Air: 95°F. Dry Bulb
79°F. Wet Bulb
250 f.p.m.

Run	Circulant[1] Temp., °F.	Dry Sheet Basis Wt., mg./cm.^{2}	Initial[2] Moisture Content, %	Constant-Rate Drying Rate, mg./cm.^{2} sec.	Critical Moisture Content, % Dry Wt.
162B	170	28.2	200	0.214	60
172B	170	3.5	200	0.40	40
160A	190	28.2	235	0.296	55
162A	190	28.2	210	0.299	50
161B	190	28.2	155	0.302	40
169A	190	14.1	200	0.395	55
171A	190	7.0	175	0.41	25
172A	190	3.5	115	0.45	35
168B	210	28.2	195	0.355	70
167B	230	28.2	195	0.45	95
169B	230	14.1	185	0.58	55
171B	230	7.0	145	0.68	30

[1] Water for temperatures up to and including 190°F., ethylene glycol for temperatures above 190°F.

[2] Estimated from drying curves

CALCULATION OF HOT-SURFACE TEMPERATURE

With the apparatus and techniques used for this work, the basic temperature measurement made is that of the fluid circulated beneath the hot surface. The precision with which the thermometer was read was about 1/2°F. Conditions were such that the temperature drop of the fluid from the time it left the reservoir until the time it returned to the reservoir was less than 0.1°F., a negligible amount.

Between the bulk of the circulating fluid and the interface of the sheet in contact with the aluminum foil, there are several thermal resistances which must have a temperature differential when heat is transferred across them. First, there is the film resistance of the fluid, which causes a temperature drop between the bulk of the fluid and the interface of the aluminum plate with the fluid. Next, there is the aluminum plate itself. Above the plate, there are two sheets of aluminum foil, the one containing the source of radioactivity and the one onto which the wet sheet was couched. While the thermal resistance of the foils is negligible, there are three interfaces between the aluminum plate and the sheet at which air may be entrapped and through which heat must be transferred.

There are three separate temperatures related to the hot surface which are to be differentiated. The first is the measured temperature, the bulk temperature of the circulating fluid. The second is the temperature at the outer surface of the aluminum plate, the hot-surface temperature. The third is the temperature at the surface of the sheet which is in contact with the aluminum foil. This will be designated as the "hot-surface interface temperature."

The hot-surface temperature equals the temperature of the circulating fluid less the temperature drop between the body of the fluid and the hot surface. This temperature drop Δt, °F. can be calculated from the heat-transfer coefficient, U, B.t.u. /(hr.)(ft.^{2})(°F.), and the rate of heat transfer, q/A (B.t.u./hr. ft.^{2}), by the equation $\Delta t = (1/U)(q/A)$.

The over-all heat-transfer coefficient, U, is calculated from the relation $(1/U) = [(1/h_f) + (X/k)]$, in which

h_f = heat transfer coefficient for fluid, B.t.u./(hr.)(ft.^{2})(°F.)

X = thickness of aluminum plate, ft.

k = thermal conductivity of aluminum plate, B.t.u./(hr.)(ft.)(°F.).

The heat-transfer coefficient for the circulating fluid, h_f, was calculated as a function of the fluid properties and flow conditions by the Colburn correlation for forced convection in tubes, given by Perry (36), p. 468, Figure 8. For water at 190°F., this was 1650 B.t.u./(hr.)(ft.^{2})(°F.). For pure ethylene glycol, the respective coefficients at 190 and 230°F. were 280 and 370, respectively. X and k respectively were (3/16 by 12) ft. and 119 B.t.u./(hr.)(ft.)(°F.). From these values, U was calculated for the various runs. (q/A) was calculated from the heat of vaporization required for the constant-rate drying rate in each run. Thus, Δt was calculated from each run. With water circulating, this temperature drop was always between 1 and 2°F. For glycol, it ranged from 7 to 13°F. from the slowest to the fastest drying rate found. The temperature drop calculated for each run was subtracted from the fluid temperature for each run to give the hot-surface temperature during the constant-rate portion of the run, the value tabulated in Table II.

TABLE II

CALCULATED INTERFACE TEMPERATURES AND HEAT-TRANSFER COEFFICIENTS* OF SHEETS

Run	Circulant Temp., °F.	Circulant	Basis Weight of Sheet, mg./cm.^{2}	Constant-Rate Drying Rate lbs./(hr.)(ft.^{2})	Hot Surface Temp., °F.	Air-Interface Temp., °F.	Heat Transfer Coefficient, Btu/(hr.)(ft.^{2})(°F.)*
162B	170	H_2O	28.2	1.51	169	137	51
172B	170	"	3.5	3.00	168	154	225
162A	190	"	28.2	2.21	189	147	55
169A	190	"	14.1	2.88	188	153	87
171A	190	"	7.0	3.00	188	155	95
172A	190	"	3.5	3.30	188	158	110
168B	210	Glycol	28.2	2.62	202	151	54
167B	230	"	28.2	3.33	221	158	56
169B	230	"	14.1	4.28	219	164	82
171B	230	"	7.0	5.00	217	169	110
206	190	"	28.2	1.89	183	143	50
207	190	"	28.2	1.91	183	129	37
McCready	176	---	145	0.92	176	135	23

* From hot surface to air interface of sheet.

The values of h calculated from the Colburn correlation could be in considerable error, since flow conditions within the hot plate are undoubtedly not identical to those in a tube. End effects may also be significant. Furthermore, the glycol used contained a little water; this would tend to have a higher heat-transfer coefficient than would pure glycol, upon whose properties the calculated coefficient was based.

The calculated values of hot-surface temperature are used in Figure 12. From this figure, it can be seen that the lower drying rate observed for a 28.2 mg./cm.^{2} sheet dried with 190°F. ethylene glycol circulating as compared with 190°F. water circulating is predicted within experimental accuracy by the lower temperature of the hot surface when glycol was circulating. This is evidence that the calculated values of hot-surface temperature given in Table II are of satisfactory accuracy.

EFFECT OF VARIABLES ON OVER-ALL RATE OF DRYING

Tables I and III are a summary of the data which have been obtained for the over-all drying rate of sheets. The constant-rate drying rate at a given temperature was independent of the initial moisture content within experimental accuracy, but the critical moisture content appeared to be slightly higher for sheets of higher initial moisture content. The constant-rate drying rate increased with decreasing basis weight, at least down to a dry basis weight of 7 mg./cm.^{2}. The short time of a run (about 8 seconds of constant-rate drying for the 3.5 mg./cm.^{2} sheet at 190°F.) combined with the inherent statistical limitations previously discussed make it impossible to be certain whether or not a sheet of 3.5 mg./cm.^{2} basis weight was drying faster than one of 7 mg./cm.^{2} at 190°F. Figure 13 shows the effect of basis

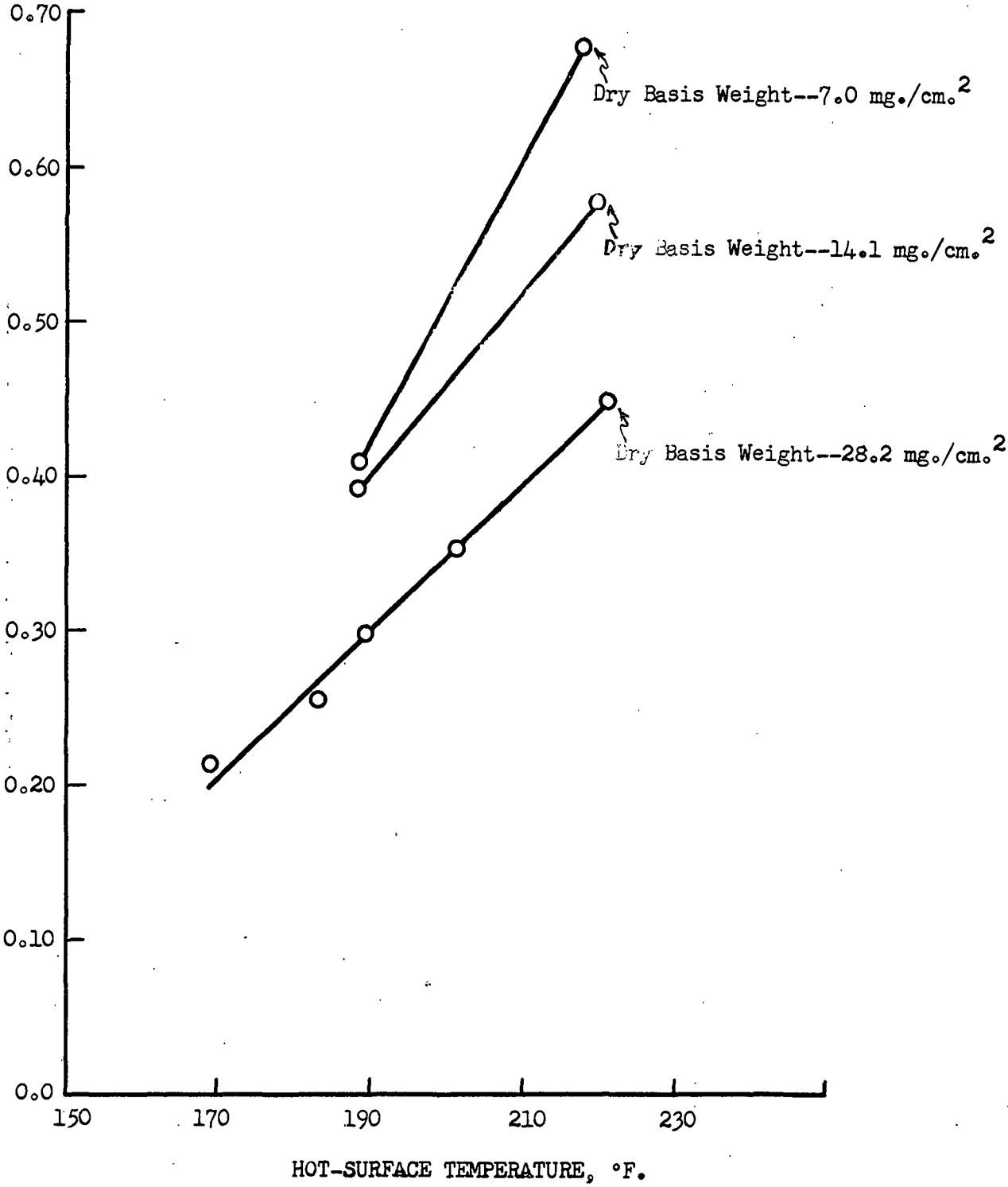

Figure 12. Effect of Hot-Surface Temperature on Constant-Rate Drying Rate of Sheets

TABLE III

CONSTANT-RATE DRYING RATE OF 28.2 MG./CM.^{2} SHEETS DRIED AT 190°F.*

Run	Circulant	Air Dry-Bulb Temp., °F.	Air Wet-Bulb Temp., °F.	Air Velocity, ft./min.	Source of Radio-activity	Constant-Rate Drying Rate, mg./cm.^{2} sec.
162A	Water	95	79	250	1-inch circle mounted on hot-surface	0.299
255	Water	85	70	250		0.301
206	Glycol	85	70	250		0.256
208	Glycol	95	79	250	"	0.256
207	Glycol	95	79	435	"	0.260
205	Glycol	85	70	250	2.37 x 3-inch imbedded in sheet at hot-surface.	0.248

* All initial moisture contents were approximately 200%.

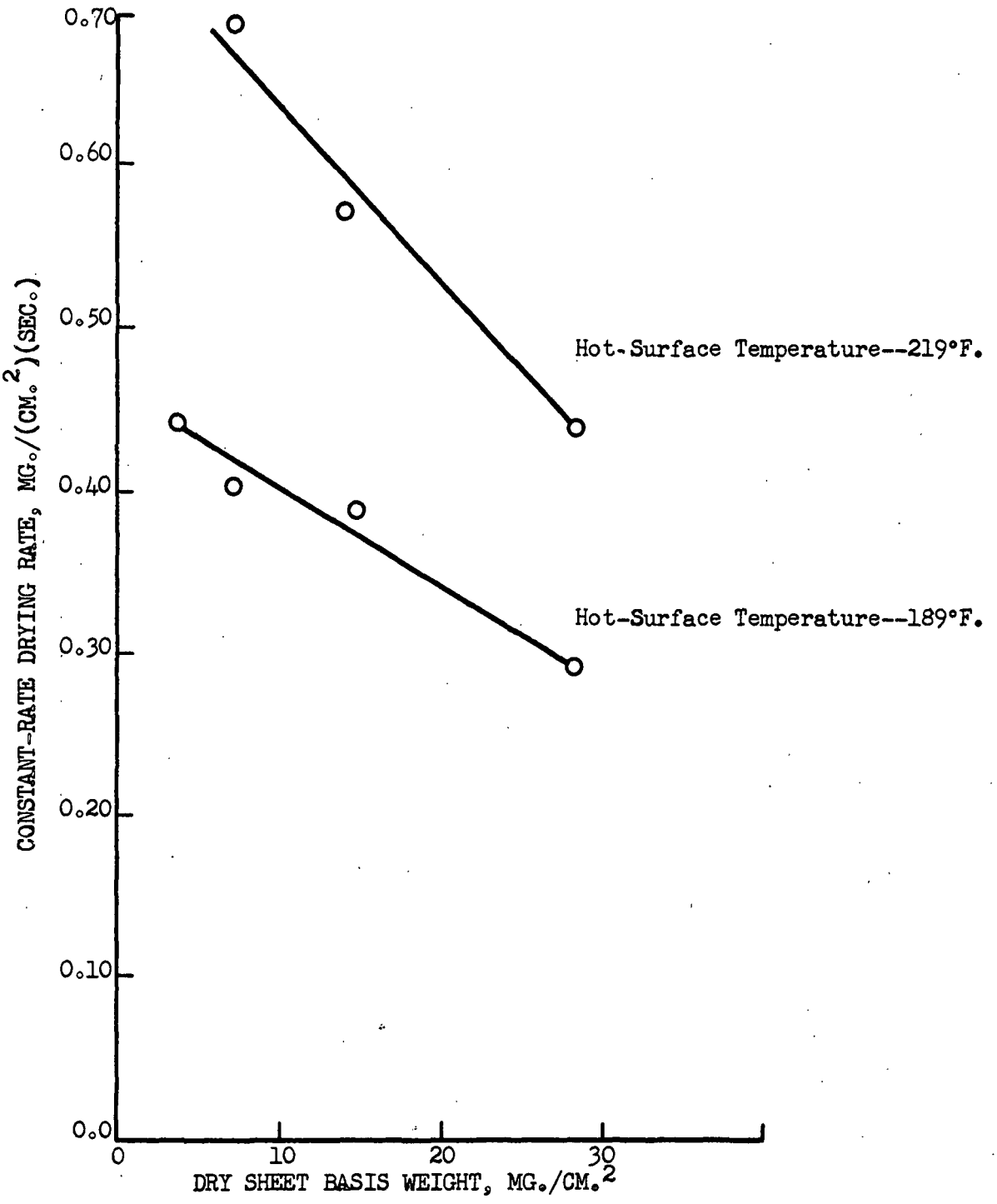

Figure 13. Effect of Dry Sheet Basis Weight on Constant-Rate Drying Rate

weight on constant-rate drying rate for two temperatures of the hot surface. Figure 12 was used to connect runs to the temperatures shown from the slightly different actual temperatures.

Figure 12 shows the effect of hot-surface temperature on drying rate. The drying rate increased as the temperature of the hot surface increased.

In Table III data are shown which indicate the effect of air conditions on drying rate. A 10°F. change in the air temperature had no measurable effect on the drying rate. Increasing the air velocity from 250 to 435 f.p.m. caused only a slight increase in drying rate.

Experimental accuracy does permit meaningful calculation of critical moisture content for 3.5 mg./cm.^{2} sheets. For sheets 7.0 mg./cm.^{2} and greater, critical moisture content increased with increasing sheet basis weight and increasing hot-surface temperature.

It is of interest to compare these data with those obtained by McCready (19), who dried thicker laps of pulp under similar experimental conditions. Both sets of data indicate that drying rate increased with the temperature of the hot surface. McCready's constant-rate drying rate values ranged from 0.12 mg./cm.^{2} sec. at 176°F. to 0.33 mg./cm.^{2} sec. at 248°F. These are lower than corresponding rates found in this work, which is in accordance with the finding that constant-rate drying rate decreased as basis weight increased.

Both sets of data also indicate that the critical moisture content increased with temperature. McCready's data on the effect of basis weight on critical moisture content are inconclusive, the probable reason being

that his slabs were brought to controlled initial thickness rather than basis weight and that his initial moisture contents were apparently not controlled. However, all his critical moisture contents are much higher than those found here, which is in agreement with the observation that critical moisture content increases with increased basis weight. In general, then, the behavior of sheets in the two sets of experiments is similar.

CALCULATED AIR INTERFACE TEMPERATURE

As discussed previously, McCready has presented data and calculations which indicate that the partial pressure of water vapor leaving the sheet was the equilibrium pressure for water at the temperature of the air interface. McCready did not present sufficient data to correlate the mass-transfer coefficient at the air interface with the properties of the circulating air. Higgins (1) has done this for the air drying of paper, and his results are shown in Figure 1. Perry (36, pg. 542) presents the generalized Chilton-Colburn correlation for heat and mass transfer. From the air conditions in the duct, either of the correlations may be used to calculate the mass-transfer coefficient for water vapor moving from the surface of the sheet to the air stream. The corresponding mass-transfer equation may then be used to calculate the partial pressure of the water vapor at the surface of the sheet. Assuming saturation equilibrium at the air interface, the corresponding temperature of the sheet at the air interface is determined.

Higgins' correlation is based on the equation

$$(\underline{dW/A}\ \underline{d\Theta}) = \underline{K}(\underline{H_{ai}} - \underline{H_a}).$$

($\frac{dW}{A\ d\theta}$) is the constant-rate drying rate of the sheet, lbs./hr. ft.^{2}. This value is determined from the drying curve for each sheet, and it is tabulated in Table II. K is the mass-transfer coefficient, lb./(hr.)(ft.^{2})(unit humidity difference). It is read from Figure 1 as a function of the air conditions in the duct. H_{ai} is the humidity of the sheet at the sheet-air interface, lb. water/lb. air. H_a is the humidity of the air in the duct.

This equation was solved for H_{ai} for each run listed in Table II. The temperature corresponding to the value of H_{ai} for each run was read from a table of the properties of saturated water vapor. These values are listed in Table II. Calculations using the Chilton-Colburn correlation have also been performed for Runs 162B and 171B, the slowest and fastest drying rates found in this work. The temperatures found by this method were respectively 1°F. less and 4°F. more than the temperatures calculated from Higgins' correlation.

Sensible heat transfer from the surface of the sheets to the air was calculated using the calculated air-interface temperatures given in Table II and heat transfer coefficients calculated from Higgins heat-transfer correlation and from the Colburn correlation. These heat-transfer coefficients agreed within 10%. The maximum sensible heat flux from the sheet to the air was 250 B.t.u./(hr.)(ft.^{2})(°F.), less than 8% of the rate of heat transfer required for vaporization in the same sheet. The average was about 5% of the rate of heat transfer required for vaporization.

CALCULATED HEAT-TRANSFER COEFFICIENTS

The heat-transfer coefficient between two planes is defined by the

equation $q/A = U(\Delta t)$, where

q/A = heat flux, B.t.u./hr. ft.^{2}

U = over-all heat-transfer coefficient, B.t.u./(hr.)(ft.^{2})(°F.)

Δt = temperature difference between planes, °F.

The temperatures of the hot surface and of the air interface of the sheet have been calculated and listed in Table II; Δt is the difference between these. (q/A) is the sum of the sensible heat flux to the air from the air interface and the heat flux required for vaporization of water during the constant-rate period. The latter is the product of the drying rate per unit area and the latent heat of vaporization.

The heat-transfer coefficient from the hot surface to the air interface has been calculated and is given in Table II. Figure 14 shows the calculated heat-transfer coefficient as a function of the dry basis weight of the sheet. The apparent heat-transfer coefficient definitely decreased as the basis weight of the sheet increased. The average heat-transfer coefficient obtained by Sherwood, Gardner, and Whitney (15) on a paper machine during the constant-rate period discussed earlier, falls close to these data when corrected for the area of the drums actually covered by the sheet. Estimates made by Montgomery (37) are also of the same order of magnitude.

The apparent thermal conductivity of the sheets was calculated as the product of the thickness of the sheet and the over-all heat-transfer coefficient. These values decreased with increasing sheet basis weight, ranging from 0.07 to 0.14 B.t.u./(hr.)(ft.^{2})(°F./ft.). The value for dry paper is given by Perry (36) as 0.075, the value for water as 0.39. The value calculated from McCready's data for his thick sheet was 0.43.

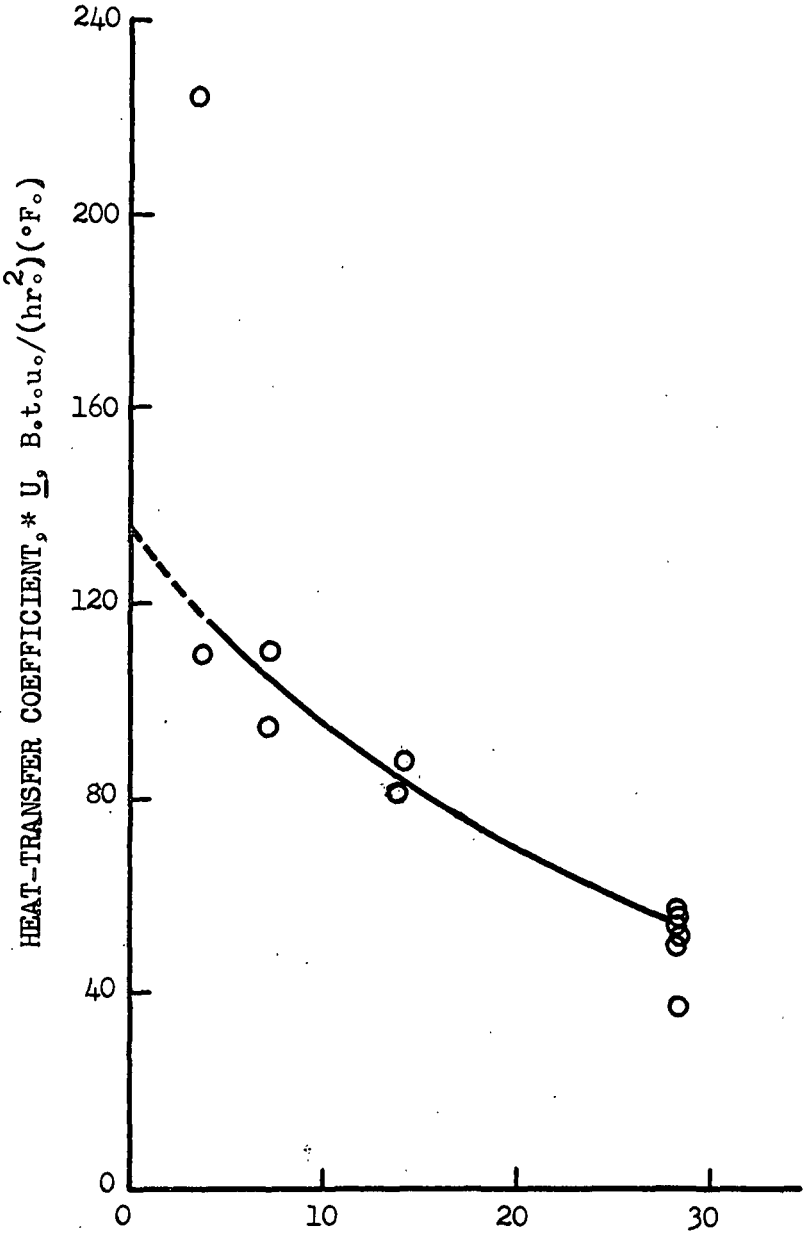

Figure 14. Calculated Heat-Transfer Coefficients

* From hot surface to air-interface of sheet.

McCready's value was based on measured temperatures at the top and bottom of the pad. The values calculated from the data of this thesis are based on the calculated temperature at the top of the sheet and the temperature of the hot surface. All air films at the hot surface are being included in the heat-transfer coefficient and thermal conductivity calculated. Air has a thermal conductivity of 0.018 B.t.u./(hr.)(ft.^{2})(°F./ft.) at 212°F. (36).

The surface of a wet sheet of paper is not smooth; high spots were therefore in contact with the hot surface, but low spots, such as area between fibers at the surface, were not. Thus, an effective air film occurred at the hot-surface interface. In addition, there was probably a small effective air film between the foil on which the sheets were couched and the hot-surface unit. Referring to Figure 14, the heat-transfer coefficient intercept at 0 sheet basis weight is about 145 B.t.u./(hr.)(ft.^{2})(°F.), though this value is obviously subject to considerable uncertainty. Using 0.018 for the thermal conductivity of air, the effective total air film at the hot surface was 0.0012 inches. This value would appear to be of a reasonable order of magnitude, being somewhat less than one fiber diameter.

In view of the assumptions required to calculate heat-transfer coefficients and the uncertainty of the extrapolation to determine the heat-transfer coefficient of the air film at the hot-surface interface, calculation of the true heat-transfer coefficient and the thermal conductivity of the sheets is not warranted. The air-film resistance was approximately 1/3 of the total resistance to heat transfer for the 28.2 mg./cm.^{2} sheets and an even greater fraction of the total resistance for lighter sheets.

The temperature drop across this resistance is the same fraction of the total temperature drop from the hot surface to the air interface. It is, therefore, certain that in no case did the average temperature of the sheet at the hot-surface interface reach 212°F. during the constant-rate period.

The procedure used to form and handle sheets gave reproducible results for constant-rate drying rate. Therefore, the air film, while representing an appreciable portion of the total resistance to heat transfer, was apparently constant in this work.

TRANSVERSE MOISTURE DISTRIBUTION DURING DRYING

PREPARATION OF SHEETS

To determine the transverse moisture distribution by the technique proposed, the source of radioactivity must be deposited in a plane within the sheet. A suitable method for doing this requires that the radioactive source be insoluble and firmly fixed at the desired plane of the sheet. This plane must be small both in thickness and basis weight compared to the sheet. The presence of the plane in which a source of beta radiation has been deposited must not affect measurably the distribution or the movement of moisture within the sheet during drying.

In the method finally adopted, the radioactive thallium was made insoluble by absorbing it on finely ground cation-exchange resin. This resin was affixed to a thin sheet of paper with a resorcinol-formaldehyde resin. The coated sheet was then wet pressed between two laminates made in the British sheet mold such that the composite sheet was of the desired total basis weight and contained the radioactive laminate at the desired depth. Development work leading to this technique and details of the procedure are given in Appendix VII.

The inclusion of a small amount of soluble dye (tartrazine) in the sheets proved to be of value. After a sheet had been dried, the presence of any delamination or air inclusion at the radioactive plane could be detected by delaminating the sheet and examining the interfaces for dye spots. Air inclusion at the hot-surface interface could be detected by examining that interface for spots lacking dye. Drying data were discarded from sheets in which either type of spot was found.

EXPERIMENTAL RESULTS

ACCURACY AND REPRODUCIBILITY

Since all sheets were brought to the same initial total weight, small differences in the area and basis weight of sheets caused small differences in initial moisture content of sheets in any given series being used to determine internal moisture distribution. Consequently, a small difference existed between the moisture contents of various sheets after drying for any given length of time. A correction of the drying curve of each sheet to that of a sheet having the average initial moisture content was required. Table I shows that the constant-rate drying rate was independent of initial moisture content within experimental accuracy, so the over-all drying curves were separated by a constant value of moisture content at any time of drying. The slopes of the lines in Figure 15 show that this was also true for the 40% fractional basis weight of the sheet, fractional basis weight in this thesis being measured from 0% at the air surface to 100% at the hot-surface interface. Thus, if the moisture content of a sheet is known, a correction of the drying curve of each sheet to the average drying curve for the series of similar sheets can be and was made by adding the initial difference in moisture content between that sheet and the average of the series to values obtained at other times during the drying run. The differences in critical moisture content caused by small differences in initial moisture content were less than the experimental accuracy with which critical moisture content could be determined. These differences were therefore neglected.

Figure 15 also shows data points for two pairs of duplicate runs. In no case was the discrepancy between the runs greater than 1 mg./cm.^{2}.

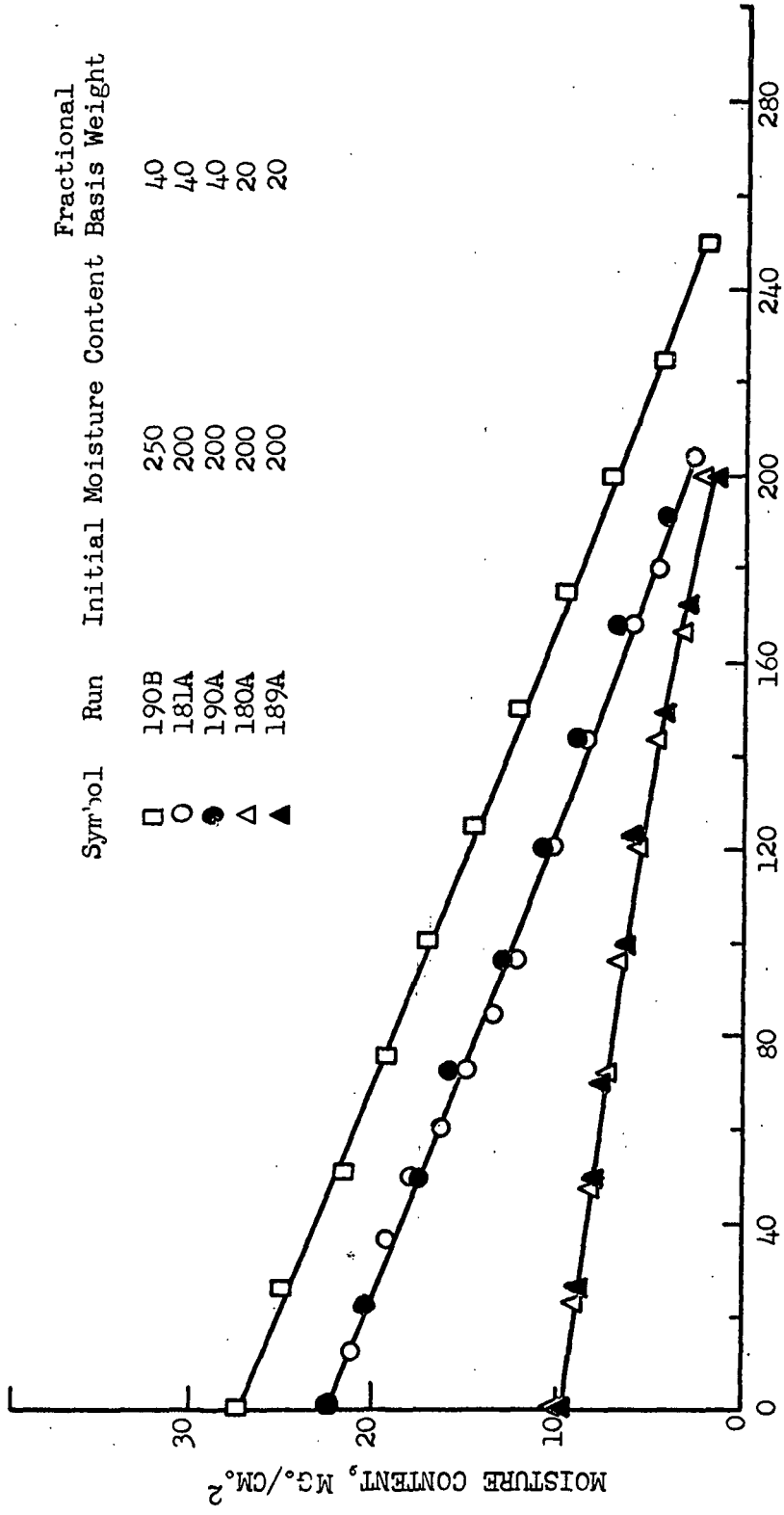

Figure 15. Drying Curves for Fractional Basis Weight of Sheets

Sheet Basis Weight--28.2 mg./cm.^{2}
Hot-Surface Temperature--183°F.

Another pair of duplicate runs (Runs 237 and 246) showed the same agreement.

The drying rate and critical moisture content of sheets were also functions of the dry basis weight of the sheets. The maximum variation from the average basis weight of any set of sheets was less than 3%, and the average deviation was less than half of this. The corresponding changes in drying rate and critical moisture content are not significantly greater than the precision with which these quantities can be determined, so no correction was made for variations in basis weight.

A better method of correcting for the effect of various small differences in similar sheets would have been to obtain an independent measure of the total moisture content of each sheet as a function of time. Then, each calculated datum point could have been corrected for the actual moisture content of the particular sheet in which it was determined. Without these data, similar sheets must be compared at the given times after the start of drying, and a certain amount of scatter is inevitable. This scatter became relatively more serious at low moisture content, so that the calculated results at very low moisture content lacked sufficient precision to be meaningful.

Figure 16 is a graph of cumulative moisture content through sheets of 28.2 mg./cm.^{2} dry basis weight. The sheets were dried at a hot-surface temperature of 221°F. The calculated values of moisture content for each selected time of drying shown were obtained by calculating the moisture content of the fractional thickness measured in each sheet. The points shown for the zero-time line are the values obtained by extrapolating the drying curves of each fractional thickness to zero time. The points on

on the curves for subsequent times have been corrected to average initial moisture content by adding to the values the difference between the zero-time points and line.

Four points are shown on the zero-time line but not on the other curves. These represent sheets which were discarded either because dye was found at the radioactive plane, or because a spot without dye was found at the hot-surface interface.

The moisture content at any point within the sheet at any of the values of drying time shown is the slope of the curves in Figure 16 at that point and time. Figure 17 was obtained by taking derivatives from Figure 16. It shows the moisture distribution within the sheet at various times after the start of drying. Figures 18 and 19 show moisture distributions obtained in similar fashion for a 28.2 mg./cm.^{2} sheet dried at 189°F. and for a 14.1 mg./cm.^{2} sheet dried at 219°F., respectively. The respective cumulative moisture curves for these figures contained 12 and 5 points, excluding the origin. The data for the 14.1 mg./cm.^{2} sheet was not screened by dye inclusion, so delamination could have occurred in those sheets without having been detected.

The fact that moisture distribution is obtained from the derivative of the cumulative moisture data is an inherent limitation of the accuracy of the method. It is obvious that a number of slightly different curves could be fitted to the data of Figure 16, and these curves would have a different derivative from the curve shown. It is, therefore, difficult to estimate the probable accuracy of the work. Separate independent estimates from the same data have given values differing from those given in Figures 17 to 19 by as much as 10 to 15% at some internal points.

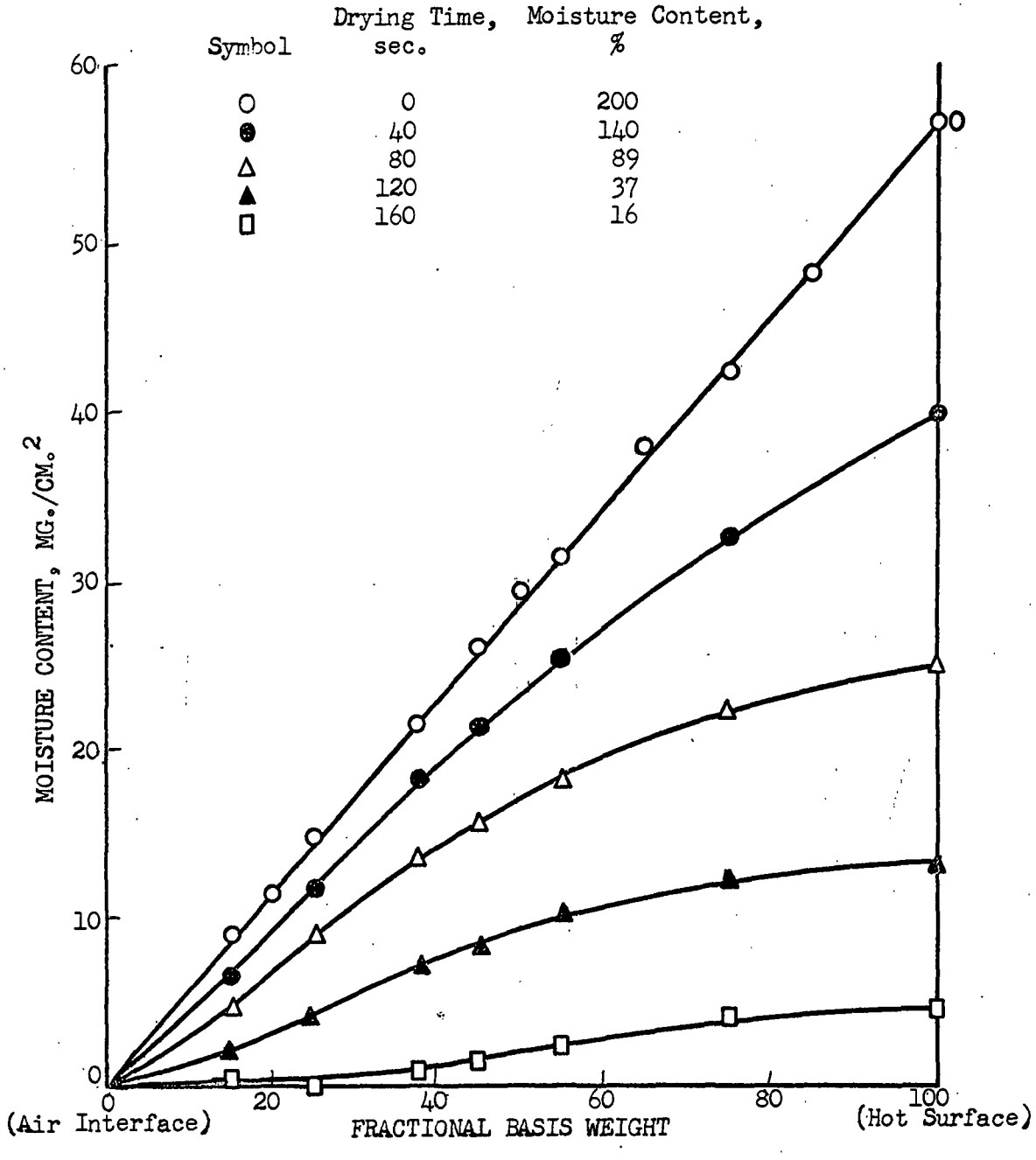

Figure 16. Cumulative Moisture Content

Sheet Basis Weight--28.2 mg./cm.^{2}
Hot Surface Temperature--221°F.

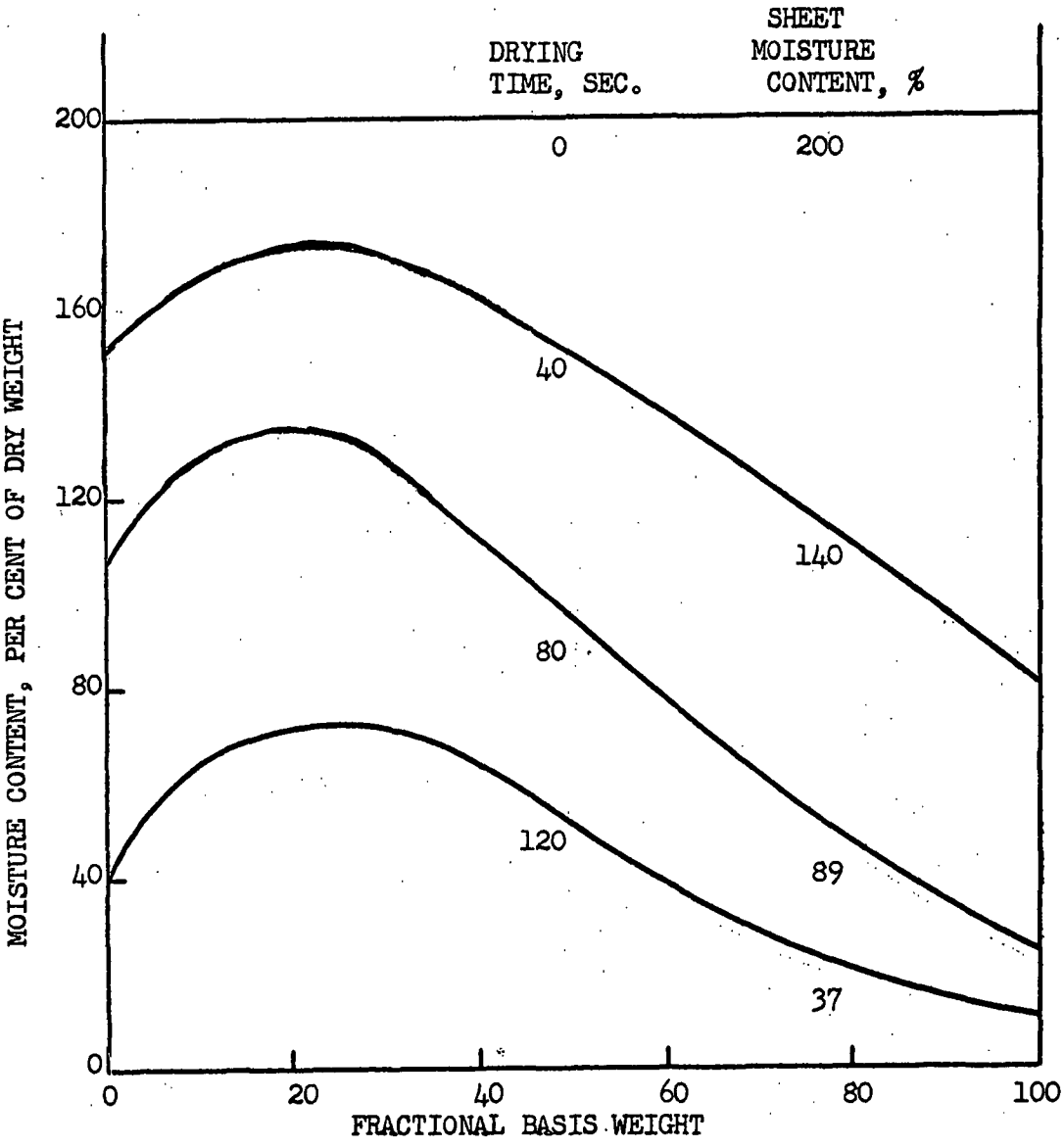

Figure 17. Moisture Distribution in 28.2 mg./cm.^{2} Sheet
Hot Surface Temperature--221°F.

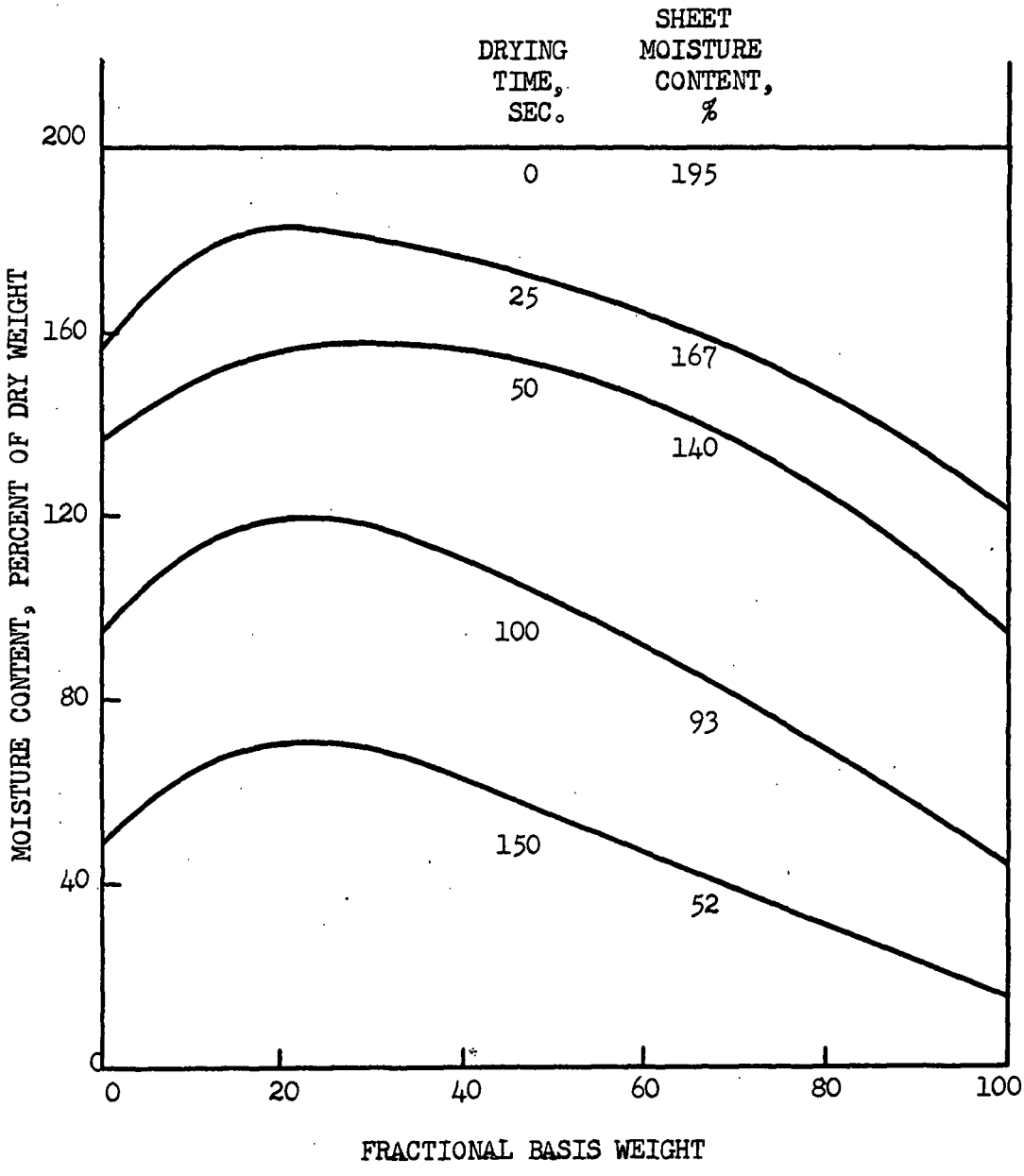

Figure 18. Moisture Distribution in a 28.2 mg./cm.^{2} Sheet
Hot Surface Temperature--189°F.

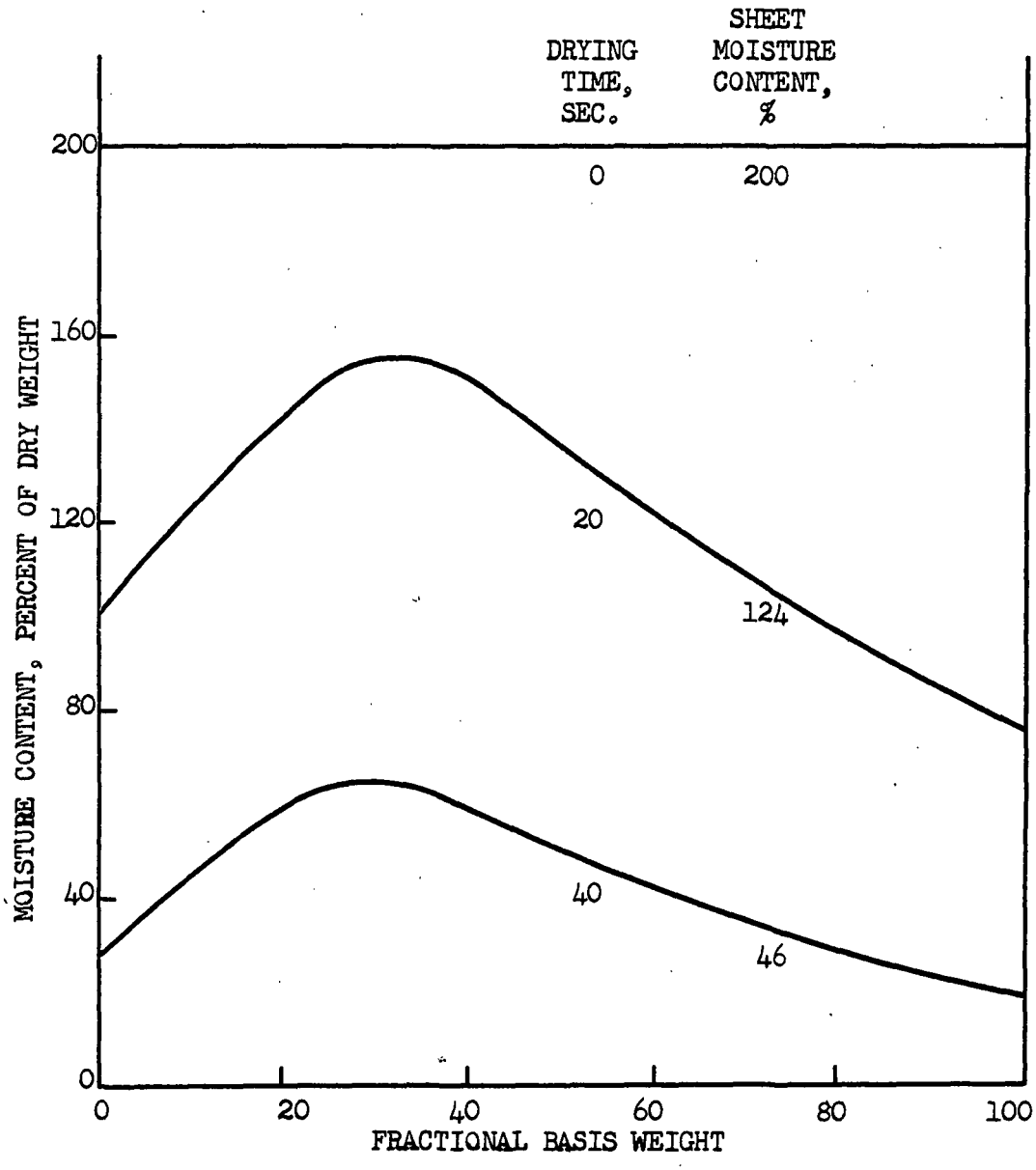

Figure 19. Moisture Distribution in a 14.1 mg./cm.^{2} Sheet
Hot Surface Temperature--219°F.

CHARACTERISTICS OF INTERNAL MOISTURE GRADIENTS

Figures 17, 18, and 19 represent the internal moisture gradients in the sheets which have been studied. The distribution of water in all sheets was similar. Starting at the air interface of a sheet, the moisture content at points within the sheet increased with fractional basis weight until a zone from about 20 to 30% of the fractional sheet thickness was reached. Somewhere within this zone, the moisture content was a maximum. From this zone to the hot surface, the moisture content of internal points decreased continuously, and the dryest point within the sheet was at the hot-surface interface. As the sheet dried, the moisture content in all portions of the sheet decreased. The general nature of the distribution did not change significantly during the constant-rate period nor as far into the falling-rate period as could be profitably followed.

For the two sheets having the same basis weight, (Figures 17 and 18), the moisture gradient over most of the sheet was steeper in the sheet dried at the higher temperature. For the two sheets dried at nearly the same hot-surface temperature, (Figures 17 and 19), the moisture gradient over most of the sheet was steeper in the sheet having the higher basis weight.

DISCUSSION OF MOISTURE GRADIENTS

As discussed previously, McCready (19) has determined the moisture distribution in a sheet 1/4-inch thick at one time during drying under experimental conditions similar to those used for this work. Table IV shows a comparison at equal total moisture content of the moisture distribution in the sheet studied by McCready with the slowest-dried sheet studied in this work. The 28.2 mg./cm.^{2} sheet was still drying at constant

rate at this moisture content, while McCready's sheet was well into the falling-rate period.

TABLE IV

COMPARISON OF MOISTURE GRADIENTS

Source of Data	This Work	McCready (19)
Hot-surface temperature, °F.	190	176
Sheet basis weight, mg./cm.^{2}	28.2	ca. 145
Initial apparent density, mg./cm.^{3}	350	ca. 230
Moisture content of upper third of sheet, %	118	128
Moisture content of middle third of sheet, %	107	128
Moisture content of lower third of sheet, %	68	37

Exact agreement of the moisture distributions would not be expected because of the greater basis weight, lower apparent density, and lower hot-surface temperature of McCready's sheet. Both sheets were dryest near the hot surface; the moisture gradient in McCready's sheet was steeper. The amount of data presented by McCready was not sufficient to detect a zone of maximum moisture content. As discussed in the Introduction, McCready did find a zone of maximum moisture content near the middle of a sheet dried with the air at the same temperature as the hot surface. In this case, however, the sheet had minimum temperature within it, so heat was being added from both faces.

The moisture gradients found in the sheets studied definitely show that capillary suction equilibrium did not exist within the sheets during drying. A nonuniform moisture distribution under capillary suction equilibrium could be caused only by nonuniform sheet properties [a gradient in r in Equation (1)] or by a gradient in γ within the sheet.

The maximum gradient in interfacial tension through a sheet corresponding to the calculated temperature drop through the sheet would be about 7%. Equation (1) indicates that capillary suction is directly proportional to interfacial tension, so a 7% difference in capillary suction could exist between the two faces of the sheet. According to the data of Barkas and Hallan (22), this could account for a difference of less than 4% between the moisture content at the two faces of the sheet.

If there were variations in the properties of the sheet serious enough to cause the distribution found during drying, a similar distribution would be found initially. Higgins (1) made sheets similar to those used in this work, and he found uniform initial moisture distribution. Furthermore, there are no reasonable conditions which could cause a maximum moisture content within a sheet in which capillary suction equilibrium exists. Therefore, unlike the situation which may exist during air drying, capillary suction equilibrium is not maintained nor even approached in the operation of hot-surface drying.

SOLUTE MIGRATION DURING DRYING

EXPERIMENTAL PROCEDURES

Sheets were prepared by wet pressing together laminates of the basis weight into which the sheets were subsequently to be delaminated. To facilitate delamination, a small piece of tea-bag stock was included between successive laminates at one end of each sheet.

Drying was conducted in the same fashion as for sheets in which moisture distribution was determined. After the desired amount of time, the sheets were removed from the tunnel and were delaminated. Mutually corresponding portions of each laminate were cut from each sheet with a die punch.

The dye from each of these portions was extracted with water and diluted to a known volume. The optical transmittance at 425 mmu. of each solution relative to distilled water, was determined with a General Electric Recording Spectrophotometer. Appendix XI contains the data which relate optical transmittance to dye concentration. Appendix XII contains details of the experimental procedures.

EXPERIMENTAL RESULTS

ACCURACY AND REPRODUCIBILITY

Sheets for dye distribution studies were made by wet-pressing together up to four laminates to form a composite sheet of the basis weight desired. To determine whether this procedure had changed the characteristics of the sheets, over-all drying curves were obtained for some of the sheets in

which solute migration was measured. One of these is shown on Figure 10. In no case did the lamination procedure cause a measurable change in the rate of drying of sheets.

To determine the magnitude of migration possible during handling of a hot, wet sheet, a sheet of presumed uniform initial dye distribution was mounted on the C-frame, inserted into the tunnel, and pulled onto the hot surface, which was at 190°F., in the usual fashion. After about 1 second on the hot surface, the sheet was removed from the tunnel and delaminated. Table V shows the dye distribution found in the sheet. Laminates are lettered from the top to the bottom of the sheet; A is the top laminate.

TABLE V

DYE MIGRATION DURING MANIPULATION

Laminate	A	B	C	D
Laminate weight, % of total sheet	15	35	35	15
Dye in laminate, % of total dye	19	30	33	18

It is apparent that some dye migration occurred during the time required to remove the sheet from the tunnel and to delaminate it. Because of this, results obtained from the delamination of wet sheets cannot be quantitatively compared with the moisture content of the sheet at the time the sheet was removed from the hot surface.

For sheets which were completely dried before delamination, dye migration during handling was undoubtedly negligible. However, as Preston and Chen (30) have remarked, the correspondence of dye movement to liquid

water movement probably was less good at low sheet moisture content. In view of this effect in dry sheets and of migration during handling of wet sheets, the results of dye migration studies cannot be construed as a quantitative measure of liquid water migration. The results should be considered only as showing the direction and the approximate amount of liquid movement and the location of zones of vaporization.

Because of these limitations of the accuracy of the results in terms of liquid water movement, a thorough study of precision was not made. In Table VII, p. 74, the results of analyses for two pairs of duplicate sheets can be found. The maximum difference between the percentage of total dye found in duplicate laminates was less than 2%. In one case, however, a discrepancy of over 10% was noted. The reason for this is not known, but the results from the one sheet were completely out of line with other data; these results were discarded.

CHARACTERISTICS OF INTERNAL DYE DISTRIBUTION

Figures 20 and 21 show the distribution of dye in sheets of 28.2 mg./cm.^{2} dry basis weight dried from 200% initial moisture content at respective hot-surface temperatures of 221 and 189°F. At any moisture content, the distance between lines represents the amount of dye which was in the portion of the sheet indicated. In all dye migration studies, it was visually obvious that there was a very marked concentration of dye at both surfaces of the sheet. Most of the dye in the upper and lower 15% fractional thicknesses was concentrated at the air interface and the hot-surface interface, respectively.

Dry Sheet Basis Weight--28.2 mg./cm.^{2}
Hot-Surface Temperature--221°F.
Initial Moisture Content--200%

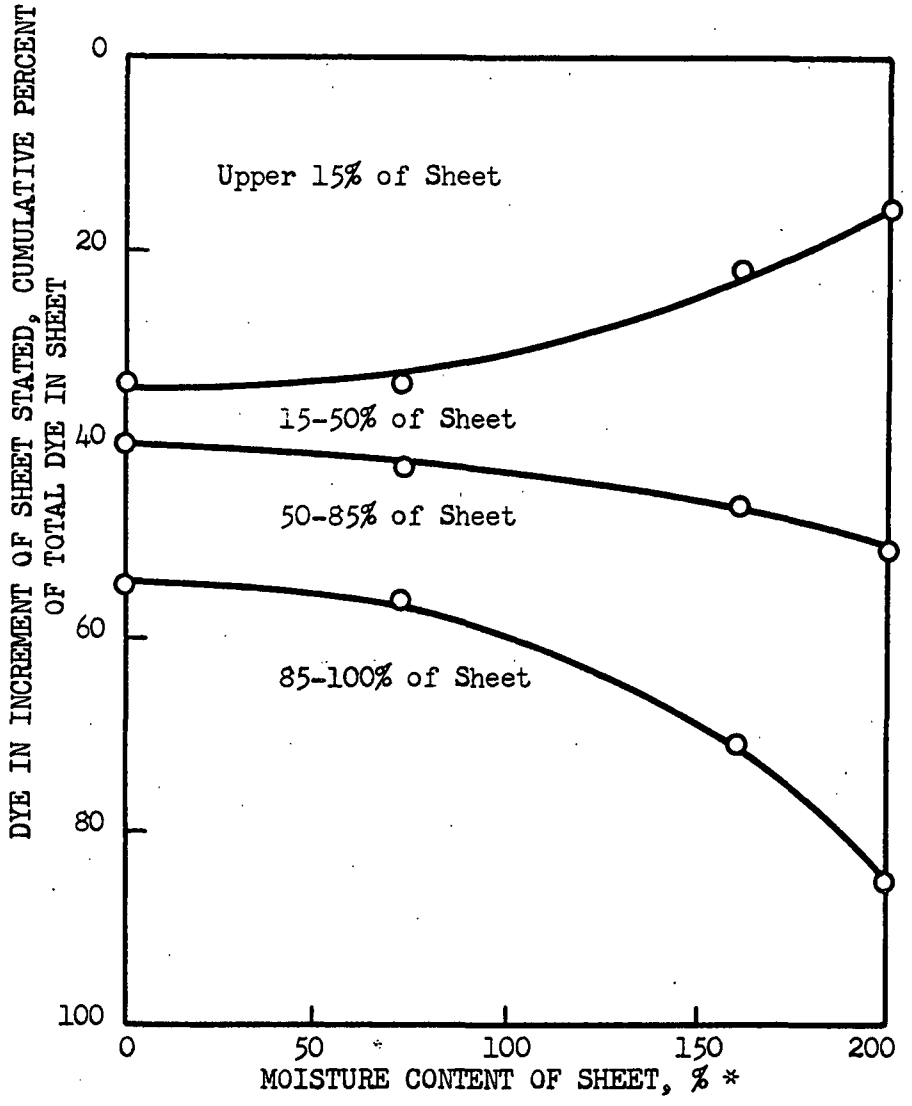

* At time sheet was removed from tunnel.

Figure 20. Dye Distribution in Sheet During Drying

Dry Sheet Basis Weight--28.2 mg./cm.^{2}
Hot-Surface Temperature--189°F.
Initial Moisture Content--200%

* At time sheet was removed from tunnel.

Figure 21. Dye Distribution in Sheet During Drying

Figures 20 and 21 indicate that the general behavior of the sheets dried at the two different hot-surface temperatures was similar. In both, the dye moved from the interior of the sheet to both the hot and cold surfaces of the sheet. This migration started very early during drying and continued at least part way into the falling-rate period.

An interesting finding was the fact that a zone of minimum dye concentration existed within the sheets. The 35% of the sheet just above the midplane contained less dye at all times during drying than did the 35% of the sheet just below the midplane of the sheet. The implications of this finding will be discussed later in the thesis.

Data in Table VI show the effects of initial moisture content and hot-surface temperature on the final dye distribution in similar sheets.

TABLE VI

DYE DISTRIBUTION IN DRY SHEETS

Dry Basis Weight-28.2 mg./cm.^{2}

Hot-Surface Temp., °F.	Initial Moisture Content, %	Dye in Laminates Listed, % of Total Dye in Sheets			
		0-15%	15-50%	50-85%	85-100%*
221	200	31	9	15	45
221	150	27	14	21	37
189	200	35	9	15	41

In all sheets, the dye was concentrated at both surfaces, and the zone of minimum dye concentration was 15-50%.* A greater percentage of dye migrated to the surfaces in the sheets of higher initial moisture content. Increasing

* Percentage basis weight of the sheet measured from 0% at the air interface to 100% at the hot-surface interface.

the hot-surface temperature did not cause a measurable change in the total migration to the surfaces of the sheet, but a greater amount of dye moved to the hot surface and a correspondingly smaller amount to the air surface. The net migration across the midplane of the sheet was greater in the sheet dried at the higher hot-surface temperature.

Table VII shows the location of dye in dry sheets of different basis weight which have been dried from the same initial moisture content. Duplicate analyses for two conditions are shown. The 0-25%* fraction and 75-100% fraction for the 28.2 mg./cm.^{2} sheets were obtained by assuming that the dye distributions in 15-50% and 50-85% fractions, which were the ones actually measured, were uniform. This was undoubtedly not true, so the estimates are not exact. However, the dye content of these sections was small compared with the dye content of outer zones, so the error introduced should not be serious.

TABLE VII

DYE DISTRIBUTION IN DRY SHEETS

Initial Moisture Content - 200%

Basis Weight, mg./cm.^{2}	Hot Surface Temp., °F.	Dye in Laminates Listed, % of Total Dye in Sheet		
		0-25%	50-100%	75-100%*
28.2	221	34.5	59.9	49.4
14.1	219	35.6	--	45.3
14.1	219	36.3	--	45.8
7.1	217	--	58.7	--
7.1	217	--	60.5	--
28.2	189	38.0	--	45.5
14.1	189	36.0	--	43.0

* See footnote on previous page.

Within experimental error, there was no significant difference in the final dye distribution in sheets of different basis weight.

A series of qualitative experiments was also performed using stacks of filter paper in which one sheet initially contained dye. The sheets were brought to approximately the same initial moisture content, were stacked together and clamped on an electrically-heated drum drier with a spring-loaded wire screen. When a stack had dried, it was removed from the drier, and each sheet was examined for dye. Excluding the edges of the sheets, it was observed that dye initially in the upper 20% of a stack was found concentrated at the upper surface of the sheet, the air interface. Dye initially in the lower 60% of a stack was found concentrated at the lower surface. Dye initially in the region 20-40% of the stack fractional thickness was found to have moved to both the hot and the cold surfaces.

MECHANISM OF HOT-SURFACE DRYING

The results obtained in this work have indicated that the same general behavior was occurring throughout the range of conditions studied. Comparison of these results with the findings of McCready (19) for heavier sheets dried under similar conditions have shown no important differences between the nature of drying of light and of heavy sheets. It is true that numerical values of the rate of drying and the internal moisture distribution were dependent upon sheet basis weight and hot-surface temperature. The importance of the air-film at the interface between the sheet and the hot surface was much less for heavy sheets, and the falling-rate period accounted for a much larger fraction of the total drying cycle for heavy sheets than for light ones. Thus, the relative importance of these phenomena was dependent upon sheet weight and drying conditions. Within the constant-rate period and within the falling-rate period, there appeared to be no difference in the mechanism of drying over the entire range from the lightest sheets studied in this work to the heaviest sheets studied by McCready.

The general conditions existing within sheets during the constant-rate period and the first part of the falling-rate period are summarized by Figure 22. In all sheets studied, the maximum moisture content was found in a zone from 20 to 30% of the distance from the cold to the hot surface. In this same region, a zone of minimum dye content existed. There appeared to be no movement of dye and therefore no movement of liquid water across this zone. Liquid water, which was initially between this zone and the hot surface moved toward the hot surface; liquid water which was between this zone and the cold surface moved toward the cold surface. Liquid water

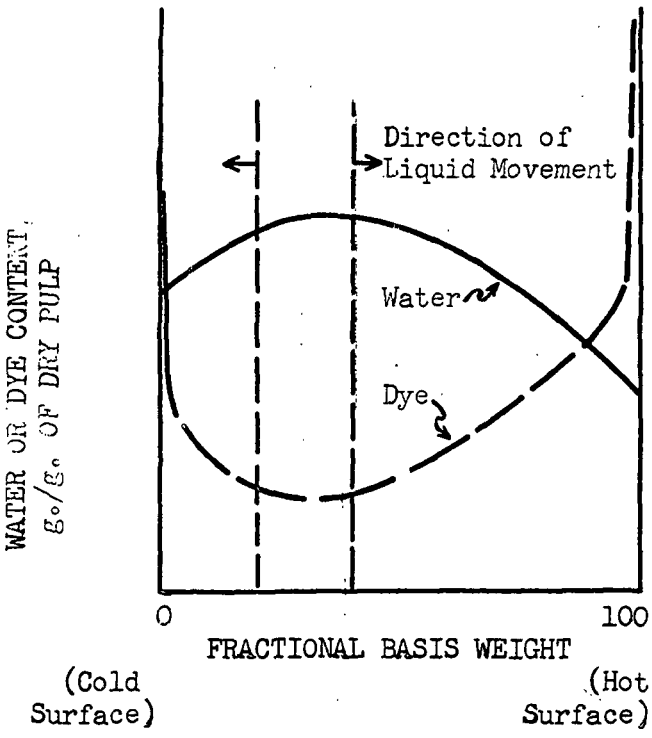

Figure 22. Typical Distribution and Movement of Water and Dye Within Sheets During Drying

movement was in the direction of decreasing moisture content and was predominantly toward the hot surface of the sheet.

Water vapor could leave the sheet only at the air interface. Therefore, the liquid water moving to the hot surface must have been vaporized there, and this vapor must have moved back through the sheet in order to escape from the open surface. The sharp concentration of dye right at the hot-surface interface indicates that most of the vaporization occurred right at the interface.

A sharp concentration of dye was also found at the air interface of the sheet. This indicates that a significant amount of vaporization occurred there. Calculations have shown that the temperature at this surface was definitely higher than the temperature of the air, so sensible heat transfer was from the sheet to the air. The heat required for vaporization at the air interface as well as the sensible heat transferred to the air must have been propagated through the sheet from the hot surface.

Within the sheet, the dye content of the sheet was at a minimum in the same region that the moisture content was at a maximum. The dye concentration in the water, the ratio of the dye content of the sheet to the water content of the sheet at the same point, decreased continuously from the hot surface to the zone of maximum water content.

Figure 23 shows the expected water and dye distribution for various mechanisms of hot-surface drying. If the only phenomena involved in hot-surface drying were liquid migration to the surfaces of the sheet and vaporization at the surfaces, the distributions shown in Figure 23A should have been found. The dye concentration in liquid water would have been

Figure 23A
Vaporization at Both Surfaces

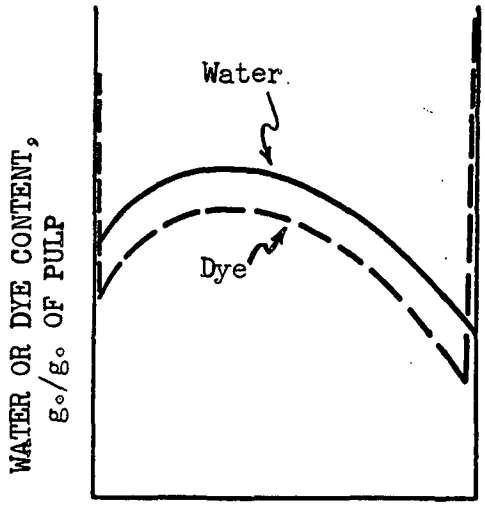

Figure 23B
Vaporization at Air Surface

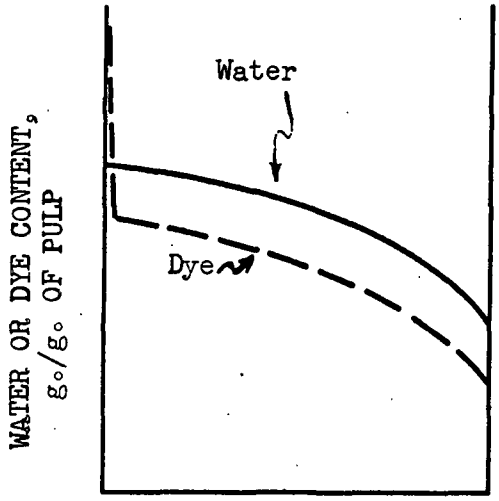

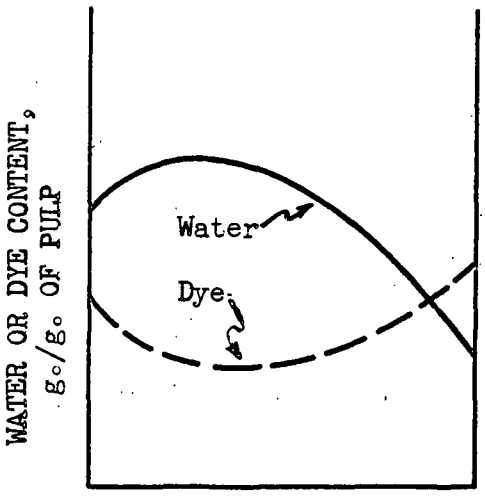

Figure 23C
Progressive Internal
Vaporization

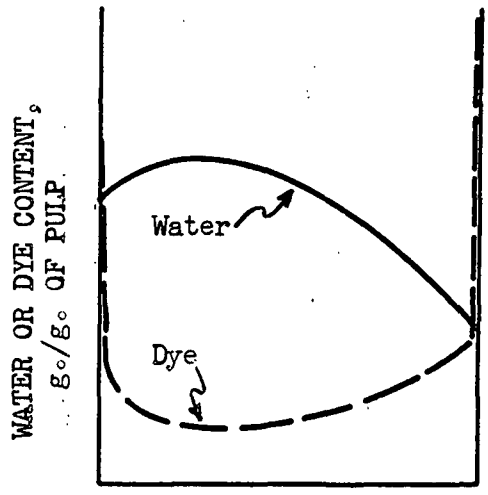

Figure 23D
Vaporization at Both
Surfaces with Internal
Recondensation

Figure 23. Predicted Water and Dye Distribution Within Sheets for Various Mechanisms of Drying

constant within the sheet, or might even have increased slightly in the center of the sheet, since dye migration may lag slightly behind liquid water migration. The sheet would have had a maximum dye content in the same region as the maximum water content.

Figure 23B indicates the expected findings if an external pressure gradient caused by heating of vapor at the hot-surface interface were the cause of liquid movement. With no felt present, liquid water would have moved from the hot to the cold surface and presumably would have vaporized at the cold surface. The dye content of the sheet would have corresponded to the moisture content, so there would have been a minimum in the dye content of the sheet at the hot-surface interface instead of the sharp concentration of dye actually found.

Figure 23C shows expected results for one possible type of internal vaporization. It is assumed for this case that the relative amount of vaporization is greatest at the surfaces and is continuously less in zones toward some zone in which the rate of vaporization is minimum. Assuming further that liquid water moved in the direction of minimum moisture content, a zone of maximum moisture content corresponding to a zone of minimum dye concentration would be observed. If this mechanism existed, there would not be a sharp concentration of dye at the surfaces of the sheet; instead a dye gradient which increased smoothly right up to and including the surfaces would be expected.

The actual distribution found corresponded to Figure 23D. Dye was concentrated at the surfaces of the sheet, indicating that liquid water had moved to and evaporated from these regions. Within the sheet, the

dye concentration in liquid water decreased continuously from just below each surface to the region of maximum water content, which was also the region of minimum dye content. This indicates that the liquid water originally within the sheet (the water containing dye) must have been diluted with water that did not contain dye. Such water could only be condensate from vapor which had been formed elsewhere.

It has already been noted that the vapor formed at the hot surface must pass through the sheet and escape into the air at the air interface. Figure 2 shows that the temperature of the sheet decreased continuously from the hot to the cold surface. Thus, the partial pressure of vapor formed at the hot surface was greater than the saturation pressure of the rest of the sheet. Calculations by McCready indicated that the vapor leaving the cold surface was probably in saturation equilibrium with respect to the cold surface. If vapor within the sheet was also at or near saturation equilibrium, there must have been condensation-vaporization cycles within the interior of the sheet. The observed dilution of dye indicates that net condensation occurred in these cycles.

The heat of condensation transferred to the sheet by these cycles would be propagated by conduction to the open surface. Here this heat plus heat transferred by direct conduction from the hot surface caused net vaporization at the air interface of the sheet, since this is the only place at which subsequent condensation would not occur.

It is now possible to present a description of the mechanism and phenomena of hot-surface drying which explains the findings of this work and of the work of McCready. At the start of a drying run, there is a

short period during which the sheet is coming to the constant-rate drying rate and temperature distribution. During the constant-rate period, heat is being added to the sheet at the hot surface, and vaporization of water occurs there. This vapor has a partial pressure greater than the equilibrium vapor pressure of the rest of the sheet, and there is net internal condensation as the vapor passes through the sheet and enters the air stream over the open surface. The heat transferred to the sheet by the condensing vapor is moved in the direction of decreasing temperature by conduction. At the open surface, a small fraction of the heat is transferred to the air by convection; the remainder causes net vaporization.

The vaporization at the two surfaces depletes the liquid water content of the sheet at these places. The process occurs too rapidly for capillary-suction equilibrium to be maintained, so moisture gradients toward the surfaces are established. These cause movement of liquid water to the surfaces. The rate of drying is determined by a complex balance of heat and mass transfer, the terms of which cannot be determined.

This process continues until the zone at the hot surface becomes too dry to maintain the initial rate of vaporization. This probably occurs as the zone at the hot-surface interface approaches the "fiber saturation point,"* although the experimental data are not sufficiently precise to support this observation with certainty. The temperature drop across this zone increases and the heat transfer across this zone decreases. The temperature of the rest of the sheet decreases; consequently, the vapor pressure of water at the air interface decreases and the rate of drying decreases. The critical moisture content is thus related primarily to the moisture content at the hot-surface interface. For a given moisture

* See footnote on page 11.

content at the hot surface, the average moisture content of a sheet becomes greater as the moisture gradient becomes greater. Any change which increases the moisture gradient, such as an increase in basis weight or in hot-surface temperature, causes an increase in the critical moisture content.

Below the critical moisture content, the zone in which vaporization occurs moves slowly away from the hot surface, and a continual readjustment of temperature within the sheet occurs. Liquid migration continues to occur in the falling-rate period, probably until the front of the zone of vaporization has reached the zone of maximum moisture content within the sheet. By this time, the moisture content of the sheet is very low, there is no longer any continuous liquid water network, and the remaining water is removed by vaporization <u>in situ</u> and diffusion of water vapor from the interior.

SIGNIFICANCE OF RESULTS

The major results of this thesis have been the determination of the transverse location and movement of water during the hot-surface drying of paper. This knowledge is intermediate between a fundamental understanding of factors causing and limiting drying rate on one hand and a pilot-plant approach to drying on the other hand. As such, it should serve primarily as a basis of comparison for future work of both types.

From a practical standpoint, the heat-transfer coefficients obtained in this work reaffirm the fact that the interface between a sheet and a hot surface represents a very important fraction of the total resistance to heat transfer, even for grades as heavy as paperboard. Improvement of heat transfer across this interface represents a real opportunity to increase the efficiency of operation of a paper machine.

The importance of the falling-rate period upon the drying time required is well known. The data in this thesis show that it becomes of relatively greater importance as the basis weight of the sheet is increased. The low drying rate at low moisture content mitigates against drying to a moisture content below that necessary to obtain desired sheet properties. Since vaporization is occurring internally during the falling-rate period, the drying rate during this period could be increased either by causing the water to move more rapidly toward the surfaces or by causing the heat to be transferred more rapidly to the interior of the sheet. It is beyond the scope of this thesis to speculate whether the former can be done. Any auxiliary apparatus which can accomplish the latter, such as dielectric or infrared heaters, would be used most efficiently at the dry end of a drier section.

The fact that liquid water migrates to a hot surface indicates that solutes would tend to concentrate at the surface of sheets. This could be of importance in a product where a solute is of importance or in any product where the surface is important. As an example, in a tub-sizing operation the distribution of sizing agent and consequently the characteristics of the sized sheet might be expected to depend to some extent upon the moisture content of the sheet when the size was applied and upon the temperature at which drying was subsequently conducted.

On a machine in which heat is added alternately from each side, the sheet is undoubtedly dryest on each side with a zone of maximum moisture content in the interior. Whether or not this zone moves appreciably as the sheet progresses from one heated surface to another would depend upon the length of time the sheet spends on a drum and in a draw. This distribution of moisture is that which was deduced by Burstein (6).

SUGGESTIONS FOR FUTURE RESEARCH

1.) VARIABLES IN YANKEE DRYING

The experimental apparatus used for this work simulates a Yankee drier to the extent that a sheet is continuously heated from one side with the other side exposed to air. Because the sheets used in this work were much thicker than those ordinarily dried on a Yankee, the conclusions drawn concerning the effect of external variables on the rate of drying are not necessarily valid. As discussed in Appendix 1, a beta emitter less energetic than thallium 204 might be used to follow more accurately the drying of light sheets. A program could be conducted to determine the effect of the temperature, velocity, and relative humidity of the circulating air on the drying rate of light sheets. The results of such a study should answer the oft debated but still moot questions concerning the importance of these factors on the rate of drying.

2.) MECHANISM OF FALLING-RATE DRYING

The falling-rate period has not been studied thoroughly on this work because of the limitations of the experimental technique. First is the limitation imposed by isotope statistics and sensitivity; second and more important is the necessity of using data from several different sheets which are presumed to be identical. An independent measure of the total moisture content of each sheet used is needed in order to obtain meaningful moisture gradients at low moisture content.

There are several modifications of the apparatus which are theoretically possible but which might offer severe practical difficulties. One would be to

obtain a continuous record of the weight of the sheet plus the hot surface during drying. Alternatively, the hot surface might be made very thin and beta-ray transmission data be obtained from both sides of the sheet.

From the work which has been done, it appears that the mechanism of drying did not change from sheets of the basis weight used in this study to the sheets of much greater basis weight used by McCready. It may, therefore, be desirable to use a heavy sheet and to determine moisture gradients by interrupting a drying run, delaminating a sheet, and determining the moisture content of the laminates gravimetrically, as was done by McCready.

3.) DRYING ON A PAPER MACHINE

Paper-machine drying differs from drying on a single hot surface in several respects. A sheet is alternately heated from each side, and after each heating it passes through a draw in which it is in contact with air on both sides. During part of the time that one side of a sheet is in contact with a hot surface, the other side is often in contact with a felt.

There has been some work published which contributes to understanding where water removal occurs on a paper machine (12, 15, 27), but much more work is needed.

Beta gages now make it possible to determine the moisture content of a felt while a machine is running. Furthermore, it should be possible to use a solute in water to determine how much, if any, liquid water migrates into a felt. If a radioactive solute were used, such a measurement could be made during operation; otherwise it might still be possible to perform such work just before a felt change.

Laboratory studies of the role of felts in drying would also be of value. A comparison of drying rates, moisture gradients, and liquid water movement when felts are present and when felts are absent would be of interest.

4.) FUNDAMENTALS OF LIQUID FLOW CAUSED BY CAPILLARITY

Flow of liquid in porous beds or capillary systems when air is also present is a very complex phenomenon. Some work has been done concerning the flow of oil and water through sand. Capillary suction data have been obtained for pulp (22). Pearse et al. (24) have attempted to apply capillary suction theory to the movement of water during air drying of glass beads. A more elaborate theory than theirs appears to be necessary.

An adequate knowledge of the forces causing and limiting the flow of fluid in such a system would serve as a rational basis for predicting and explaining dewatering of sheets at suction boxes and presses as well as during evaporative drying.

GENERAL SUMMARY

Apparatus suitable for conducting experimental hot-surface drying has been constructed, and a new technique for following the course of drying has been developed. In this technique, the mass per unit area of water in the sheet was determined at any time during drying by measuring the transmission of the sheet to beta-rays as a function of time during drying. To determine over-all rates of drying of sheets, a source of beta rays was mounted beneath the sheet on the hot surface and the radiation detector was mounted above the sheet. The mass per unit area of water was related to the beta-ray transmission by an empirical calibration procedure. Using thallium 204 as the source of beta rays, precision within 1 mg./cm.^{2} could be obtained.

To determine the drying rate of any fraction of the sheet from the air surface, the source of radiation was deposited in the sheet at the desired depth from the air interface, and the radiation detector was mounted above the sheet. To do this, radioactive thallium was absorbed on finely-ground cation-exchange resin. The ion-exchange resin containing the radioactive thallium was affixed to a thin sheet of paper with a resorcinol-formaldehyde resin. The sheet for drying was formed by wet-pressing the thin sheet containing the radioactive source between two laminates such that this source was at the desired depth and the laminated sheet was of the desired dry basis weight.

A series of over-all drying-rate curves for sheets made from lightly beaten, bleached sulfite pulp has been obtained. Hot-surface temperature varied from 169 to 221°F.; the dry basis weight of sheets from 3 to 28

mg./cm.^{2}. The air above the sheet was 95°F., 50% R.H., 250 f.p.m. Changes in air conditions had very little effect on the rate of drying.

Constant-rate drying rates observed were from 0.21 to 0.68 mg./cm.^{2} sec.; critical moisture contents were from 25 to 95%. Constant-rate drying rate and critical moisture content increased with hot-surface temperature. Constant-rate drying rate decreased and critical moisture content increased with increasing dry basis weight of the sheet.

The temperature of the sheet at the air interface was calculated from the drying rate and the mass-transfer coefficient, assuming that the vapor leaving the surface was in saturation equilibrium with the surface. This temperature was always higher than the dry-bulb temperature of the air; always lower than the hot-surface temperature. Heat-transfer coefficients from the hot surface to the air interface of the sheet were calculated. This heat-transfer coefficient increased as sheet basis weight decreased, and the coefficient for the air film between the sheet and the hot surface was estimated to be 145 (B.t.u./hr. ft.^{2} °F.), representing a very significant fraction of the total resistance to heat transfer even for the heaviest sheets studied.

Transverse moisture distribution within a sheet was determined by measuring the drying rate of a series of fractional thicknesses of similar sheets dried under similar conditions. This method eliminated the need for interrupting a drying run and delaminating wet sheets. It had the disadvantage that data from several different drying runs had to be obtained to determine the moisture distribution within a sheet, so small variations between similar sheets caused some scattering of the data. Moisture

gradients were obtained for 28.2 mg./cm.^{2} sheets dried at 189 and 221°F., and for 14.1 mg./cm.^{2} sheets dried at 219°F.

During the constant-rate period and as far into the falling-rate period as could be followed, all sheets were dryest at the hot-surface interface and had a zone of maximum moisture content between 20 and 30% of the distance from the cold to the hot surface. The moisture gradient became steeper as the hot-surface temperature or the basis weight of the sheet increased.

Solute migration and distribution during drying were studied as a qualitative means of following liquid moisture movement within the sheet and identifying zones in which vaporization occurred. In all sheets of uniform initial solute distribution, the solute moved to both the hot and the cold surfaces of the sheet, and a zone of minimum solute content existed in the same region as the zone of maximum moisture content. In stacks of filter paper in which only one sheet had been dyed, it was found that solute from the upper 20% of the stack moved to the cold surface; solute from the lower 60% of the stack moved to the hot surface; solute from the zone 20-40% of the distance from the cold to the hot surface moved partially to each surface.

Based on these findings a postulated mechanism of drying for the constant-rate period and the first portion of the falling-rate period is presented. All the heat for drying is supplied from the hot surface, and only a small fraction is lost to the air as sensible heat. Most of the vaporization occurs at the hot-surface interface. The vapor formed at the hot-surface interface cannot escape there but must pass through the sheet

and escape from the surface open to the air. Water vapor formed at the hot surface has a partial pressure greater than the equilibrium saturation pressure of the rest of the sheet, and it is partially condensed within the sheet. The heat liberated by condensation of part of the vapor is propagated to the air surface by conduction. At the air surface, this heat causes net vaporization. Vaporization at the two surfaces causes depletion of the liquid water content there and consequently a gradient in moisture content toward each surface. Capillary suction equilibrium does not exist within the sheet; liquid water is moved to the surfaces by the moisture gradient or the consequent capillary suction gradient.

CONCLUSIONS

The following major conclusions may be drawn as the result of this investigation:

1. Measurement of absorption by water of beta radiation from radioactive isotopes is a feasible technique for studying the drying of paper.

2. With the apparatus and techniques employed, the over-all drying rate of sheets may be studied over a wide variety of conditions.

3. With the apparatus and techniques employed, moisture distribution within sheets may be studied during the constant-rate period and the initial portion of the falling-rate period for a wide variety of conditions. Modification is required to obtain useful data in the final portion of the falling-rate period.

4. Solute migration studies are a useful qualitative adjunct for studies of liquid moisture movement during drying.

5. The important variables affecting the rate of drying of sheets with one side contacting a hot surface and the other side exposed to circulating air are the hot-surface temperature and the dry basis weight of the sheet. Air temperature, air velocity, and initial moisture content of the sheet have very little effect on drying rate in the range studied.

6. The resistance to heat transfer at the hot-surface interface of the sheet represents an important fraction of the total resistance to heat transfer between the hot surface and the air interface of the sheet.

7. During the constant-rate period and initial portion of the falling-rate period, the nature of the distribution of water within a sheet does not change appreciably. A sheet is driest next to the hot surface and has a zone of maximum moisture content at 20-30% of the distance from the cold to the hot surface.

8. The moisture gradient in sheets of given basis weight increases as the hot-surface temperature increases.

9. At a given hot-surface temperature, the moisture gradient in sheets increases as dry basis weight of the sheets increases.

10. Liquid water migration at points within a sheet is in the direction of decreasing moisture content. Liquid water, therefore, moves in both directions from the zone of maximum moisture content. Vaporization occurs at both surfaces of the sheet.

11. Internal condensation of a portion of the vapor formed at the hot surface occurs. The heat transferred to the sheet by this process accounts for at least part of the heat used for vaporization at the cold surface.

12. At the critical moisture content, there is no sudden change in the nature of the water distribution within a sheet. The zone of vaporization at the hot surface probably begins to recede into the interior of the sheet.

LITERATURE CITED

1. Higgins, James J. A study of air drying of paper. Doctor's Dissertation. Appleton, Wis., The Institute of Paper Chemistry, 1951. 122 p.; Tappi 35, no. 3:93(March, 1952).

2. Kamei, S., and Shiomi, S., J. Soc. Chem. Ind. (Japan), Supplemental Binding: 40 (1937); C.A. 31:8263.

3. McCready, D. W., Paper Trade J. 95:T125(1932); 101:T159(1935).

4. Sherwood, T. K., Paper Trade J. 88, no. 8:134(Feb. 21, 1929).

5. Sherwood, T. K., Trans. Am. Inst. Chem. Eng. 32:150(1936).

6. Burstein, Victor S. Method for rate of drying of paper and paperboard under machine conditions. Doctor's Dissertation. Appleton, Wis., The Institute of Paper Chemistry, 1944. 145 p.; Paper Trade J. 110:35(March 7, 1946).

7. TAPPI. Data Sheets no. 155. (1951).

8. Montgomery, A. E., Tappi 37:1(1954).

9. Montgomery, A. E. Drying of paper in the paper-making process. Boston, Barrett, 1954.

10. Schmidt, K., Das Papier 3, no. 5:73(1949).

11. Nuki, R. P., Proc. Tech. Soc. Brit. Paper and Board Makers' Assoc. 35:47(Feb., 1954).

12. Goumeniouk, G. I., Pulp and Paper Mag. Can. 55, no. 8:109(Aug., 1954).

13. Nissan, A. H., and Kaye, W. G., Tappi 38, no. 7:385(July, 1955).

14. Lewis, W. K., McAdams, W. H., and Adams, F. W., Paper Trade J. 84, no. 18:61(May 5, 1927).

15. Sherwood, T. K., Gardner, H. S., and Whitney, R. P., Paper Trade J. 106, no. 24:29(June 16, 1938).

16. Smith, S. F., and Attwood, B. W., Tappi 36:481(1953).

17. Attwood, B. W., and Smith, S. F., World's Paper Trade Rev. 134, no. 20:1425(1950).

18. Flyate, D. M. Bumazhnaya Prom. 21, no. 3:37(1946).

19. McCready, D. W., Paper Trade J. 101:T162(1935).

20. Marshall, W. R., Jr., and Friedman, S. J. Drying. In Chemical Engineers' Handbook. 3rd ed. p. 801ff. New York, McGraw-Hill, 1950.

21. Haines, J., J. Agric. Science 17:264(1927).

22. Barkas, W. W., and Hallan, R., World's Paper Trade Rev. 139, Technical Convention no.:52(March, 1953).

23. Ceaglske, N. H., and Hougen, O. A., Ind. Eng. Chem. 29:805(1937).

24. Pearse, J. E., Oliver, T. R., and Newitt, D. M., Trans. Inst. Chem. Eng. (London) 27:1(1949).

25. Krischer, O., Chem. Technik. 16:117(1943).

26. Hougen, O. A., McCauley, H. J., and Marshall, W. R., Jr., Trans. Am. Inst. Chem. Eng. 36:183(1940).

27. Nissan, A. H., Tappi 37, no. 12:597, 666(Dec., 1954).

28. Preston, J. M., and Chen, J. C., J. Soc. Dyers Colourists 64:60(1948).

29. Preston, J. M., Bull. Inst. Textile (France) 30:467(1952).

30. Preston, J. M., and Bennett, A., J. Soc. Dyers and Colourists 67:101 (1951).

31. Shepard, C. B., Hadlock, C., and Brewer, R. C., Ind. Eng. Chem. 30: 388(1938).

32. Hutcheon, N. B., and Paxton, J. A., Heating, Piping, Air-Conditioning 24:113(April, 1952).

33. Vassilou, B., and White, J., J. Trans. Brit. Ceram. Soc. 47:351(1948).

34. Eisenstadt, Raymond. A study of certain aspects of thermally activated moisture migration in granular media. Doctor's Dissertation. New York, N. Y., Columbia University, 1953.

35. Varder, R. W., Phil. Mag. 29:726(1915); C.A. 9:1875.

36. Perry, John H. Chemical Engineers' Handbook. 3rd ed. Section 6. New York, McGraw-Hill, 1950.

37. Montgomery, A. E., Paper Trade J. 123 no. 14:29(Oct. 3, 1946).

38. Fearnside, K., World's Paper Trade Rev. 133:1320, 1832; 134:439, 939 (1950).

39. Friedlander, G., and Kennedy, J. Introduction to radioactivity. New York, Wiley, 1949. 412 p.

40. Rutherford, E., Chadwick, J., and Ellis, C. D. Radiations from radioactive substances. Cambridge, Eng., University Press, 1930. 388 p.

41. Kaplan, I. Nuclear physics. Cambridge, Mass., Addison-Wesley, 1955. 609 p.

42. Jordan, W. H. Detection of nuclear particles. In Annual Reviews of Nuclear Science. Stanford, Stanford Press, 1952. p. 208 ff.

43. Curtiss, L. F. Measurement of radioactivity. National Bureau of Standards Circular 476, 1949. 84 p.

44. Muller, R., Phys. Rev. 93, no. 4:891(1954).

45. Corson, D. R., and Wilson, R. R., Rev. Sci. Instruments 19:207(1948).

46. Schiff, L. I., and Evans, R. D., Rev. Sci. Instruments 7:456(1936).

47. Catalog of Isotopes. Oak Ridge National Laboratories. July, 1952.

48. Tracerlab Instrument Manual for P-20 Scintillation Detector.

49. Tracerlab Instrument Manual for SC-51 Autoscaler.

50. Brinkerhof, J., Tracerlog no. 61(July, 1954).

51. Hoffpauir, C. L., and Guthrie, J. D., Textile Res. J. 20:617(1950).

APPENDIX I

THE USE OF BETA RADIATION TO MEASURE MOISTURE CONTENT

INTERACTION OF BETA RADIATION WITH MATTER

The use of beta radiation to measure moisture content depends upon the fact that beta rays (high energy electrons) interact with matter. It is beyond the scope or needs of this thesis to undertake a thorough analysis of this very complex phenomenon; however, a brief discussion of selected topics will aid in understanding the capabilities and limitations of the technique. Readers interested in pursuing the subject further are referred to Fearnside (38) for an introduction to the measurement and uses of radioactive materials in the pulp, paper, and allied industries, to Friedlander and Kennedy (39), Rutherford et al. (40), and to Kaplan (41) for more thorough analyses of work and theory. Jordan (42) and a National Bureau of Standards Circular (43) discuss techniques and instruments for measuring radioactivity.

Of a beam of electrons passing through matter, some electrons will emerge unaltered in velocity; some will emerge with a different velocity (direction changed and/or speed reduced) from that with which they entered; and some will be so dissipated that they can no longer be detected. Electrons which emerge at an angle greater than 90° to the incident angle are said to be "backscattered." It is also possible that some additional electrons will be dislodged from the material and may emerge. There will also be emitted a certain amount of "bremsstrahlung," X-rays caused by interaction of the electrons with coulombic fields of atoms.

Beta rays have velocities high enough to require relativistic mathematical treatment of interaction. In addition, all natural beta-emitters produce a continuous spectrum of radiation energy ranging from zero to a maximum energy which is characteristic of the nuclear disintegration producing the radiation. Calculation of interaction is therefore extremely complex and empirical measurement of absorption and scattering is generally employed.

It has been experimentally shown that absorption, scattering, and bremsstrahlung are functions of the energy of the electron, the atomic number of the material, and the mass per unit area of the material through which the electrons are passing. Absorption of an electron of given energy is a relatively weak function of the atomic number of the absorber but is a strong function of the mass per unit area of the absorber. Absorption decreases as the energy of the radiation increases. Beta rays are conveniently characterized by their "range," which is the maximum mass per unit area through which the radiation will pass. Various correlations of range with electron energy have been proposed (39, 41).

Backscatter increases as the atomic number of the matter increases. It increases with mass per unit area until about 1/4 the range of the electron is reached; then further increases in mass per unit area do not appreciably increase backscatter. The energy of the radiation has little effect on the percentage of radiation backscattered (39, 41).

Muller (44) has shown that an average atomic number which correlates well with the amount of backscatter from a given source is defined as

$$\bar{Z} = \underline{n}(\underline{A}_B\underline{Z}_B) + \underline{m}(\underline{A}_C\underline{Z}_C) + \ldots / \underline{n}\underline{A}_B + \underline{m}\underline{A}_C + \ldots$$

where $\bar{Z}$ = average atomic number

$\underline{Z}$ = atomic number;

$\underline{A}$ = atomic weight

for the compound $\underline{B}_n\underline{C}_n$. . .

Using this average, pulp and water have atomic numbers of 6.8 and 7.2, respectively, so the backscatter from these should be small and nearly equal for any given source of radiation. Furthermore, as shown in Appendix II, backscatter from aluminum is sufficiently similar to that of pulp and water to allow it to be used as a hot surface.

Bremsstrahlung is of importance only for high-energy electrons in materials of high atomic number (40).

Thus, for a given source of radiation, the predominant factor affecting the radiation is the mass per unit area through which the electrons pass. The greater the mass per unit area between the source of radiation and the radiation detector, the less energy will radiation received at the detector possess. With a possible exception for high-energy electrons passing through very little mass per unit area of matter, the total number of electrons received at the detector will also decrease. By providing that backscatter from material behind the source is small or constant and by standardizing relevant external variables, either the percentage transmission of electron energy or the percentage of electrons transmitted can empirically be quantitatively related to the mass per unit area of material between the source and the detector.

The technique for following drying, then, depends upon the transmission of beta rays of the mass per unit area of water between the source of radiation and the radiation detector. If this percentage transmission of beta rays can be recorded as a function of time, an empirically determined relationship can be used to convert the beta-ray transmission at any time to the mass per unit area of water between the radiation source and the radiation detector.

CHARACTERISTICS OF BETA RADIATION FROM RADIOACTIVE MATERIAL

Beta radiation is a flux of high-energy electrons emitted by the spontaneous disintegration of nuclei. The emission is independent of the chemical or physical state of the material. There is no preferred direction of emission of any electron, so the angular distribution from a source is uniform. For a given isotope, the radiation has an energy distribution between zero and a maximum which is characteristic of the isotope.

The average emission rate of beta radiation with respect to time is strictly a first-order reaction and can conveniently be characterized by the half-life of the isotope. Instantaneously, however, the rate of disintegration of nuclei is subject to statistical fluctuations about the mean value, since it is the sum of a number of random individual events. As the number of events counted becomes large, the distribution of measured emission rate approaches the Poisson distribution, in which the standard deviation of the emission rate is equal to the square root of the emission rate. The more emissions counted, the more accurate is the measurement of the emission rate. Conversely, for any given level of statistical reliability, there is a minimum number of emissions which must be counted.

When the counting rate is not changing, as long a time as is required can be used to obtain the necessary number of counts. When the counting rate is changing, the time allowed for a measurement is restricted by the rate of change. The faster the rate of change, the less time is available to accumulate the number of counts necessary for any given level of reliability; consequently, there is a minimum rate at which radiation must be incident upon the detector. This point will be given further treatment in a subsequent section of this Appendix.

APPARATUS FOR DETECTION AND MEASUREMENT OF BETA RADIATION

There are many different types of radiation detectors. The interested reader is referred to references 42, 43, and 45 for successively more complete discussions of them. The requirements and limitations of this work exclude the use of many of the types. As shown later in this Appendix, instrumental precision must be about ±1%, and counting rates up to 200,000 counts per minute are required. This rate is too low to obtain sufficient precision with an ion chamber or DC-scintillation detector with an electrometer of any existing type. Detectors operated in the Geiger region are excluded from consideration as they have a "dead-time" following each pulse of 50-150 microseconds. During this time the tube is in a discharged state and incident radiation is not detected. The percentage of radiation not counted during this time is called "coincidence loss." At the counting rate required for this work, this loss would be appreciable.

The choice is primarily limited to a proportional counter or a scintillation detector. The former is a gas-filled tube with a voltage gradient such that some secondary electrons are emitted but complete

discharge does not occur when an electron enters the tube. The latter instrument contains a phosphor which emits a light pulse when an electron strikes it. The light pulse is received by a photomultiplier tube which converts the light pulse to an amplified electronic pulse. Both of these detectors have proportional characteristics; i.e., the size of the output electrical pulse is related to the energy of the beta ray which caused it.

Correspondence and consultation with men at instrument companies and at the Argonne and Oak Ridge National Laboratories indicated that there is no clear-cut choice between the two types of detectors for this work. A proportional counter is a simpler instrument, but it produces a weaker pulse than a well-designed scintillation detector. Furthermore, it appeared that considerable experimentation concerning physical size and gas composition might be required to develop a suitable proportional counter, whereas a suitable scintillation detector was commercially available. On this basis, a scintillation detector was selected.

There are two common ways of converting the reception of pulses to rate of reception. The simpler is to measure either the time required to collect a given number of pulses or to measure the number of pulses collected in a given time interval. For this, scaling circuits are employed. These are essentially electronic digital counters; every time a pulse is received, the circuit is triggered and assumes a new configuration characteristic of the total number of pulses which it has received. The units are binary in nature but are easily designed to read directly in the decimal system.

The other method of converting pulse reception to rate of reception is to use a ratemeter. This in principle requires a capacitor shunted by

a resistor. Each pulse is made to deposit a constant charge of electricity on the capacitor. It is easily shown that the equilibrium voltage when the counting rate is constant is $V = NqR$

where V = voltage across the capacitor, volts

N = average pulse rate, counts per second

q = charge per pulse, coulombs

R = resistance of the shorting resistor, ohms.

It can be seen that the reading on a voltmeter connected across the capacitor is directly proportional to the counting rate.

Another value characteristic of a ratemeter circuit is its "time constant," RC, where C is the capacitance of the capacitor in farads and R has the definition just given. RC is the time required for a given charge on a capacitor to fall to $1/e$ of its initial value when no charge is being added.

Schiff and Evans (46) present a mathematical analysis of ratemeter statistics. They show that a ratemeter gives a better estimate of a steady or slowly changing counting rate than does a scaler, once equilibrium has been reached and provided that RC is small compared to the time derivative of the counting rate. Within this limitation, the greater is RC, the better is the estimate, since a larger number of counts is on the capacitor and is included in the estimate. However, if RC is not small compared to the time derivative of counting rate, a bias is obtained. Furthermore, the time to reach equilibrium from startup is a function of RC and N, so that for estimates of counting rate shortly after startup, a scaler is more accurate. Because of the possible bias and because of the time lag

introduced at startup with a ratemeter, a scaler was selected as the more desirable and versatile instrument for this work.

SELECTION OF A RADIOACTIVE ISOTOPE

The choice of a suitable isotope for the radioactive source is dictated by both theoretical and practical considerations. From the theoretical viewpoint, the choice of an isotope depends primarily upon the energy of emission of the radiation. This must be a compromise between sensitivity (change in transmission of beta rays per unit change in mass per unit area of water) and the range of mass per unit area which can be studied. The more energetic the electrons, the less will be the absorption by a given mass per unit area, hence the greater mass per unit area that can be studied. However, to measure a given change in mass per unit area, a greater precision of measurement of beta-ray transmission is required. This requires more stable and precise instruments and also requires a more intense source of radiation to obtain the necessary statistical accuracy within a given amount of time.

From a practical viewpoint, the isotope should be free of gamma radiation, since this would contribute a high background count even for a sheet infinitely thick to beta radiation. Gamma radiation would also contribute an additional health hazard. For these same reasons, it should decay to a gamma-free product. The isotope should also have a half-life of at least a few months. It should be obtainable in a state free of other radioactive emitters, preferably at moderate cost. The following section of this Appendix contains an analysis of isotopes which fulfill these requirements.

PRELIMINARY DESIGN CALCULATIONS FOR THE BETA GAGE

Selection of an Isotope

It is a fortuitous fact that the exponential absorption law provides a fair approximation to the transmission of beta radiation by matter (38). For design purposes, then,

$$T = \exp(-\mu_a x) \qquad (2)^*$$

where T = transmission by matter of beta rays, dimensionless

μ_a = absorption coefficient by matter of beta rays, $(mg./cm.^2)^{-2}$

x = mass per unit area of matter, $mg./cm.^2$

is used, even though it must fail badly at very low values of transmission since beta rays have a rather well-defined maximum range in matter. Friedlander and Kennedy (39, p. 164) present a graph of range in aluminum as a function of the energy electrons. Varder (35) shows data which indicate that absorption by paper is similar to absorption by aluminum.

It is also an empirical fact that the mass per unit area which absorbs 50% of the incident radiation, $x_{1/2}$, the "half thickness," is from 10 to 20% of the range, R (39). Thus,

$$x_{1/2} = R/5 \text{ to } R/10 \qquad (3)$$

depending upon the energy distribution from the isotope, the characteristics of the radiation detector, and the geometry used.

Substitution of $T = 0.5$ and $x = x_{1/2}$ into Equation (2) shows that the absorption coefficient, μ_a, is related to the half-thickness of the isotope by

$$0.693/x_{1/2} = \mu_a \qquad (4)$$

*This notation is equivalent to $T = e^{-\mu_a x}$

Taking the derivative of Equation (2),

$$dT/dx = -\mu_a \exp(-\mu_a x) = -\mu_a T. \qquad (5)$$

Substituting (4) into (5),

$$(1/T)dT/dx = 0.693/x_{1/2}. \qquad (6)$$

Thus, the "sensitivity" of the isotope, the fractional change in transmission for a unit change in mass per unit area of absorber, is equivalent to $0.693/x_{1/2}$, which is the absorption coefficient, μ_a.

Table VIII lists three isotopes available from Oak Ridge which satisfy the practical considerations given in the last section. For this table, the half-life and the maximum energy are taken from the Oak Ridge Catalog (47). The range is read from reference (39, p. 164), which is a graph of range versus maximum energy. The half-thickness of the isotope is calculated from Equation (3). The sensitivity is calculated from Equation (6), using the average value for half-thickness.

TABLE VIII

CHARACTERISTICS OF AVAILABLE BETA EMITTERS

Isotope	Half-Life, yrs.	Max. Energy, m.e.v.	Range, R mg./cm.^{2}	Half-thickness, $x_{1/2}$, mg./cm.^{2}	Sensitivity, μ_a, (mg./cm.^{2})$^{-1}$
Sr^{90}-Y^{90}	25	2.18	1200	120-240	0.0038
Tl^{204}	2.4	0.78	300	30-60	0.015
Ca^{45}	0.45	0.26	50	5-10	0.092

It can also be shown that the half-thickness of an isotope affords a reasonable estimate of the useful dry basis weight of sheets that can be studied during drying. Assuming that the sheets have an initial moisture content of 200%, a reasonable estimate for the moisture content obtained

after drainage and expression of water from a sheet, then there will be a three-fold change in mass per unit area between the initial wet sheet and the ovendry sheet. As will be shown subsequently, the minimum desirable transmission is about 10%. This would correspond to a 10-fold change in the time required for any given number of counts. Substituting Equation (4) into Equation (2),

$$\underline{T} = \exp(-0.693\ \underline{x}/\underline{x}_{1/2}), \text{ or}$$

$$\ln \underline{T} = -0.693\ \underline{x}/\underline{x}_{1/2}. \qquad (7)$$

Substituting $\underline{T} = 0.1$ and $\underline{x} = \underline{x}_{0.1}$ and combining constants,

$$\underline{x}_{0.1}/\underline{x}_{1/2} = 3.3 \qquad (8)$$

A sheet having a dry basis weight of 1.1 half-thickness and a moisture content of 200% would have a total mass per unit area of 3.3 half-thicknesses, and a transmission of 10% compared to the bare source. Sheets of twice this basis weight could be studied from only about 100% initial moisture content.

Table VIII then serves as a useful guide to isotope selection. Using Ca^{45}, it would be possible to study the drying of sheets up to a maximum basis weight of 5 to 10 mg./cm.^{2}; a 1 mg./cm.^{2} change in basis weight would cause a change in beta-ray transmission of about 9.2%. With Tl^{204}, sheets up to 30-60 mg./cm.^{2} could be studied, but the change in beta-ray transmission would be 1.5% per mg./cm.^{2}. Sr^{90}-Y^{90} is the most energetic source which meets practical considerations. The maximum dry basis weight of sheet which could be studied would be 120-240 mg./cm.^{2} from 200% initial moisture content, from 240-480 mg./cm.^{2} if an initial moisture content of 100% were satisfactory. A change of only 0.38% in beta-ray transmission can be expected from a change of 1 mg./cm.^{2} using this isotope.

Estimates from TAPPI Data Sheets 155 (7) showed that the total drying time for the heaviest sheets which could be studied with Ca^{45} might be well under one minute, even at hot surface temperatures considerably below the boiling point. In view of this, and of additional handling and detection problems which might arise with such a weak beta source, it was therefore decided to start with Tl^{204} and work with heavier sheets, even though Ca^{45} might later prove to be desirable for studies of light sheets or light increments of heavy sheets.

Estimation of Counting Rate and Instrument Precision Required

It was shown in the previous section of this Appendix that sheets up to about 7.5 mg./cm.^{2} would be most accurately studied using Ca^{45} for a beta emitter. Therefore, 15 mg./cm.^{2} is used as an estimate of the basis weight for which Tl^{204} is employed.

Estimates from TAPPI Data Sheets 155 (7) indicate that the drying rate for such sheets at 212°F. under good mill conditions is about 1.7 lb./hr. ft.^{2}, or 0.23 mg./cm.^{2} sec. McCready (19), drying laps with one side in contact with a hot surface, found drying rates somewhat higher than this. For a safe-side estimate of the length of a drying run, the TAPPI rate is doubled. The time of a run for a sheet of 200% initial moisture content is

$$\theta = 15 \times 2/0.23 \times 2 = 65 \text{ seconds.}$$

Assume that a standard deviation of 5% of the sheet weight is acceptable precision for the moisture content of a sheet. The estimated sensitivity for thallium is 0.015(mg./cm.)$^{-1}$. The change in transmission corresponding to this precision is

$$0.05 \times 15 \times 0.015 = 0.011$$

Thus, the instruments used must be precise and reproducible to within 1.1%. In addition, sufficient counts must be detected for each scaled point to have a standard deviation of 1.1%. This number of counts is given by Poisson's relationship, $\sigma_n = 1/\sqrt{n} = 0.011$. From this, $n \cong 8000$ beta rays received per scaled interval.

Assume further that 5 seconds is the longest interval which can be tolerated for a determination. This would occur in the first interval after the start of a run, when the transmission is lowest. The required initial counting rate is 8000 x 60 / 5 = 96,000 c/min. The wet sheet has a total mass per unit area of 45 mg./cm.^{2}. This corresponds approximately to the estimated half-thickness of the isotope, so the initial transmission is about 0.5. Reception from the source must, therefore, be 96,000/0.5 = 192,000 c/min. At 1% geometry, the total source required is 192,000/0.01 = 1.9×10^7 c/min. One microcurie, (μc), equals 3.7×10^4 c/sec. so the source required is approximately 9 μc. The product obtainable from Oak Ridge (47) contains 50-300 mc./g. Nine μc. corresponds to 0.55-0.17 mg. of solids.

The maximum mass per unit area which can be studied is limited by the minimum transmission which can be tolerated. In the previous section, this was assumed to be 0.1. This is defined as $N_{min.}/N_s$. The maximum value of N_s, the counting rate from the source, is limited by the resolution time of pulse amplifying and scaling circuits. The coincidence loss when the source is being counted must be less than the minimum precision required; otherwise there would be bias introduced which would be a function of the counting rate from the source. About 1 μ sec. is the smallest resolution

time for available standard instruments. The coincidence loss becomes 1% at 600,000 c/min. for such an instrument, so this represents the approximate maximum rate.

The minimum counting rate is determined by the maximum length of time available to obtain a statistically reliable estimate of the initial moisture content. Assuming that 10 seconds is allowable for the heaviest sheets to be studied, and 1% statistical accuracy is desired, 10^4 counts must be obtained in 10 seconds; the counting rate is 60,000 c./min. Thus, the minimum transmission is about 60,000/600,000, or 0.1.

In view of the many interrelated estimates and assumptions required, calculated values are only approximations. They show, however, that extraordinary precision is not required of the instruments, nor is a prohibitively large amount of radioactive material needed to obtain sufficient precision for this work.

APPENDIX II

COMPARISON OF BACKSCATTER FROM PULP AND ALUMINUM

Because aluminum has a higher atomic number than pulp or water, a greater percentage of beta radiation incident on it is backscattered. For studies of over-all drying rates of sheets, this is of no importance. The effective source of radiation would be direct radiation from the isotope mounted on the hot surface plus radiation backscattered from the hot surface into the solid angle subtended by the detector. The empirical calibration curve obtained would be for this invariant effective source.

For studies of the drying of fractional thicknesses of sheets, backscatter could introduce an error if backscatter from the hot surface were appreciably different from backscatter from the matrix being dried. As the material between the source of radioactivity and the hot surface dried, the intensity of the radiation reaching the hot surface would increase. As a result, the fraction of radiation being backscattered would change. The net radiation received at the detector would then depend not only upon the mass per unit area of material between the source and the detector, but also upon the mass per unit area of material between the source and the hot surface.

An attempt was made to construct a surface which could be uniformly heated by passing an electric current through a carbon resistance painted on a slab of Masonite. Such a unit would have an average atomic number very close to that of pulp and water. Uniform heating of such a surface was found to be possible, but sensitive, accurate control of the temperature proved to be very difficult. Heating of an aluminum plate by circulating

liquid appeared to be simple and more convenient if the difference in backscatter between pulp and aluminum could be tolerated.

The following experiment was conducted to see whether the difference in backscatter between aluminum and pulp could be tolerated. The radioactive source for this work consisted of material from a RaE capsule which was dissolved in aqua regia and precipitated with sodium hydrogen sulfide. The material was washed and mounted between two strips of Scotch tape. Scotch tape is infinitely thick to alpha radiation but transmits most of the beta radiation. RaE emits very little gamma radiation, and Geiger tubes are much less sensitive to gamma than to beta radiation, so the effective source being counted was a beta emitter of $E_{max.}$ = 1.17 M.e.v.

Two backings of equal thickness were made up, one of aluminum and the other of Masonite. Both were infinitely thick to the beta radiation. A thin-window Geiger tube was mounted 2 inches above the source. The counting rate for the source on the two different backing materials with various amounts of paper between the source and the detector is given in Table IX. The data are seconds for 10,000 counts. The values are averages for at least 10,000 counts, so have a standard deviation of 1% or less.

TABLE IX

COMPARISON OF ALUMINUM AND MASONITE BACKING

Paper Over Source, mg./cm.^{2}	Counting Rate, sec./10^4c. with Backing Material Stated, Aluminum	Masonite
0	65.1	65.7
7.6	70.8	71.4
15.2	78.8	78.4
25.0	84.8	86.4

From these data, it appears that the difference in the amount of radiation backscattered from Masonite as compared to aluminum is less than 1% of the total amount of radiation.

As an additional check, an infinite aluminum backing was used and various amounts of paper were placed between the source and the backing. Various amounts of paper were also placed between the source and the detector. The results are given in Table X. The data are seconds for 10,000 counts and have a standard deviation of 1% or less.

TABLE X

EFFECT OF INSERTION OF PAPER BACKING ON COUNTING RATE

Paper Over Source, mg./cm.^{2}	Counting Rate, sec./10^4c., with mg./cm.^{2} Paper Stated Between Aluminum and Source,		
	0	7.6	25.0
0	68.1	67.8	68.7
7.6	74.1	73.9	74.5
25.0	89.1	86.8	86.6

These data show no significant effect caused by the insertion of paper between the source of radiation and the aluminum backing.

APPENDIX III

DEPOSITION OF THALLIUM ON ALUMINUM FOIL

In the first attempt, the thallium nitrate was deposited by evaporation of the solution onto a sheet of 0.0015-inch aluminum foil. This was backed by a sheet of 0.003-inch foil, and the edges were sealed. It proved impossible to draw this taut over the hot plate, so the backing foil was discarded and only the top foil was used. After several days use, the foil was removed, and it and the hot plate were scanned. The radioactive material was found to have migrated over the hot surface, apparently due to water which had seeped past one of the screws. A better method of deposition had to be found.

Thallium has valence states of +1 and +3. The former behaves similarly to the alkali metal salts, forming soluble hydroxides and insoluble sulfides. The latter is similar to aluminum. Thallium is lower in the electromotive series than aluminum. $TlNO_3$ melts at 810°F.

Based on these facts, it appeared that precipitation of thallium as the sulfide might prevent solution in any water seeping over it. Fusing of it to the foil should prevent mechanical transport by moving water.

A series of experiments was conducted using a solution of radioactive thallous nitrate diluted with carrier thallous nitrate to an activity of about 1 μc./mg. The solution contained about 8 μc./ml. In the experiments, 50 ml. of thallous nitrate solution was deposited evenly on sheets of 0.0015-inch aluminum foil which were on a hot plate at about 140°F. Each foil was then monitored under constant geometry with a thin-window Geiger tube. The foils were heated in a muffle furnace at 900°F., then monitored

again. They were rubbed with a piece of cotton containing 20% ammonium sulfide solution, rinsed with warm water, and soaked at 120°F. for one hour. Between each treatment, the foils were monitored under constant geometry with the Geiger counter.

It was found that fusion followed by sulfide treatment did present a satisfactory means of immobilizing the thallium; however, much of the radioactive material was vaporized in the muffle furnace. This could be reduced by using a preheated muffle furnace and by shielding the foil from direct radiation from the heating elements of the furnace. Further significant reduction of losses during heating was obtained by treating the foil with hydrochloric acid solution after the thallium had been deposited on it. Increasing acid concentration up to about 0.5 N decreased losses during heating; increasing concentration above 0.5 N had less effect. Precleaning the foil with steel wool caused no change in vaporization loss or in resistance to removal by water. Dilution of the thallous nitrate solution from 50 µl. to 2 ml. before adding it to the foil caused a slight increase in loss during heating.

Based on these experiments, the following procedure for source preparation was adopted:

1. Radioactive thallous nitrate solution containing the desired amount of radioactivity was spread in a 1-inch circle on the center of a 0.0015 by 3.5 by 9-inch sheet of clean aluminum foil. The foil was on a hot plate at about 140°F. and was held at that temperature until the foil had dried.

2. The area over which the radioactive material had been spread was treated with 4 drops of 2 N hydrochloric acid.

3. The foil was heated for 1/2 hr. in a muffle furnace which had been preheated to 850°F. The foil was shielded from direct radiation of the heating coils with a separate sheet of aluminum foil.

4. After the foil had cooled, ammonium sulfide solution was spread on the foil area containing the radioactive material.

5. The foil was rinsed with warm water.

As a precaution against water seepage around the screws holding the top of the hot surface to the base, a piece of tissue paper was placed at each end of the hot plate with one edge of the tissue covering the screws and the other edge extending over the end of the hot surface. This served to conduct any water seepage from the screws off of the hot surface.

The foil on which the source was deposited was mounted on the hot plate, the side containing the thallium down, by wrapping each end around a strip of aluminum 1/8 by 1/4 by 4 inches. Each aluminum strip contained three holes; wood screws were passed through the holes and were screwed into the wooden base on which the hot surface was mounted, thus pulling the foil taut over the hot surface. Using this procedure, less than 1/3 of the radioactive material may be lost by vaporization in the muffle furnace; losses in other steps during preparation of the source are less than 5%. Vaporization losses could probably be minimized by further investigation of the temperature-time conditions in the muffle furnace. Since only one source was to be prepared, the above loss could be tolerated, so no further refinements were attempted.

A 20 μc. source was made by this procedure. The source was mounted on the hot surface without any tissue over the screws, and water at 200°F. was circulated through the hot plate for 18 hours. The source was removed, and it was found that over 95% of the radioactive material was still in its initial position on the foil. Of the radioactive material on the hot surface, 85% was found to be on the area in direct contact with the radioactive portion of the foil.

On subsequent occasions, tissue was used to cover the screws. At various times during the conduct of the work, the hot surface was monitored. Radiation from any area except that directly in contact with the radioactive area of the foil was never more than 0.4% of that from the source.

APPENDIX IV

CALIBRATION OF THE SOURCE FOR OVER-ALL DRYING-RATE STUDIES

FACTORS AFFECTING THE CALIBRATION CURVE

The factors influencing the selection of an isotope and instruments suitable for this work have been discussed in Appendix I. For a given isotope and for the particular detector and scaler used, the following factors could influence the calibration curve:

1. the atomic number of the absorber being calibrated,
2. the size and shape of the source,
3. the distance and position of the detector with respect to the source,
4. the amount of other materials between the source and detector,
5. certain instrument settings; viz., the gain of the preamplifier, the voltage across the photomultiplier dynodes, and the input sensitivity of the scaler.

In addition, any external factors which affect preamplifier gain or scaler sensitivity, such as ambient temperature changes, drafts, large stray magnetic fields, and variations in input voltage might be expected to influence the calibration curve. At high counting rates where the coincidence loss of the circuit becomes appreciable, the calibration curve becomes a function of the absolute counting rate of the source. Changes in backscatter could affect the calibration curve, but the data in Appendix II show that this effect is small enough to be tolerated in this work.

Of the major variables affecting calibration, the atomic number of pulp and water are fixed. For the others, there are, in general, factors which limit and influence the choice.

The size and shape of the source can be varied from a point up to the size of the sample being dried. However, the source should be large enough to give the average mass per unit area of a fairly large area, but when possible should be somewhat smaller than the sheet so that drying of the area near the edges will not be included in the results. Theoretical considerations also indicate that the sensitivity of the beta gage is increased, but that the counting rate for any given amount of radioactivity is decreased, as the source becomes larger. A 1-inch circular source was selected for studying the over-all drying-rate of sheets.

The detector head was placed directly above the center of the source since this position minimizes the percentage backscatter. The distance from the source to the detector is primarily dictated by a compromise between interference with insertion and startup procedures and the amount of radiation required, although certain other factors also deserve consideration. Changes in the mass per unit area of air between the source and detector caused by heating or by barometric fluctuation would have to be accounted for if the distance were great. If the distance were small, difficulty would be encountered in positioning the head with sufficient accuracy, should it have to be removed and replaced for any reason. A distance of 1-5/8 inches from the center of the detector head to the center of the hot surface has been selected.

The choice of instrument settings should not be critical when the scintillation head and scaler are functioning properly (48, 49). A

discussion of their effect is given in references (49) and (50). It has become customary to preset all scalers to 0.25 v. input sensitivity and to design detectors to generate pulses of this size. The choice of instrument settings thus devolves into choosing a suitable combination of preamplifier gain and dynode supply voltage. For any gain setting, there is a voltage "plateau," a range in which the percentage change of counting rate is a minimum for a given change in voltage. Instruments are operated on this plateau, and it was found that the sensitivity of the beta gage was independent of the voltage setting on the plateau. As the gain of the preamplifier is increased, the plateau counting rate increases, the sensitivity of the beta gage increases, the plateau slope decreases, and the plateau length decreases. A fairly high amplifier gain was selected, and the dynode supply voltage operated just below the middle of the plateau.

CALIBRATION PROCEDURE

To determine the calibration curve for water, wet handsheets were made and cut to approximately 2.5 inches square. These sheets were air dried to approximately the desired moisture content, were sealed in aluminum foil 0.00035-inch thick, and were allowed to stand overnight in polyethylene bags. Each wrapped sheet was weighed on an analytical balance, clamped to the hot surface beneath the wire-and-shim clamp, and the counting rate at the detector determined. The counting rate of the bare source was also determined. Each sheet was unwrapped and clamped on a cold drier with a spring-loaded screen. The sheet was air dried while clamped, then heat was applied and the last of the moisture in the sheet removed. The dry sheet weight and the dry weight of the foil used for wrapping the sheet

were determined. The percentage transmission of each dry sheet was determined; then each dry sheet was trimmed, weighed, and measured to determine the mass per unit area.

It was necessary to correct the data thus obtained for the presence of the 0.00035-inch foil used for wrapping the wet sheets. To do this, the transmission of a series of dry sheets was determined with and without the foil being present. It was also necessary to correct the data thus obtained for the extra sheet of 0.0015-inch foil which would be present when sheets were being dried. The presence of this extra sheet of aluminum foil is explained in the section concerning preparation of sheets for drying studies. The data for this correction were obtained by determining the beta radiation transmission of a series of sheets with and without the extra sheet of foil present.

To provide a convenient check of the performance of the instruments over a period of time, a sheet of 0.003-inch aluminum foil was selected and used as a standard absorber. Before every set of runs, or whenever equipment was moved or changed, the transmission of this foil was checked to determine whether the beta-gaging apparatus was in calibration.

CALIBRATION DATA

Tables XI and XII contain the data for calibration of the beta gage for over-all drying-rate studies. The source was 1 inch in diameter, prepared as described in Appendix III. The scintillation head was mounted 1-5/8 inches directly above it. The preamplifier gain was approximately 12. The high voltage was 1400 v. The transmission of the calibrated foil was 0.757 when the wet sheets were counted, 0.770 when the dry sheets were counted.

TABLE XI

CALIBRATION OF SOURCE FOR OVER-ALL DRYING-RATE STUDIES

Sheet No.	Wt. of Wet Sheet and Foil, g.	Foil Wt. g.	Wet Counting Rate, c./min.x10^{-4}	Dry Sheet Wt., g.	Dry Counting Rate, c./min.x10^{-4}	Source Counting Rate for Dry Sheet, c./min.x10^{-4}	Dry Trimmed Sheet Length, in.	Dry Trimmed Sheet Width, in.	Dry Trimmed Sheet Wt., g.
no sheet	--	--	60.7	--	--	--	--	--	--
35	0.49	0.38	56.4	0.07	45.0	45.6	2.25	2.62	0.064
37	0.69	0.39	53.5	0.15	44.4	45.5	2.31	2.62	0.126
38	0.65	0.43	54.3	0.14	44.5	45.7	2.62	2.25	0.123
39	0.83	0.37	50.8	0.24	43.6	45.8	2.69	2.38	0.208
41	0.97	0.38	48.9	0.31	43.0	45.9	2.31	2.69	0.268
42	1.18	0.40	45.4	0.31	42.6	45.3	2.38	2.69	0.277
43	1.23	0.39	44.3	0.31	42.6	45.4	2.31	2.69	0.266
44	1.40	0.39	41.4	0.32	--	--	2.38	2.75	0.279
45	1.41	0.39	41.9	0.59	39.4	45.6	2.38	2.75	0.533
46	1.56	0.40	39.3	0.59	39.6	45.3	2.38	2.81	0.551
47	1.89	0.40	34.9	0.59	39.3	45.5	2.06	2.31	0.389
48	2.04	0.41	32.7	0.60	40.6	46.1	2.44	2.81	0.560
49	2.90	0.41	22.8	0.99	34.7	45.6	2.62	2.75	0.887
50	3.43	0.39	18.3	0.91	35.9	45.5	2.31	2.69	0.762
52	4.03	0.41	13.2	1.25	32.0	46.1	2.44	2.69	1.11
53	4.32	0.39	10.7	1.23	31.9	45.5	2.38	2.69	1.06
54	5.63	0.39	5.0	1.25	--	--	2.44	2.75	1.11
55	5.82	0.40	4.2	1.78	25.0	45.4	2.38	2.69	1.54

TABLE XII*

BETA-RAY TRANSMISSION OF ALUMINUM FOILS

Sheet	0	0.0007-inch Al Foil	0.0015-inch Al Foil	Bare Source Only
none	--	43.6	41.2	44.8
55	24.2	22.0	19.7	44.7
53	31.0	28.7	25.8	44.7
49	34.0	31.7	28.6	44.6
47	38.6	36.3	33.3	44.6
43	41.7	39.9	36.9	44.5
53+55	13.3	12.1	10.6	44.4
55	24.1	--	--	44.4

*Data are counts per minute times 10^{-4} with the given sheet of paper and the given amount of aluminum foil between the source of radiation and the radiation detector.

SAMPLE CALCULATION

Sheet 47

1. The mass per unit area of a dry sheet, $\underline{x}_d$, is mass of the sheet divided by the area of the sheet. The mass of the dry sheet in grams is numerically equal to the weight of the dry sheet in grams.

$\underline{x}_d = (1000)(0.389)/(2.06)(2.31)(2.54)^2 = 12.7$ mg./cm.^{2}

The factor 1000 converts the weight in grams to the weight in milligrams. The factor $(2.54)^2$ converts the area in square inches to the area in square centimeters.

2. The beta-ray transmission of dry sheets is the ratio of the counting rate observed when the sheet is between the radiation source and the radiation detector to the counting rate observed when no sheet is between the source and the detector.

$$T_d = 39.3/45.5 = 0.864$$

The calibration for dry sheets placed between the source and the detector is obtained by plotting (2) as ordinate against (1) as abscissa. This corresponds to the time when the instruments show a transmission of 0.77 for the calibration foil.

3. The wet weight of the sheet is the weight of the wet sheet and foil less the weight of the foil.

Wet wt. = 1.89 - 0.40 = 1.49 g.

4. The weight of water in the sheet is the wet weight of the sheet less the dry weight of the sheet.

= 1.49 - 0.59 = 0.90 g.

5. The mass of water per unit area in a sheet is the mass per unit area of the dry sheet times the ratio of the weight of water in the sheet to the dry weight of the sheet.

$\underline{x}_w = (12.7) \times (0.90)/(0.59) = 19.4$ mg./cm.^{2}

6. The transmission of the wet sheets and foil is the ratio of the counting rate when the wet sheet and foil are between the source and detector of radiation to the counting rate when nothing is between the source and the detector.

$\underline{T} = N/N_o = 34.9/60.7 = 0.574$

This corresponds to a calibration foil transmission of 0.757.

7. The transmission of wet sheet and foil corresponding to a calibrated foil transmission of 0.757 is converted to the equivalent transmission when the calibration foil transmission is 0.770. This is done by assuming that the relative absorption (1 minus transmission) of a sheet is proportional to the relative absorption of the calibrated foil.

The absorption of sheet 47 is

$= 1 - 0.574 = 0.426$

when calibration foil absorption is

$= 1 - 0.757 = 0.243.$

When calibration foil absorption is

$= 1 - 0.770 = 0.230,$

the corresponding absorption of sheet 47 is

$= 0.426 \times (0.230/0.243) = 0.404.$

The transmission of sheet 47 corresponding to a calibration foil transmission of 0.770 is

$$= 1 - 0.404 = 0.596.$$

8. The transmission of the foil used for wrapping the wet sheets is determined. To do this the data of Table XII are employed. For each sheet in Table XII the transmission of the foil is calculated as the ratio of the counting rate when the sheet and foil are between the source and detector to the counting rate when only the sheet is between the source and detector. The transmission of the sheet and foil is calculated as the ratio of the counting rate when the sheet and foil are between the source and detector to the counting rate when nothing is between the source and detector. These results are put into graphical form with the transmission of the sheet and foil as the abscissa and the transmission of the foil only as the ordinate. For sheet 47, the transmission of the sheet plus foil is 0.596. The foil transmission corresponding to this, read from the graph, is 0.918.

9. The transmission of the wet sheet only is the transmission of the wet sheet plus foil divided by the transmission of the foil.

$$= 0.596/0.918 = 0.649.$$

10. The transmission of the water in the sheet is the transmission of the wet sheet divided by the transmission of the dry sheet.

$$T_W = 0.649/0.864 = 0.752.$$

The calibration curve for water is obtained by plotting (10) as the ordinate against (5) as the abscissa. This corresponds to conditions when the instruments show a transmission of 0.770 for the calibration foil.

11. The calibration curves for both dry sheets and water must be corrected for the fact that a sheet of 0.0015-inch aluminum foil will be present when a drying run is made. This is the foil onto which the wet sheets are couched. To do this, the data of Table XII are employed. The transmission of the 0.0015-inch aluminum foil when no sheet of paper is present is

    = 41.2/44.8 = 0.918.

    The transmission of each sheet when no foil is present is calculated as described in (2). The transmission of each sheet plus 0.0015-inch aluminum foil is calculated and is divided by 0.918. The quotient is the transmission of each sheet when 0.0015-inch foil is present. A graph is prepared from these results showing the transmission of sheets when foil is present, the condition which will exist during a drying run, as a function of the transmission when no foil is present, the value of which was calculated from the calibration data. Using this graph to convert the values calculated for sheet 47, the value for pulp corresponding to 0.864 is 0.813. This value is plotted for the calibration curve for pulp in Figure 9. The value corresponding to 0.752, the transmission of water in sheet 47 is 0.686. This value is plotted for the calibration curve for water in Figure 9.

APPENDIX V

PREPARATION OF SHEETS FOR OVER-ALL DRYING-RATE STUDIES

The sheets used for this work were made from Weyerhaeuser bleached sulfite pulp. Three hundred sixty grams of pulp were soaked overnight in nine liters of deionized water, dispersed for 10 minutes with a Williams stirrer, placed in a 1-pound Valley beater and diluted to 23 liters with deionized water. The beater was run for 5 minutes with no load on the bedplate followed by 20 minutes with 5500 g. on the bed plate. The resulting freeness was 800 ml. Schopper-Riegler.

The sheets for drying were made to the desired basis weight in a British sheet mold. The volume of water used in the sheet mold was the same for all sheets, so the consistency was proportional to the basis weight. The sheets were not couched onto blotters but were couched directly onto a 7 by 7-inch sheet of 0.0015-inch aluminum foil which had previously been cleaned with acetone. The interface with this sheet of aluminum foil subsequently became the hot-surface interface; in this manner, the contact between the hot surface and the sheet was reproducible.

Each sheet was pressed lightly in a flat press with a dry blotter below the foil, a wet blotter in contact with the sheet, and a dry blotter above that. The top blotter was then removed, a fresh dry blotter put in its place, and the stack was run through the Noble and Wood rotary sheet press.

Two sheets for drying studies were cut from each pressed sheet with a guillotine cutter. Each of these sheets was 2.55 by 3.62 inches. Each

sheet was air dried to 0.25 g. less than the desired final weight, and then sprayed with 0.25 g. of a solution of 10% dextrinized starch. The starch solution was prepared by heating in a steam cone for 20 minutes just prior to use. Each sheet was sealed in a polyethylene bag and allowed to stand overnight at 73°F. before being dried.

APPENDIX VI

SAMPLE CALCULATION OF DRYING RUN

As explained in the description of the apparatus, the raw data for a drying run is obtained as a series of photographs of a 1-second full-sweep clock taken at intervals of 10,000 scaled counts. These readings are transcribed into a research notebook. The difference between successive readings is calculated to the nearest 0.01 seconds, and the average time of the interval from the start of a run is calculated to the nearest 0.5 second. These values are shown below for Run 169A.

Frame Reading, sec.	Time for 10^4 Counts, sec.	Time from Start of Run, sec.	Frame Reading, sec.	Time for 10^4 Counts, sec.	Time from Start of Run, sec.
3.39	3.39	1.5	75.37	2.02	74.5
6.67	3.28	5.0	77.40	2.03	76.5
9.87	3.20	8.0	79.39	1.99	78.5
13.03	3.16	11.5	81.39	2.00	80.5
16.09	3.06	14.5	83.40	2.01	82.5
19.09	3.00	17.5	85.37	1.97	84.5
22.00	2.91	20.5	87.36	1.99	86.5
24.75	2.75	23.5	89.31	1.95	88.5
27.49	2.74	26.0	91.26	1.95	90.5
30.21	2.72	28.5	93.23	1.97	92.5
32.83	2.62	31.5	95.15	1.92	94.0
35.40	2.57	34.0	97.13	1.98	96.0
37.89	2.49	36.5	99.06	1.93	98.0
40.35	2.46	39.0	101.01	1.95	100.0
42.80	2.45	41.5	102.95	1.94	102.0
45.20	2.40	44.0	104.90	1.95	104.0
47.52	2.32	46.5	106.84	1.94	106.0
49.80	2.28	48.5	108.78	1.94	108.0
52.06	2.26	51.0	110.67	1.89	109.5
54.31	2.25	53.0	112.58	1.91	111.5
56.54	2.23	55.5	114.51	1.93	113.5
58.71	2.17	57.5	116.41	1.90	115.5
60.87	2.16	59.5	118.30	1.89	117.5
63.01	2.14	62.0	120.22	1.92	119.0
65.14	2.13	64.0	122.14	1.92	121.0
67.19	2.05	66.0	124.06	1.92	123.0
69.27	2.08	68.0	125.98	1.92	125.0
71.32	2.05	70.5	127.89	1.91	127.0
73.35	2.03	72.5	129.82	1.93	129.0

These results are plotted on semilogarithmic paper with the time from the start of a run as the abscissa and the interval for each 10,000 counts as the ordinate. The results for Run 169A are shown in Figure 10. Toward the end of a run, where the counting rate is changing very slowly, the results of averaging 2 or 3 consecutive intervals are plotted. A line of best fit is faired through these points.

At selected times from the start of a run, the faired value of the interval for 10,000 counts is read from the graph. The interval required for 10,000 counts when the sheet is dry (the constant counting rate at the end of a run, $\theta = \infty$) is divided by the interval required for 10,000 counts at each of the selected times. This quotient is the percentage beta-ray transmission of the water in the sheet at that time, T_w. This value is converted to the mass per unit area of water in the sheet at that time by the appropriate calibration curve, Figure 9 for sheet 169A and other sheets for which the 1-inch source mounted on the hot surface was used, Figure 25 for sheets in which the source was deposited within the sheets. These sample calculations for sheet 169A are shown below. These calculated points and the resulting drying curve are shown in Figure 11.

Run 169A

Time from Start of Run, sec.	Faired Time for 10^4 Counts, sec.	Beta-Ray Transmission of Water, T_w	Water in Sheet, X_w mg./cm.^{2}
0	3.45	0.555	28.2
12	3.14	0.610	24.1
24	2.81	0.683	18.8
36	2.54	0.755	13.5
48	2.29	0.837	8.9
54	2.22	0.865	7.5
60	2.15	0.891	5.7
64	2.11	0.910	4.7
68	2.08	0.920	3.2
76	2.03	0.945	2.5
90	1.96	0.977	1.1
∞	1.92	1.00	0.0

For over-all drying-rate studies, such as sheet 169A, the counting rate of the bare source is known, so an independent check of the dry mass per unit area of the sheet is available. The measured counting rate from the bare source is 43.9×10^4 counts per minute.

$$1/N_s = 60/43.9 = 1.365 \text{ sec.}/10^4 \text{ counts.}$$

The transmission of the aluminum foil on which the sheet was mounted is 0.918. The count interval through the foil is $1.365/0.918 = 1.485$ sec./10^4 counts. The transmission of the dry sheet is

$$T_d = 1.485/1.92 = 0.773.$$

Using the curve for pulp of Figure 9, the dry basis weight of this sheet is 15.4 mg./cm.^{2}. This compares with the value of 15.0 mg./cm.^{2} obtained by trimming, weighing, and measuring the dry sheet.

APPENDIX VII

IMMOBILIZATION OF THALLIUM WITHIN A SHEET

There are several requirements for the technique for immobilizing radioactive thallium within a sheet so that the drying of fractional portions of the sheet can be followed. The radioactive material must not move from the zone in which it is originally placed. Therefore, it must not only be insoluble and nonvolatile, but it must be in such a form that it cannot be moved mechanically. The zone in which it is placed must be small both in thickness and in mass per unit area compared to the entire sheet. The presence of the radioactive zone must not affect the moisture distribution or the movement of moisture within the sheet.

PRECIPITATION OF THALLIUM SULFIDE

The first attempt to immobilize radioactive thallium within a sheet was to precipitate it on and in fibers as thallous sulfide. These fibers were to be incorporated into sheets by the procedure described in Appendix VII.

A preliminary experiment was conducted in which radioactive thallium diluted with stable thallium was precipitated on fibers. Thallium 204 diluted 230:1 with stable thallium was used. The pulp was dried to about 20% moisture content, in which condition it absorbed liquid readily. One-fourth cubic centimeter of 3% potassium hydroxide was added to the thallous nitrate solution to make it basic, and the solution was added to 300 mg. of pulp which was on a fritted glass funnel. Six per cent thallium nitrate,

based on pulp weight, was added, and the pulp was allowed to stand overnight, sealed to prevent evaporation. Following this, the pulp was again dried to about 20% moisture content and hydrogen sulfide gas was drawn slowly through the pulp for 4 hours. The pulp was then removed from the funnel, moistened with 20% ammonium sulfide solution, and dispersed in 100 ml. of warm water. It was filtered on a suction funnel, washed 3 times with 10-ml. portions of warm water, and then with 50 ml. The filtrate from each of the last three washes contained less than 0.5% of the radioactive material in the pulp.

The same procedure was used to prepare fibers containing thallium 204 with no additional carrier thallium added. Approximately 2300 microcuries of thallium were precipitated on 1.7 dry grams of pulp. These fibers were suspended in 1 liter of water and incorporated into sheets by the procedure described in Appendix VIII. Each sheet made in the British sheet mold contained about 60 microcuries of radioactive material. Two samples for drying, each 2.55 by 3.62-inches were cut from each sheet. Checks of these sheets after drying showed that much of the initial radioactive material had been lost. Furthermore, the remaining radioactive material was distributed through the sheets. In some cases, more than 50% of the radioactive material was found in parts of the sheet other than that which was intended; the average was about 20%.

An investigation was conducted to determine the cause of this failure and to overcome it. Stable thallium was added to the radioactive thallium which was precipitated onto fibers. Stable thallium sulfide was also precipitated onto pulp from which the nonradioactive laminates of the sheets for drying studies were made. Neither of these procedures reduced the

migration of radioactive material appreciably. An aliquot of the slurry of radioactive fibers used for preparation of the first set of sheets was checked for radioactivity. As much radioactive material could be decanted with the supernatant liquid as was retained with the fibers. Filtration of the supernatant liquid through a fine sintered glass crucible removed nearly all of the radioactive material.

These findings indicate that the migration of thallium was not due primarily to solution of the thallium sulfide but was primarily a mechanical removal of thallium sulfide particles from the fibers. The preliminary experiment was repeated, and it was found that the sintered glass crucible through which the wash liquors were extracted was retaining much of the radioactive thallium.

Attempts were made to reduce the losses of thallium sulfide from fibers by extended washing of the fibers, by pH control during washing, and by using other types of pulp. None of these changes showed any promise of yielding a pulp from which the radioactive material was not dislodged during the sheet-forming process, so the technique of precipitating thallium as the sulfide was abandoned.

INSOLUVILIZATION OF THALLIUM BY ION EXCHANGE

Absorption of metal ions from solution by insoluble derivatives of cellulose is known (51). The reaction involved is

$$\underline{R} - \underline{A} - \underline{H} + \underline{M}^{+} = \underline{R} - \underline{A} - \underline{M} + \underline{H}^{+}$$

where $\underline{R}$ is a cellulose chain, $\underline{A}$ is an acidic group attached to the chain, $\underline{H}$ is a hydrogen atom, and $\underline{M}$ is a metal atom. Attempts were made to attach thallium to oxycellulose of degree of substitution (D.S.) 0.6, to

carboxymethylcellulose of D.S. 0.04, and to cellulose phosphate of D.S. 0.2, and to a hard-cooked neutral sulfite semichemical pulp. The best retention of thallium was obtained by allowing the initial absorption of thallium to occur from an unbuffered solution of thallous nitrate, then to buffer all subsequent slurries of the material containing the thallium at a pH above that at which absorption occurred. Of these materials, cellulose phosphate showed the best retention of thallium. In a 1% slurry of this material in water at 95°C. and pH 10, 91% of the radioactive thallium was retained on the fibers.

Amberlite IR-120, a nuclear sulfonic acid cation-exchange resin retained over 99% of the radioactive thallium under similar conditions. This material, however, comes in the form of pellets, and there was no indication that it had ever been prepared in fibrous form.

Some Amberlite IR-120 was wet ground in a ball mill and fractionated into several cuts of various size by settling in water. Attempts were made to deposit these particles on the surface of laminates formed in a sheet mold and on the surface of sheets of filter paper. In both cases, microscopic examination of the sheets indicated that the particles were distributed through the pores of the sheet. Twenty microns, about 7% of the thickness of a 14 mg./cm.^{2} sheet, was chosen as the maximum particles diameter which could be tolerated. No means could be found of preventing particles of this size from distributing through the pores of a wet sheet.

MECHANICAL ATTACHMENT OF ION-EXCHANGE RESIN TO FIBERS

A possible means of preventing distribution of the ion-exchange resin through a sheet is to attach the resin to fibers with a binder or glue.

Such a material is most conveniently applied to a thin sheet of paper, since the material will bind the fibers together as well as binding ion-exchange particles to fibers.

The first binder tried was animal glue hardened with formaldehyde. Dip coating and brush coating were tried, and the latter was found to be more satisfactory. Spray coating might also have been satisfactory, but special precautions would have been required to spray a slurry containing radioactive material.

A little thallium was added to some -5 μ Amberlite resin so that the resin could be easily located. This resin was dispersed in glue, and the glue was brushed onto 1.1 mg./cm.^{2} hemp teabag stock. The sheets were dipped in a 10% formaldehyde solution, allowed to air dry, then oven dried at 60°C. The sheets were dipped into distilled water and wet-pressed between 14 mg./cm.^{2} laminates made from bleached sulfite. These sheets were then delaminated and the intensity of radiation from each laminate determined under conditions of approximately equal geometry with respect to the detector. With 12% glue on the teabag stock, 25% of the radioactive material was found in the other laminates of the sheet after wet pressing. The teabag stock containing 12% glue was very stiff and had been noticeably decreased in porosity.

Other experiments were conducted in which formaldehyde was mixed directly with the glue solution, and in which a second coat of glue was put over the layer containing the ion-exchange resin. In all cases, excessive migration of radioactive material occurred during wet pressing of the coated laminate into a sheet. An aliquot of the suspension of

Amberlite in glue used to coat the sheets was centrifuged, and over 96% of the radioactive material was removed. Thus, the Amberlite particles were retaining the radioactive thallium, but the glue was not binding the particles to the fibers.

Properties of Sheets Coated with Penacolite G-1131

Penacolite G-1131, a resorcinol-formaldehyde resin made by Koppers, was the next resin tried. Teabag stock was coated with 50, 25, and 12% of resin. Microscopic examination of the coated sheets showed that the resin spread uniformly over the fibers but tended to fillet at fiber crossings. The sheet containing 50% resin was stiff and contained some balls of resin along the fibers. All sheets were too porous to be measured with the Gurley porosity tester. Some sheets were later checked with apparatus which measures the flow rate of air through the sheet at 20 inches water pressure drop across the sheet. Table XIII contains these data. The flow rate of air through the sheet is expressed as air velocity in f.p.m. through a 2-inch tube when the pressure drop across the sheet is 20 inches of water.

TABLE XIII

AIR PERMEABILITY OF COATED SHEETS

Coating Weight, % of 1.1 mg./cm.^{2} Sheet	Air Flow through Sheet, f.p.m.
0	1720
9	1720
25	1510
31	1440
37	1300
55	1170

The porosity of a 3.5 mg./cm.^{2} sheet made from Weyerhaeuser bleached sulfite, prepared as described in the body of the thesis, was less than 300 f.p.m. In this range, the apparatus is very insensitive.

Retention of Radioactive Thallium by Penacolite G-1131

For a preliminary experiment, some Amberlite resin ground to -5μ was made slightly radioactive with thallium 204. This was dispersed in Penacolite resin, and a sheet of 1.1 mg./cm.^{2} teabag stock was coated with about 20% total solids. The initial net counting rate of the sheet was 5.0 counts per second. After soaking for 1 hour in warm, deionized water, the counting rate under the same geometry with respect to the detector was 4.6 counts per second. After being wet pressed between two blotters in the Noble and Wood rotary sheet press, the counting rate was 4.3 counts per second. Each blotter had a net counting rate of 0.05 counts per second. The standard deviation of the counts on the sheet was ±3%.

To determine the effect of coating weight and of the particle size of the Amberlite resin on retention of radioactive thallium, the following experiments were conducted. Some Amberlite was wet ground in a ball mill and fractionated by sedimentation in water into cuts of approximately -20+5, -5+1, and -1μ. The solids content of each cut was determined by oven drying an aliquot. Some $Tl^{204}NO_3$ was added to a portion of each fraction.

Nine sheets were coated by the procedure finally used, described subsequently in this Appendix. The size of the Amberlite particles and the weight of coating on each sheet are given in Table XIV. After being oven dried, each sheet was counted, dipped in distilled water, air dried, and counted again.

Sheets 11, 14, and 16 were torn up, placed in a Waring blender in 400 ml. of deionized water, and defibered by running the blender for 2 minutes. This stock from each sheet was reformed into a sheet in a British sheet mold. Each of these sheets was air dried, cut into approximately the same size as the original sheet and counted.

The six remaining sheets were rewetted by dipping in deionized water and were wet pressed between blotters in the Noble and Wood rotary sheet press. These sheets and the blotters between which they were pressed were air dried and counted.

The radioactive sheets were then wet pressed between two 13.5 mg./cm.^{2} laminates made from bleached sulfite in the manner described in the body of the thesis. These laminated sheets were air dried to 200% moisture content and were stored overnight in sealed polyethylene bags. Sheets 10, 12, 17, and 18 were delaminated. The sheets and the laminates between which they had been pressed were counted. Sheets 13 and 15 were cut in half; one half of each sheet was air dried; the other half was dried on a hot surface at 220°F. These sheets were then counted.

Table XIV contains the results of these experiments. All data are obtained from at least 1000 counts and are corrected for a background count of 0.8 c./sec.

These results indicate that about 75% of the radioactive thallium is lost from coated sheets which are subsequently dispersed and reformed. However, the coating is sufficiently good to withstand dipping into water, wet-pressing into sheets, and drying. The larger the particle size of the Amberlite resin, the better is the retention. The average retention

TABLE XIV

RETENTION OF RADIOACTIVE THALLIUM ON SHEETS

Sheet	Amberlite Particle Size, m.	Coating Weight, % of Dry Sheet	Initial Sheet Activity, c./sec.	Activity after Water Dip, c./sec.	Activity after Dispersing and Reforming, c./sec.	Activity after 1st Wet Pressing, c./sec.[1]	Activity after 2nd Wet Pressing, c./sec.[2]	Activity after Drying, c./sec.[2,3]
10	-20+5	30	16.7	15.6	--	15.1	14.7	--
11	-20+5	30	15.4	15.1	3.8	--	--	--
12	-20+5	15	8.1	7.7	--	7.6	7.2	--
13	-5+1	30	15.1	14.8	--	14.6	--	13.9
14	-5+1	30	16.4	15.9	3.8	--	--	--
15	-5+1	15	8.5	8.1	--	8.0	--	7.2
16	-1	30	14.4	14.1	3.5	--	--	--
17	-1	30	13.7	13.5	--	12.7	11.8	--
18	-1	15	8.3	7.6	--	7.3	6.8	--

Notes:

1. The activity of the blotters between which the sheets were pressed was too low to be measured.

2. The laminates between which the radioactive sheets had been pressed had net counts of 0.3-0.4 c./sec.

3. Comparison of the air-dried and hot-surface dried portions of each sheet is as follows:

Sheet	Portion Dried on Hot Surface, c./sec.	Portion Air Dried, c./sec.
13	6.4	7.1
15	3.2	3.7

during wet pressing for the -20+5 μ cut was 96%; the average retention for the -1μ cut was only 91%. Increasing the coating weight from 15 to 30% of the sheet weight also increased retention on the laminate. Losses upon delamination after hot-surface drying were greater than losses upon delamination after air drying. However, the air-dried sheets were much easier to delaminate, and it was visually obvious that there was more coating pulled away from the radioactive laminate but located at the interface which had been in contact with that laminate for sheets dried on a hot surface than for air-dried sheets. In all cases, the presence of Amberlite particles at the interface could be seen after delamination.

At a later date, a series of sheets for drying studies was made up. These contained about 25 μc. per sheet absorbed on approximately 2 mg. of -20+5 μ Amberlite IR-120. The radioactive laminate was made from 1.1 mg./cm.^{2} teabag stock containing a coating of about 25% of the dry sheet weight. After the sheets had been hot-surface dried, some were delaminated and the relative activity of the laminates determined. These data are given in Table XV.

TABLE XV

DISTRIBUTION OF RADIOACTIVE MATERIAL IN DRIED SHEETS

Sheet	Dry Basis Weight, mg./cm.^{2}	Upper Laminate, % of Sheet	Counting Rate per Minute x 10^{-4} from Laminate		
			Upper	Coated	Lower
180A	28.2	20	0.89	18.4	1.42
193A	14.1	50	2.39	18.7	0.09
185A	28.2	25	1.04	17.0	0.84
188B	7.1	50	1.81	20.2	1.71

In all sheets, there was a dark layer at the interface of the outer laminates which had been in contact with the radioactive laminate. Examination showed that this consisted of particles of Amberlite. Thus, the actual retention of radioactive material in the proper zone of the sheet was considerably higher than indicated from the data of Table XV.

Effect of Lamination Procedure on Drying Characteristics of Sheets

Teabag laminates 3.25 by 6 inches were coated with various amounts of resin. The procedure used for making these laminates was that described in the next section of this appendix, except that no radioactive thallium was included in the laminates.

These laminates were wet pressed into the center of sheets by the procedure described in the body of the thesis. Two samples for drying, each 2.55 by 3.62 inches, were cut from each of these sheets. These samples were then prepared and dried as sheets in which the over-all rate of drying was determined. The 1-inch circular thallium source was mounted on the hot surface and used to follow drying.

Figure 10 contains the results obtained. There was no measurable difference in over-all drying rate between sheets containing a laminate with up to 20% resin on it and nonlaminated sheets of equal dry basis weight dried under the same conditions. With 30% resin on the laminate, a 28.2 mg./cm.^{2} sheet had the same constant-rate drying rate as a nonlaminated sheet, but the critical moisture content was higher.

A sheet was also made with a 2.55-by 3.25-inch radioactive laminate containing about 25% resin wet pressed at the hot-surface interface. This sheet had a constant-rate drying rate 3% less than a nonlaminated sheet of equal dry basis weight dried under the same conditions but measured with

the 1-inch circular source of radiation mounted on the hot surface. This difference is very plausibly due to poorer contact by the coated laminate with the hot surface compared to contact by a sheet which has never been dried or pressed since the pulp was beaten. It was in fact observed that sheets of the latter type left fibers attached to the foil with which it was in contact if the wet sheet was stripped from the foil. With sheets containing a coated laminate at the interface with the foil, care was required at all times during handling to prevent separation of the sheet from the foil.

The results of these experiments indicate that the technique developed for immobilizing and including radioactive thallium within sheets, while undoubtedly amenable to further improvement, is satisfactory for the study of the drying rate of fractional thicknesses of a sheet. For studies of the drying rate of an entire sheet, the source of radioactivity must be mounted below the foil with which the sheet makes contact in order that reproducible contact with the hot surface be attained.

PROCEDURE FOR SHEET PREPARATION

The first step in preparing sheets was to affix the necessary amount of radioactive material on the thin laminate sheets. Three and one-quarter by eight-inch sheets were cut from the 1.1 mg./cm.^{2} bleached manila teabag stock. Each end was secured between two strips of 0.005-inch brass shim stock with a spring-loaded paper clip.

Allowing for 33% waste in handling, the following formulation coats about 15 sheets over a 3.25 by 6-inch area, each sheet containing about 20% solids and 50 microcuries of radioactive material:

2.5 g. Penacolite A (a solution of partially condensed resorcinol-formaldehyde resin)

0.5 g. Penacolite B (a catalyst and filler)

1000 microcuries of $Tl^{204}NO_3$ specific activity 200 mc./g.

25 ml. water total (includes the water with the thallium and the Amberlite)

100 mg. Amberlite IR-120, ground to less than 20 microns

0.5 ml. 3% ammonium hydroxide.

The Penacolite A and B were mixed well, and a little dilution water was added. This mixture had a useful working life of about 2 hr. at room temperature.

In a separate container, the Amberlite slurry and the radioactive thallium solution were mixed. After about 15 minutes, ammonia was added dropwise to bring this slurry to approximately pH 7.

The Penacolite solution was added to the resin slurry. Any required remaining dilution water was used to rinse the Penacolite container before adding it to the total mix.

The sheets for coating were laid one at a time on a piece of plate glass. The coating was added with a 1-inch brush. The sheet was uniformly wetted and coated, then was turned over and brushed on the reverse side. It was then hung up to dry, any streaks being removed by doctoring the sheet lightly with the edge of a folded paper towel. After about 2 hours at room temperature, the sheets were hung overnight in an oven at 55°C. Following this, they were dipped in a water bath and allowed to dry again. Two sheets 2.38 by 3.25 inches were cut from the coated section of each sheet.

The nonradioactive laminates of the sheets to be dried were made from pulp prepared in the same fashion as for sheets of which the over-all drying rate was being studied. The two nonradioactive laminates were made separately in a British sheet mold. The upper laminate was couched onto blotters in the normal fashion. The lower laminate was couched directly onto a 7 by 7-inch piece of 0.0015-inch aluminum foil which had previously been cleaned with acetone.

The radioactive laminate was placed on a blotter and wetted with distilled water, then was carefully placed on the lower laminate so that no wrinkles or air bubbles formed. The upper laminate was removed from its blotter and carefully placed in contact with the lower and the radioactive laminates.

A wet blotter was placed in contact with the top of the laminated sheet, and dry blotters were placed above this and below the stack. This was pressed lightly by hand to remove excess water. A new wet and a new dry blotter were placed above the laminated sheet, and the sheet with the two blotters above and one below was run through the Noble and Wood rotary sheet press.

The portion of the sheet finally used for drying was 2.62 by 3.75 inches. This was so cut from the entire laminated sheet that the radioactive laminate was centered in it. Care was exercised to avoid bending of the wet sheet. Any sheets which delaminated during cutting or handling were discarded.

The cut sheets were air dried to 0.25 g. less than the desired final weight. They were sprayed with 0.25 g. of a solution of 10% dextrinized starch and 0.2% tartrazine, a soluble dye. The sheets were sealed in polyethylene bags and stored overnight at 73°F.

APPENDIX VIII

FORMATION OF LAMINATED SHEETS IN THE BRITISH SHEET MOLD

As explained in Appendix VII the original plan for depositing radioactive material within sheets was to deposit the radioactive thallium on and in fibers and subsequently to deposit the fibers at the desired depth within sheets. The mass per unit area of the fibers containing radioactive material was to be about 0.4 mg./cm.^{2}, too little to be formed and couched as a sheet. It was therefore necessary to form this laminate and another in the sheet mold and to couch the two together. The success of this venture depended upon being able to add slurry containing pulp for a second laminate to the sheet mold without disturbing a laminate which had already been formed on the wire.

After several fruitless attempts, a simple device was developed which enabled this to be done. This device is shown in Figure 24. It consists of two discs of the same diameter as the internal diameter of the sheet mold. These discs are mounted on concentric shafts, the lower disc connected to the inner shaft. They are so perforated that in one position all the holes line up, but when one disc is rotated 45° with respect to the other, all the holes in each disc are sealed by the other disc. A bar affixed to the inner shaft with an Allen screw allowed the unit to be adjusted so that it was supported with this bar on the top rim of the sheet mold and the discs at any height, within limits, in the sheet mold. A pointer attached to the outer shaft just below the supporting bar indicated the relative position of the discs.

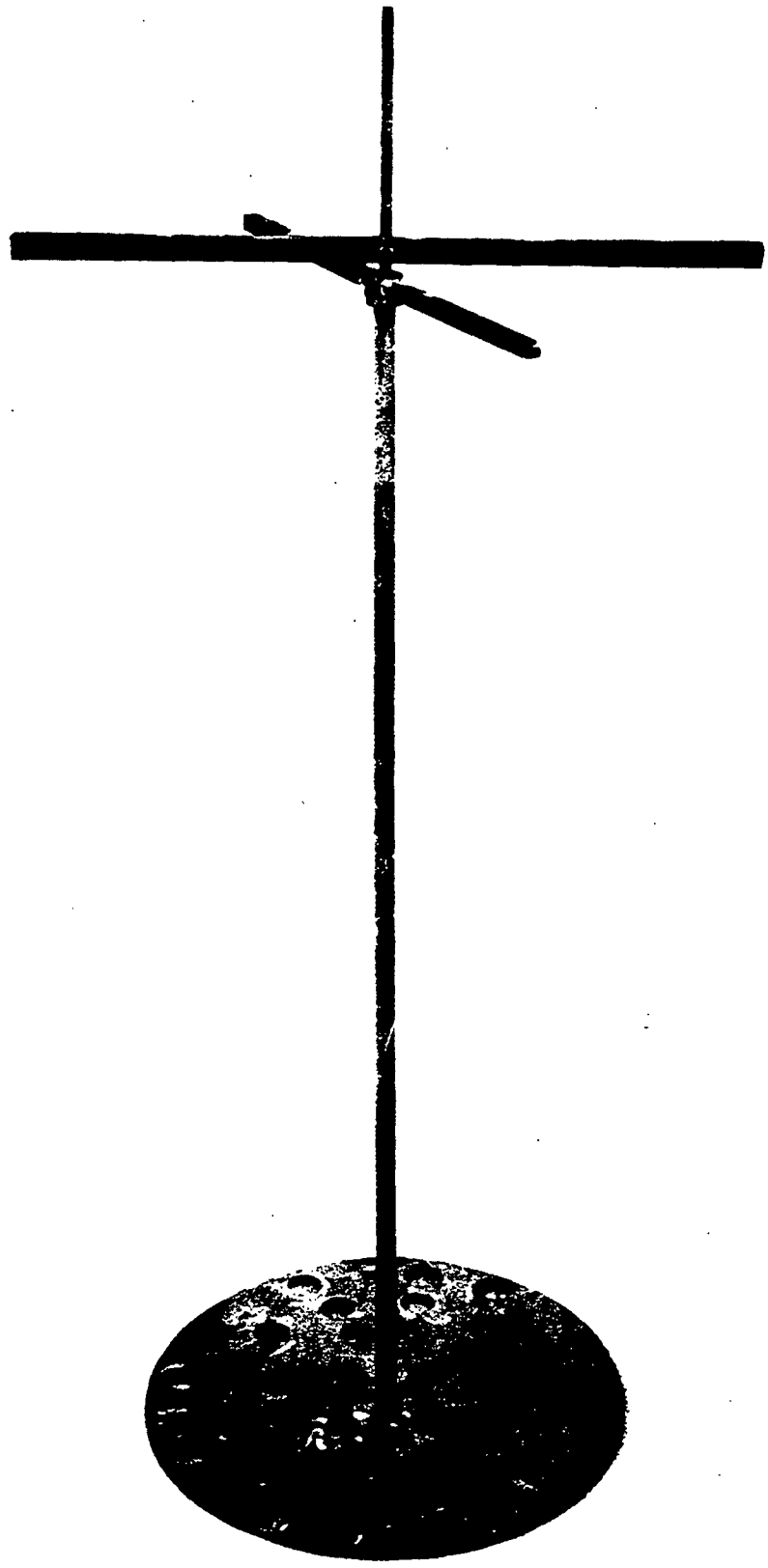

Figure 24. Sketch of Accessory for Forming Laminated Sheets in the British Sheetmold

The procedure for forming sheets was as follows:

1. The pulp slurry for the first laminate was added to the mold in normal fashion.

2. The first laminate was formed, but the mold drain was closed when about 1/4 inch of water remained above the surface of the laminate.

3. The disc device with holes open was lowered into the sheet mold, moving it very slowly downward as it approached the liquid surface and stopping it with the discs in contact with the water surface.

4. The device was closed by rotating the upper disc 45°.

5. Water was allowed to drain very slowly down the shaft until about an inch of water covered the discs. After this, the rate of water addition could be increased.

6. After 2-3 inches of water covered the discs, the slurry containing pulp for the next laminate was added to the sheet mold simultaneously with the water.

7. When the sheet mold was full, the slurry was stirred with a rod, taking care not to touch the shaft or the discs.

8. The holes were opened by rotating the outer shaft 45°, and the unit was removed from the sheet mold. Care was required to move the discs slowly upward until they were about 1 foot above the wire; then the rate of extraction was increased. The sheet-mold drain was barely open during this procedure. It was found satisfactory if the extraction of the discs took about 30 seconds, during which time about 1 liter of water drained from the sheet mold.

9. After the discs were removed from the mold, the drain was opened fully and formation of the sheet was completed in the normal manner.

The device as used was crude, but satisfactory sheets could be made with it. It was not used in the course of the thesis work, since the precipitation of thallium on fibers did not prove satisfactory.

The discs used were made by perforating two discs normally used for drying handsheets for physical testing. These discs were too thin and tended to flex during use and to allow leakage. Thicker discs which sealed more completely would have eased the work.

APPENDIX IX

CALIBRATION OF THE BETA GAGE FOR DRYING STUDIES OF FRACTIONAL SHEET THICKNESS

The source of beta radiation used for studies of fractional thicknesses of sheets was 2.38 by 3.00 inches. There was no aluminum foil between the source and the detector of radiation. Therefore, a different calibration curve obtains for these conditions than for the conditions when drying of the entire sheet was being studied with the 1-inch circular source mounted on the hot surface.

In Figure 9, the calibration curve for the 1-inch circular source, it was shown that the data obtained from the zero-time beta-ray transmission of sheets were in satisfactory agreement with the data obtained by the steady-state calibration procedure. Furthermore, the calibration data for this source indicated that within experimental accuracy the beta-ray transmission of water was independent of the amount of pulp that was present.

Since a large number of zero-time estimates were available, statistical variations of the estimate as well as small variations in initial moisture content could be tolerated and a curve of beta-ray transmission of water as a function of the mass per unit area of water faired in.

Figure 25 is the graph of beta-ray transmission as a function of the mass per unit area of water which was used. The points shown on it are calculated from sheets 210-246. The mass per unit area corresponding to each point is the percentage initial moisture content of each sheet (200% for all sheets) multiplied by the mass per unit area of the fractional thickness which is measured in each sheet. One-half of the mass per unit area of the radioactive laminate is included in this value.

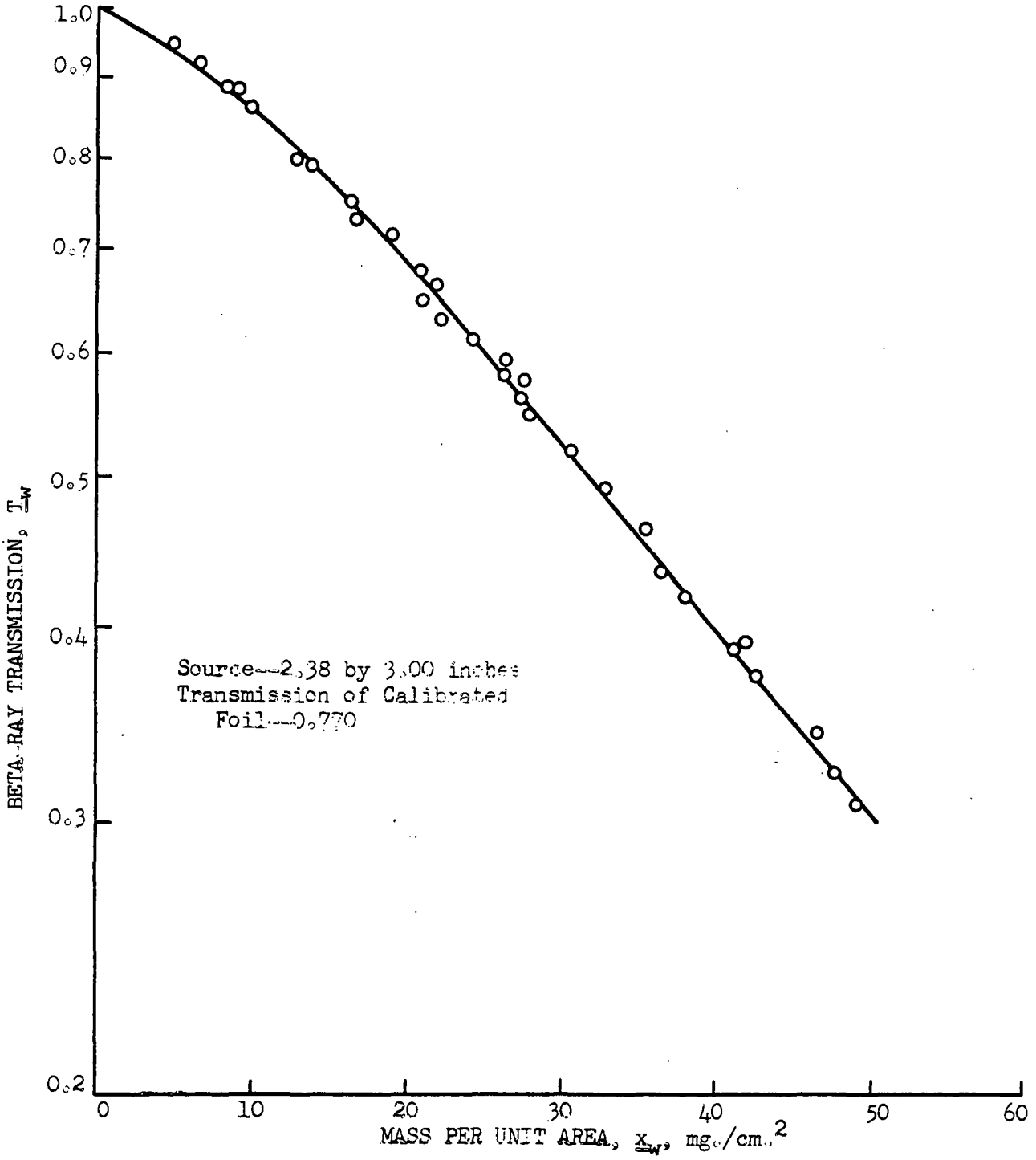

Figure 25. Calibration Curve for Water with Thallium^{204} Imbedded Within Sheets

APPENDIX X

SELECTION OF A SOLUTE FOR LIQUID MIGRATION STUDIES

The ultimate criterion for a suitable solute for liquid migration studies is that the movement of the solute correspond to the movement of the liquid in which it is dissolved. A simple way of checking this property for paper is to run a paper chromatogram of the solute.

A spot of the material being checked was placed on a 24-inch sheet of Whatman No. 1 filter paper. The paper was supported in a sealed tank containing water in the bottom of it in order to minimize evaporation from the sheet. The upper end of the sheet was immersed in water. After the water had traveled at least 10 inches down the sheet from the initial position of the spot, the sheet was removed from the tank. The distance from the initial position of the spot to the center of the spot and to the water front were measured. The ratio of these two distances is the relative migration of the solute to water, R_f, of the solute.

Dyes were located visually. Sugar was located by spraying the sheet with aniline hydrogen phthalate solution followed by heating the sheet in an oven. Halides were located by spraying the sheet with a solution of alcoholic silver nitrate containing traces of fluorescein and ammonium hydroxide. The sheet was then placed under ultraviolet light to develop the spot.

The R_f values of various substances are given in Table XVI. The dyes listed are acid dyes; this group is less substantive to cellulose than are basic or direct dyes.

TABLE XVI

R_f VALUES FOR SOLUTES IN WATER

Solute	Color Index	R_f
Pontacyl Carmen 2B	PR 100	0.5
Pontacyl Carmen 6B	57	0.25
Fast Acid Violet 4R	758	0.2
Tartrazine	640	0.93
Naphthol Yellow	10	0.8
Sodium chloride	--	1.0
Glucose	--	0.93
Sodium bromide	--	0.95
Copper sulfate	--	streaked out

The effect of other solutes on the migration of glucose and sodium chloride are given in Table XVII.

TABLE XVII

EFFECT OF OTHER SOLUTES ON MIGRATION OF DYE AND SODIUM CHLORIDE

Solution	R_f of Tartrazine	R_f of Sodium Chloride
1% Na_2SO_4	0.88	--
5% Na_2SO_4	0.86	--
1% acetic acid	0.7	1.0
1% NaOH	0.7	1.0
1% alum	0.7	--
5% alum	0.5	1.0
10% starch	0.9	--

Because of the ease of locating a dye visually, the ease of colorimetric analysis for a dye, and the decreased likelihood of contamination from extraneous sources, tartrazine was selected as a solute for following liquid migration, even though the movement of sodium chloride corresponds somewhat better to the movement of liquid water than does the movement of tartrazine.

APPENDIX XI

OPTICAL TRANSMITTANCE OF TARTRAZINE SOLUTIONS

Solutions of approximately 0.05 and 0.005 g./l. were made. A graph of transmittance of light as a function of wavelength from 400 to 700 mmu was obtained with a General Electric Recording Spectrophotometer (GERS). The dye exhibited a minimum transmittance from 420 to 440 mmu.

A solution of 1.000 g./l. was made, and more dilute solutions were made by quantitative dilution. A 5-mm. cell was used in the GERS, and the transmittance at 425 mmu relative to distilled water was measured. These data are given in Table XVIII.

TABLE XVIII

TRANSMITTANCE OF TARTRAZINE SOLUTIONS AT 425 MMU

Dye Concentration, mg./l.	Transmittance, %
100	1.7
50.0	13.4
25.0	36.8
10.0	66.9
5.0	81.3
2.50	90.7
1.00	95.7

Figure 26, a graph of these data on semilogarithmic paper, is a straight line, showing that the dye obeys Beer's law at this wavelength.

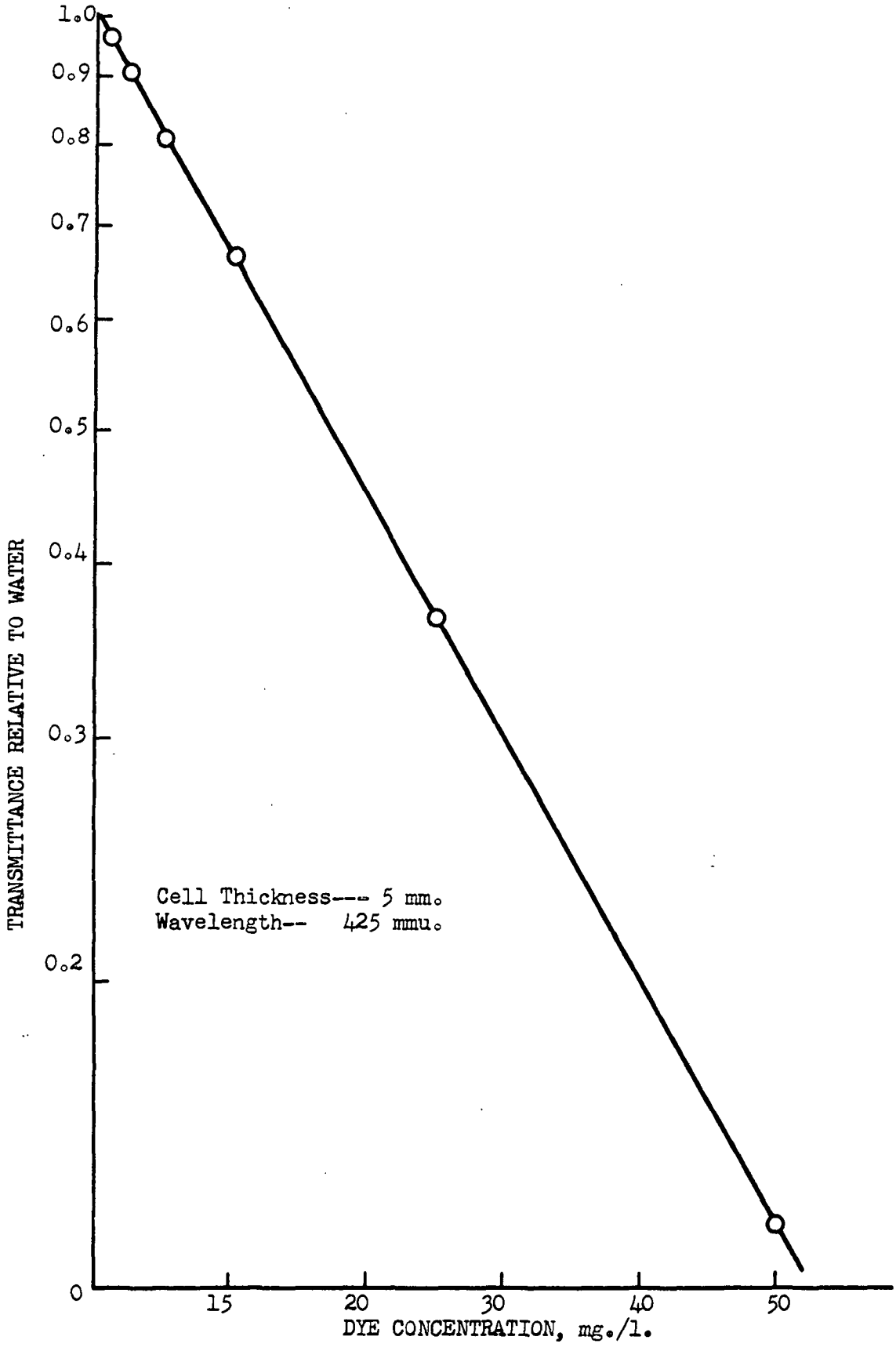

Figure 26. Transmittance of Tartrazine Solutions

Effect of Heating Tartrazine on Transmittance

Fifty milliliters of a 25.0 mg./l. solution of tartrazine was boiled vigorously for 15 minutes in a 125-ml. beaker. It was allowed to cool and diluted to 50 ml. The transmittance of the solution was 37.2%, compared with an original transmittance of 36.8%. The concentration corresponding to 37.2%, read from Figure 26, is 24.7 mg./l. It thus appears that changes in dye transmittance caused by heating the dye can be tolerated.

Effect of pH on Transmittance of Tartrazine

Three 25-ml. portions of a solution of tartrazine in distilled water were used. Sample A was used as a control; to Sample B was added 2 drops of 2% sulfuric acid; to Sample C was added 2 drops of 2% sulfuric acid, then 2 drops of 10% sodium carbonate. The pH and transmittance of each sample were measured. These data are given in Table XIX.

TABLE XIX

EFFECT OF pH ON TRANSMITTANCE OF TARTRAZINE SOLUTIONS

Sample	pH	Transmittance
A	7.7	24.8
B	3.2	25.4
C	10.0	34.5

It appears that pH has only a slight effect on transmittance provided that the solution is kept slightly acidic.

APPENDIX XII

PREPARATION OF SHEETS FOR SOLUTE MIGRATION STUDIES

The sheets were made from pulp prepared in the same manner as for sheets in which drying was followed. The sheets were made by wet-pressing together laminates of the thickness desired for later delamination.

The bottom laminate was couched directly onto a 7 by 7-inch sheet of 0.0015-inch aluminum foil which had previously been cleaned with acetone. A strip of teabag stock 0.5 by 6 inches was laid across the laminate with the center of the strip about 1 inch from the side of the sheet.

Subsequent laminates were couched from the wire onto blotters, then carefully removed from the blotter and laid on the stack, avoiding the formation of any air bubbles at the interface. After each laminate was laid on the stack, another strip of teabag stock was laid down, superimposed on the ones below. The stack was then sprinkled with water, which facilitated the elimination of air bubbles when subsequent laminates were put in place.

After all laminates had been put in place, a wet blotter was put over the laminated sheet, then dry blotters were placed over this one at a time and were pressed lightly by hand. Three dry blotters were usually used. A fresh wet blotter was then placed above the sheet, a dry blotter above that, and a dry blotter below the aluminum foil. The sheet was run through the Noble and Wood rotary sheet press.

The specimen for drying was 2.62 by 3.75 inches. This was so cut that about half of the width of the teabag strips remained at one end of the sheet.

Each sheet was air dried to 0.25 g. less than the desired final weight, then sprayed with 0.25 g. of a solution of 10% dextrinized starch and 6% tartrazine. The sheets were sealed in polyethylene bags and stored for 72 hours at 73°F. before being used.

DETERMINATION OF SOLUTE DISTRIBUTION

Before a sheet was used, a 0.2 by 2-inch tab was cut in each end of it. The sheet was weighed, placed in the C-frame, and the tab at each end was folded up to hold the sheet on the frame. The teabag strips, now outside of the clamped area, were removed from the sheet, leaving one end of the sheet with the laminates separated. The sheet was inserted into the tunnel in the same manner as sheets for drying rate determinations.

The sheet was dried for the desired length of time. The C-frame and sheet were removed from the tunnel and the sheet removed from the C-frame. The sheet was delaminated from the end containing the teabag strips up to about 1 inch from the opposite end. A piece of 0.0015-inch aluminum foil was placed between each laminate; the laminates were folded back into their original relative positions above one another; and a circular section 1.25 inches in diameter was stamped out with a die punch. In sheets used for moisture distribution determination, delamination interfaces were inspected for areas of dye concentration, and any sheets in which such were found were discarded.

The dye from each section was extracted with distilled water. Successive portions of water were used until the pulp and the extract were colorless. A Hirsch funnel and qualitative creped filter paper were used. For the laminate in contact with the hot surface, it was necessary

to add a drop of 2% sulfuric acid to the second extract to obtain complete extraction of the dye.

The total extract from each laminate was diluted to a measured volume, and the pH was checked to be certain that it was below 7. The General Electric Recording Spectrophotometer was used to measure the transmittance of the dye solution at 425 mmu, relative to distilled water, in a 5-mm. cell. Figure 26, presented in Appendix XI was used to convert the measured transmittance value to dye concentration.

APPENDIX XIII

TABULATED DRYING DATA*

TABLE XX

DRYING RATE OF LAMINATED SHEETS

Description of Sheets

161A 28.2 mg./cm.^{2} nonlaminated sheet

162A 2 - 14.1 mg./cm.^{2} laminates

163A 2 - 13.5 mg./cm.^{2} laminates with uncoated 1.1 mg./cm.^{2} teabag laminate

164A 2 - 13.3 mg./cm.^{2} laminates with teabag laminate containing 55% resin

165A 2 - 13.4 mg./cm.^{2} laminates with teabag laminate containing 31% resin

165B same as 165A

167A 2 - 13.5 mg./cm.^{2} laminates with teabag laminate containing 10% resin

167B same as 167A

169A 14.1 mg./cm.^{2} nonlaminate sheet

169B same as 169A

170A 2 - 6.5 mg./cm.^{2} laminates with teabag laminate containing 15% resin

170B same as 170A

255 2 - 9.9 mg./cm.^{2} laminates and 2 - 4.2 mg./cm.^{2} laminates

Intended initial moisture content of all sheets - 200% of dry sheet weight.

Source of radiation - 1-inch circular thallium source mounted on hot surface.

Transmission of calibrated foil - 0.770 $\pm$ 0.03.

---

* The counting-rate values tabulated in this appendix are read from the curve faired through the incremental values calculated from the film readings.

TABLE XX (Continued)

DRYING RATE OF LAMINATED SHEETS

Sheet,	161A	162A	163A	164A	165A	167A	255	165B	167B
Circulant,	Water	Water	Water	Water	Water	Water	Water	Glycol	Glycol
Circulant, temp., °F.	190	190	190	190	190	190	190	230	230
Air temperature, °F.	95	95	95	95	95	95	85	95	95
Air wet-bulb temp., °F.	79	79	79	79	79	79	70	79	79
Air velocity, f.p.m.	250	250	250	250	250	250	250	250	250
Drying Time, sec.	Faired Counting Rate, sec./10^4 c.								
0	--*	10.7	10.3	10.3	10.1	10.9	9.60	9.10	9.00
20	9.20	9.05	8.60	8.60	8.40	8.90	8.10	7.15	7.05
40	7.90	7.75	7.25	7.30	7.15	7.45	6.80	5.60	5.45
60	6.50	6.40	6.05	6.10	5.90	6.30	5.80	4.40	4.40
80	5.60	5.45	5.07	5.30	5.20	5.33	3.95	3.78	3.80
100	4.70	4.61	4.37	4.65	4.45	4.65	4.23	3.33	3.30
120	4.16	4.00	3.87	4.20	4.03	4.03	3.73	3.00	2.97
140	3.63	3.55	3.48	3.80	3.48	3.63	3.32	2.84	2.75
160	--*	3.25	3.16	3.45	3.27	3.27	3.05	2.66	2.58
180	--*	3.00	2.90	3.20	3.05	3.03	2.84	2.58	2.48
200	2.81	2.80	2.70	2.97	2.85	2.80	2.70	2.50	2.43
220	2.71	2.68	2.57	2.84	2.71	2.66	2.61	--	--
240	--*	2.61	2.47	2.73	2.66	2.59	2.53	--	--
260	--*	2.56	--	2.66	2.61	2.55	2.47	--	--
∞	--*	2.55	2.44	2.58	2.56	2.51	2.43	2.48	2.43
Counting rate from bare source, c./min. x 10^{-4}	43.6	43.8	44.0	44.0	44.0	43.9	45.2	45.4	45.3

* Camera damaged

TABLE XX (Continued)

DRYING RATE OF LAMINATED SHEETS

Sheet,	169A	170A	169B	170B
Circulant,	Water	Water	Glycol	Glycol
Circulant temp., °F.	190	190	230	230
Air temperature, °F.	95	95	95	95
Air wet-bulb temp., °F.	79	79	79	79
Air velocity, f.p.m.	250	250	250	250
Drying Time, sec.	Faired Counting Rate, sec./10^4 c.			
0	3.44	3.40	3.34	3.29
10	3.16	3.12	2.90	2.86
20	2.91	2.86	2.52	2.49
30	2.67	2.64	2.19	2.24
40	2.45	2.44	2.03	2.05
50	2.27	2.26	1.93	1.97
60	2.15	2.15	1.85	1.90
70	2.07	2.07	--	--
80	2.01	2.01	--	--
90	1.95	1.95	--	--
100	1.94	1.93	--	--
∞	1.92	1.92	1.83	1.89
Counting rate from bare source, c./min. x 10^{-4}	43.9	43.9	45.1	45.0

TABLE XXI

EFFECT OF DRYING VARIABLES ON DRYING RATE

Same source of radioactivity as Table XX
Same instrument sensitivity as Table XX

Sheet,	160A	161A	161B	162B	168B	206	207	208	167B
Intended dry basis weight, mg./cm.^{2}	28.2	28.2	28.2	28.2	28.2	28.2	28.2	28.2	28.2
Intended initial moisture content, %	240	200	150	200	200	200	200	200	200
Circulant,	Water	Water	Water	Water	Glycol	Glycol	Glycol	Glycol	Glycol
Circulant temp., °F.	190	190	190	170	210	190	190	190	230
Air temperature, °F.	95	95	95	95	95	85	85	95	95
Air wet-bulb temp., °F.	79	79	79	79	79	70	70	79	79
Air velocity, f.p.m.	250	250	250	250	250	250	435	250	250

TABLE XXI (Continued)

EFFECT OF DRYING VARIABLES ON DRYING RATE

Drying Time, sec.	Faired Counting Rate, sec./10^4 c.								
0	--*		6.65	9.75	9.25	11.3	11.7	11.5	
20	--*		5.67	8.63	7.55	9.95	10.2	10.1	
40	--*	See	4.87	7.71	6.15	8.63	8.70	8.70	See
60	--*	Table	4.18	6.44	5.07	7.47	7.50	7.55	Table
80	6.55	XX	3.62	6.15	4.21	6.47	6.50	6.53	XX
100	5.55		3.22	5.48	3.68	5.67	5.60	5.65	
120	4.84		2.90	4.90	3.33	5.01	4.91	5.01	
140	4.14		2.72	4.37	3.00	4.45	4.40	4.45	
160	3.65		2.59	3.89	2.76	4.07	4.00	4.06	
180	3.27		2.52	3.62	2.65	3.77	3.68	3.75	
200	3.03		2.48	3.36	2.56	3.53	3.48	3.49	
220	--*		--	3.14	2.53	3.33	3.25	3.31	
240	2.67		--	2.95	--	3.17	3.11	3.17	
260	2.64		--	2.78	--	3.04	3.00	3.03	
280	2.53		--	2.70	--	2.88	2.88	2.91	
300	2.48		--	2.64	--	2.85	2.81	2.82	
320	--*		--	2.55	--	--	--	--	
340	--*		--	2.49	--	--	--	--	
∞	--*		2.45	2.46	2.45	--	--	--	
Counting rate from bare source, c./min. x 10^{-4}	43.8		45.6	45.7	45.4	40.8	41.7	41.1	

Camera jammed

TABLE XXI (Continued)

EFFECT OF DRYING VARIABLES ON DRYING RATE

Sheet,	169A	169B	171A	171B	172A	172B
Intended dry basis weight, mg./cm.^{2}	141	141	7.0	7.0	3.5	3.5
Intended initial moisture content, %	200	200	200	200	200	200
Circulant,	Water	Glycol	Water	Glycol	Water	Water
Circulant temp., °F.	190	230	190	230	190	170
Air temperature, °F.	95	95	95	95	95	95
Air wet-bulb temp., °F.	79	79	79	79	79	79
Air velocity, f.p.m.	250	250	250	250	250	250
Drying Time, sec.			Faired Counting Rate, sec./10^4 c.			
0			2.19	2.05	1.72	1.77
5			2.11	1.91	1.66	1.69
10	See	See	2.03	1.77	1.61	1.63
15	Table	Table	1.95	1.70	1.58	1.60
20	XX	XX	1.89	1.66	--	1.55
25			1.83	1.65	--	1.53
30			1.76	--	--	--
35			1.72	--	--	--
40			1.71	--	--	--
∞			1.70	1.64	1.58	1.51
Counting rate from bare source, c./min. x 10^{-4}			43.7	44.9	43.7	45.9

TABLE XXII

REPLICATE DRYING RATE OF FRACTIONAL PORTIONS OF SHEETS

Circulant - Glycol
Circulant temperature - 190°F.
Air temperature - 85°F.
Air wet-bulb temperature - 70°F.
Air velocity - 250 f.p.m.
Radioactive source - 300 by 2.55 inches imbedded within sheet

Sheet	193A	193B	180A	189A	181A	190A	190B	205*
Intended dry basis weight, mg./cm.^{2}	28.2	28.2	28.2	28.2	28.2	28.2	28.2	28.2
Intended fraction being measured, %	100	100	20	20	40	40	40	100
Intended initial moisture content, %	200	250	200	200	200	200	250	200
Drying Time, sec.	Faired Counting Rate, sec./10^4 c.							
0	18.3	28.4	3.58	4.35	4.48	6.15	7.10	13.7
20	16.2	25.2	3.51	4.27	4.30	5.95	6.55	12.2
40	14.5	22.1	3.47	4.23	4.08	5.64	6.28	10.8
60	12.9	19.6	3.40	4.16	3.88	5.39	5.99	9.15
80	11.5	17.4	3.31	4.12	3.72	5.17	5.71	7.95
100	10.2	15.3	3.29	4.07	3.56	5.02	5.48	7.03
120	9.05	13.6	3.24	4.02	3.44	4.87	5.28	6.18
140	8.30	12.1	3.17	4.00	3.34	4.70	5.06	5.53
160	7.65	10.8	3.13	3.93	3.20	4.50	4.88	4.98
180	7.30	9.8	3.11	3.88	3.09	4.33	4.67	4.61
200	7.00	8.9	3.10	3.80	3.02	4.20	4.49	4.26
220	6.85	8.1	--	--	3.00	4.12	4.33	3.99
240	--	7.6	--	--	--	--	4.24	3.80
260	--	7.2	--	--	--	--	4.19	3.74
280	--	6.9	--	--	--	--	--	--
300	--	6.8	--	--	--	--	--	--
320	--	6.7	--	--	--	--	--	--
∞	6.77	6.62	3.05	3.74	2.95	4.04	4.10	3.68

* Source size for sheet 205-3.00 by 2.38 inches

TABLE XXIII

MOISTURE DISTRIBUTION DETERMINATION DATA

Circulant - Glycol
Circulant temperature - 230°F.
Air temperature - 85°F.
Air wet-bulb temperature - 70°F.
Air velocity - 250 f.p.m.
Intended sheet dry basis weight - 28.2 mg./cm.^{2}
Intended initial moisture content - 200%
Source of radioactivity - 2.38 by 300 inches

Sheet	210	211	212	213	214	215	216	217	218	219	220
Intended measured fraction, %[1]	15	25	37.5	45	55	65	75	85	97.5	50	40
Drying Time, sec.	Faired Counting Rate[2] sec./10^4 c.										
0	3.02	6.90	4.62	6.55	7.81	9.35	9.35	12.5	13.3	6.48	5.75
20	2.93	6.73	4.40	6.17	7.27		8.18				
40	2.89	6.42	4.27	5.75	6.67		7.15				
60	2.85	6.32	4.06	5.38	6.12		6.15				
80	2.80	6.18	3.84	5.00	5.57	(3)	5.35	(3)	(3)	(3)	(3)
100	2.76	5.92	3.63	4.68	5.09		4.71				
120	2.72	5.69	3.37	4.35	4.65		4.22				
140	2.70	5.52	3.23	4.14	4.32		3.89				
160	2.68	5.48	3.15	3.98	4.16		3.73				
180	2.66	5.46	3.14	3.89	4.10		3.62				
∞	2.66	5.46	3.11	3.91	4.06	4.07	3.55	4.01	4.45	3.54	3.61

[1]Fractional dry basis weight measured from air interface,

[2]Time in seconds from start of scaler

[3]Drying data discarded because of delamination or poor hot-surface contact.

TABLE XXIV*

MOISTURE DISTRIBUTION DETERMINATION DATA

Circulant - Glycol
Circulant temperature - 230°F.
Air temperature - 85°F.
Air wet-bulb temperature - 70°F.
Air velocity - 250 f.p.m.
Intended sheet dry basis weight - 14.1 mg./cm.^{2}
Intended initial moisture content - 200%
Source of radioactivity - 2.38 by 3.00 inches

Sheet	221	222	223	224	225	226
Intended measured fraction, %	25	35	45	60	75	95
Drying Time, sec.	Faired Counting Rate, sec./10^4 c.					
0	4.80	2.13	5.28	5.55	5.63	7.00
10	4.70	2.05	5.00	5.28	5.08	6.07
20	4.63	1.98	4.77	5.00	4.60	5.38
30	4.55	1.93	4.58	4.69	4.19	4.85
40	4.49	1.89	4.37	4.36	3.86	4.46
50	4.45	1.86	4.25	4.18	3.70	4.21
∞	4.43	1.84	4.21	4.05	3.63	4.05

*These data not screened by dye inclusion.

TABLE XXV

MOISTURE DISTRIBUTION DETERMINATION DATA

Circulant - Water
Circulant temperature - 190°F.
Air temperature - 85°F.
Air wet-bulb temperature - 70°F.
Air velocity - 250 f.p.m.
Intended sheet dry basis weight - 28.2 mg./cm.^{2}
Intended initial moisture content - 200%
Source of radioactivity - 2.38 by 3.00 inches

Sheet	230	231	232	233	234	235	236	237	246
Intended measured fraction, %	10	17.5	25	30	35	40	45	50	50
Drying Time, sec.	Faired Counting Rate, sec./10^4 c.								
0	4.87	5.74	4.48	8.58	5.73	9.75	14.1	10.4	8.62
25	4.80	5.63		8.34	5.48			9.60	7.85
50	4.71	5.53		8.04	5.25			8.70	7.21
75	4.70	5.44	*	7.88	5.06			8.07	6.69
100	4.68	5.36		7.50	4.86	*	*	7.56	6.27
125	4.66	5.29		7.25	4.67			7.11	5.88
150	4.65	5.21		6.96	4.47			6.66	5.54
175	4.64	5.16		6.70	4.33			6.00	5.26
200	4.63	5.12		6.55	4.20			5.87	5.09
225	--	--		6.48	4.12			5.83	5.00
∞	4.64	5.05	3.59	6.42	4.12	6.48	8.61	5.80	4.97

*Drying data discarded because of delamination or poor hot-surface contact.

TABLE XXV (Continued)

MOISTURE DISTRIBUTION DETERMINATION DATA

Sheet	238	239	245	244	243	242	241	240
Intended measured fraction, %	55	60	65	70	75	80	85	90
Drying Time, sec.	Faired Counting Rate, sec./10^4 c.							
0	8.45	11.6	15.2	15.7	17.6	14.1	15.3	11.2
25	7.60	10.5		13.7	15.3	12.3	13.1	
50	6.94	9.63		12.1	13.2	10.6	11.4	
75	6.38	8.83	*	10.6	11.7	9.26	9.75	*
100	5.95	8.10		9.75	10.5	8.12	8.40	
125	5.56	7.42		8.70	9.10	7.18	7.27	
150	5.16	6.80		7.85	8.10	6.38	6.45	
175	4.79	6.30		7.15	7.50	5.85	5.87	
200	4.56	6.02		6.83	7.11	5.53	5.49	
225	4.46	5.82		6.65	6.88	5.37	5.27	
∞	4.38	5.69	7.02	6.54	6.83	5.25	5.13	3.41

*Drying data discarded because of delamination or poor hot-surface contact.

TABLE XXVI

DYE DISTRIBUTION DATA

Air temperature - 85°F.
Air wet-bulb temperature - 70°F.
Air velocity - 250 f.p.m.

Sheet		253	250	251	254	255	256	260	261	262
Circulant		Water	Water	Water	Water	Water	Water	Glycol	Glycol	Glycol
Circulant temperature, °F.		190	190	190	190	190	190	230	230	230
Drying time, sec.		0	25	50	200	300	120	20	80	150
Intended sheet dry basis weight, mg./cm.^{2}		28.2	28.2	28.2	28.2	28.2	14.1	28.2	28.2	28.2
Intended initial moisture content, %		200	200	200	200	2200	200	200	200	200
Laminate dry basis weight, %[1]										
	A	15	10	15	15	15	25	15	15	15
	B	35	35	35	35	35	50	35	35	35
	C	35	40	35	35	35	25	35	35	35
	D	15	15	15	15	15	--	15	15	15
Extract volume from laminate, ml.										
	A	35.0	21.0	30.0	23.0	21.7	22.5	26.5	27.9	22.5
	B	25.0	20.0	25.0	17.0	17.5	38.0	29.0	22.0	25.7
	C	25.0	41.0	31.0	22.5	33.0	44.0	36.0	32.2	25.5
	D	46.0	71.0	39.2	34.2	$\frac{36.7}{21.0}$(2)	--	40.5	46.1	38.8
Extract transmittance at 425 mmu., %										
	A	59.5	50.1	50.2	18.1	20.2	25.7	42.5	30.6	16.1
	B	33.1	29.7	47.3	51.3	61.0	63.2	41.3	70.0	65.8
	C	28.7	49.6	52.9	45.4	64.1	42.8	47.9	64.7	52.6
	D	67.7	74.7	56.1	34.2	$\frac{35.0}{92.8}$(2)	--	46.5	39.2	27.5

1. Laminates are lettered successively from A at the air interface.
2. Extract 255D consisted of 2 portions.

TABLE XXVI (Continued)

DYE DISTRIBUTION DATA

Sheet		263	269	265	266	267	268
Circulant		Glycol	Glycol	Glycol	Glycol	Glycol	Glycol
Circulant Temperature, °F.		230	230	230	230	230	230
Drying time, sec.		240	240	100	100	60	60
Intended sheet dry basis weight, mg./cm.^{2}		28.2	28.2	14.1	14.1	7.0	7.0
Intended initial moisture content, %		200	150	200	200	200	200
Laminate dry basis weight, %							
	A	15	15	25	25	50	50
	B	35	35	50	50	50	50
	C	35	35	25	25	--	--
	D	15	15	--	--	--	--
Extract volume from laminate, ml.							
	A	47.8	34.1	36.9	34.7	28.4	52.0
	B	37.5	44.7	38.9	38.0	28.7	37.4
	C	44.0	36.1	62.5	51.8	--	--
	D	53.5	41.4	--	--	--	--
Extract transmittance at 425 mmu., %							
	A	47.8	43.5	35.5	36.3	33.2	61.4
	B	75.8	70.9	61.4	61.1	38.9	55.8
	C	67.9	53.9	47.8	41.5	--	--
	D	36.5	39.1	--	--	--	--